In: Dyes and Pigments: New Research
Editor: Arnold R. Lang
ISBN 978-1-60692-027-5

Chapter 1

PHOTODYNAMIC THERAPY

Petr Zimcik**[*] and Miroslav Miletin
Department of Pharmaceutical Chemistry and Drug Control,
Faculty of Pharmacy in Hradec Kralove, Charles University in Prague,
Heyrovskeho 1203, 500 05 Hradec Kralove, Czech Republic

ABSTRACT

Photodynamic therapy (PDT) is a cancer treatment based on activation of a drug by light. The drug, called photosensitizer, absorbs the energy of light of the proper wavelength and transfers it to surrounding molecules, mainly oxygen, forming reactive oxygen forms like radicals and singlet oxygen. These highly reactive species are responsible for destruction of targeted cells. Besides the direct effect on the cells, vascular shutdown develops as well and immune response is activated, both being important for long-term control over the tumor. Most of the photosensitizers are recruited from the group of porphyrins and related compounds like chlorins, bacteriochlorins, porphycenes, texaphyrins, and phthalocyanines. However, other dyes also entered the trials for photodynamic evaluation, e.g. some tricyclic dyes or hypericine. We discuss in this chapter, the history, photophysical and photochemical principles of PDT, as well as the biological effects of the photosensitizers. The main structural groups of photosensitizers are discussed and the most important drugs, either approved or in trials are described. Also, other approaches closely connected with PDT (catalytic therapy, sonodynamic therapy, photothermal therapy, and photochemical internalisation) are mentioned in this chapter.

HISTORY OF PDT

The sun's radiation is one of the essential prerequisites for existence of life on Earth, the visible light being the most important part of the sun's radiation spectrum. Photosynthesis, realized by chlorophyll, an essential natural dye built on a tetrapyrrolic porphyrin molecule,

[*] E-mail: petr.zimcik@faf.cuni.cz, tel.:+420 49 5067257, fax: +420 49 5067167.

employs the visible light to transfer the sun's light energy into the energy of organic bonds thus building basic conditions for the actual terrestrial life existence. However, the porphyrin skeleton is a nature´s patent, enabling more than just the transfer of energy for life.

Human beings, since the ancient civilizations including the Egyptian, Indian and Chinese cultures, realized the potential of light for treatment of some skin disorders like vitiligo, psoriasis, and also saw its importance for mental health [1]. The ancient Mediterranean civilizations extended this knowledge: the heliotherapy was introduced by ancient Greeks (Herodotus) for health renovation, and they used the light for treatment of many diseases [2]. However, people always realized both positive effects of the sun's radiation and its damaging potential. It was probably one of the reasons for light skin to be considered a sign of higher society and therefore people protected their skin against radiation [3-5].

There are two basic ways people have used light therapeutically:

Phototherapy, which usually does not require oxygen or any drug, could be defined as an exposure to non-ionizing radiation to treat a disease. It may be realized by an exposure to visible light, UVB or UVA radiation, or their combination [6, 7]. It was widely practiced hundreds of years B.C. in Ayurvedic medicine. Today it is employed in several medical areas, particularly in dermatology and psychiatry for the treatment of internal depressions, sleeping changes, the circadian rhythm, regulation and some other disorders.

Photochemotherapy is a therapeutic technique employing a photosensitizing chemical substance that is subsequently activated by a non-ionizing radiation [6]. Also, this type of treatment we could observe in ancient civilizations where naturally occurring plant ingredients psoralens were used by Egyptians to treat a wide spectrum of skin diseases [8]. Also, in the Indian Ayurvedic medicine system the psoralen/light combination was being used already around 1400 B.C. [9], and it was rediscovered again about 30 years ago [10].

Photodynamic therapy is usually considered as a type of photochemotherapy, which requires oxygen as the third component, along with a photosensitizer and light, necessary to be effective.

In the course of the 19th century, a lot of important work for the future development of PDT was done on exploring the structure, function and properties of the blood-red dye hem, a structural base of future clinically important photosensitizers. Among others, several German scientists [11-13] reported the removal of iron from hem and the resulting changes of such a modified molecule, which was called hematoporphyrin. The onset of fluorescence was also noted, but still not appreciated. An important step in phototherapy development was the treatment of smallpox using red light and of cutaneous tuberculosis with ultraviolet light, reported in 1901 by Danish physician Niels Finsen [14], who was awarded the Nobel Prize in 1903 for this discovery.

The milestone of photodynamic therapy was the concept of cell death induced by the interaction of chemicals and light, formulated by Oscar Raab, a medical student at Hermann von Tappeiner in Germany. More than 100 years ago, in 1900, he reported the lethal effect of acridine red and light simultaneously acting on the paramecium *Infusoria* [15], while both agents alone were harmless. This accidental famous discovery happened thanks to a flash during a thunderstorm, when the ambient lighting was very low. Around the same time as Raab's discovery, a French neurologist, Prime, reported photosensibilisation in sun-exposed areas in an epileptic patient treated with parental eosin [16].

Employing the above findings, von Tappeiner and the dermatologist Jesionek, at Munich Dermatological Clinic in 1903, performed a topical treatment of skin tumors by eosin and

white light [17]. Subsequently (1904), von Tappeiner and Jodlbauer evidenced the oxygen as an integral part in photosensitization reactions. They also established the term ‘‘photodynamic action’’ (1907) [18, 19].

Concurrently with this crucial improvement in the understanding of the photodynamic action mechanisms, scientists recalled the fluorescence of heme derivatives described almost half a century ago and started a period of exploration of photodynamic properties and potential clinical use of hematoporphyrin derivatives. In 1908-1911 Hausmann reported on fluorescence and photosensitized cell destruction with hematoporphyrin [20, 21]. The consideration of porphyrins as photodynamic agents arose from an explanation of porphyria, an inborn error of heme synthesis and metabolism in the 1900s. This type of disease is accompanied by considerable photosensitivity. The patients with porphyria were found to produce various porphyrins in abundance, among them some behaving as endogenous photosensitizers which accumulate in many tissues, particularly in the skin. This results in an unintended PDT when exposed to light. In the early to mid 1900s, Fisher did much of the work in the field of porphyrin metabolism [22] and treatment of porphyrias for which he was awarded the Nobel Prize in 1943. He revealed the potency of porphyrins for PDT, however, he did not use them for clinical PDT. This step was done by Meyer-Betz in 1913, when he intentionally applied himself a potential effective dose of hematoporphyrin and after light exposure experienced the first intentional porphyrin-based PDT reaction [23]. Unfortunately, the clinical significance of this risky experiment was not appreciated for several decades.

In 1924, French physician Policard noted enhanced tumor fluorescence when exposed to a Woods lamp, which indicated possible selective localization of endogenous porphyrins to tumor tissue [24]. After more than 20 years, Figge et al. [25] and Rasmussen-Taxdal et al. [26] paid attention to the selectivity of porphyrin tumor localization, and they could confirm the observations of Policard. In the 1950s, Schwartz and Lipson continued in the work of Fisher and Meyer-Betz to develop more refined and more active forms of hematoporphyrin, which was called Hematoporphyrin Derivative (HpD), and employed it at first only for fluorescent diagnosis of human tumors [27-29].

Experimental studies performed in the 1970s confirmed the hypothesis of von Tappeiner and Jodlbauer that singlet oxygen is the main cytotoxic agent in the photodynamic treatment [30]. Utilizing the above knowledge and experience, Dougherty appreciated the relatively high singlet oxygen quantum yield of HpD after absorption in the Q-band region of spectrum and he used the HpD/red light combination for treatment of 25 patients suffering from several types of both primary and secondary skin tumors with considerable effects [31]. In this key study, of the 113 cancer lesions 98 were cured completely, 13 responded partially, and only two were resistant to the PDT. The success of Dougherty was followed by more clinical studies of PDT treatment, performed mainly with HpD, e.g. for treatment of lung [32], esophageal [33], colon [34] cancer, cerebral glioma [35], and other brain tumors [36].

Their discoveries and experience started an era of modern PDT development realized by the introduction of HpD as standard medicinal preparation Photofrin® into clinical use by QLT PhotoTherapeutics in 1993, even if it still was not a structurally uniform and defined product.

PHOTOPHYSICS AND PHOTOCHEMISTRY IN PDT

Actually, the mechanism of action of PDT is nothing else than transfer of absorbed energy from photosensitizer to various substrates, oxygen being the most important, with subsequent formation of highly reactive cytotoxic species. The energy absorbed after illumination with light of appropriate wavelength excites the sensitizer from ground singlet state (S_0) to excited singlet state (S_1). Excited singlet state is only short-lived with lifetimes in nanosecond range and that is why it does not cause any PDT-important interactions with surrounding molecules. The deactivation (Figure 1) of singlet excited state is done *via* either radiative emission (fluorescence) or non-radiative decay (internal conversion). The energy dissipates also through non-radiative intersystem crossing to excited triplet state (T_1) with somewhat lower energy than S_1. This process is accompanied by change of the spin of one of the outermost electrons.

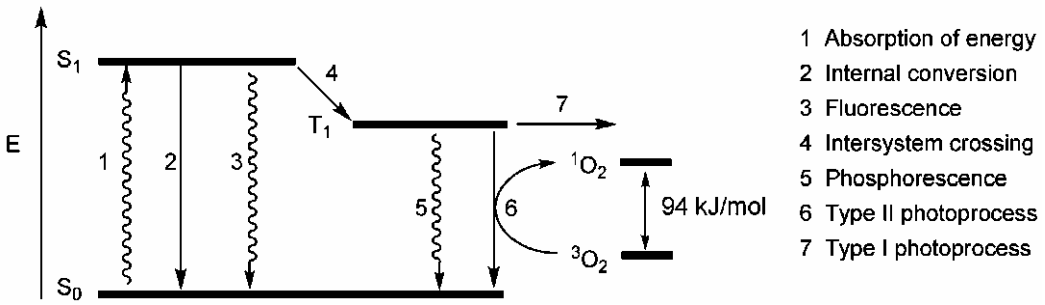

Figure 1. Modified Jablonski diagram.

Excitation of PS

$$^1PS + h\nu \rightarrow {}^1PS^* \rightarrow {}^3PS^* \quad (1)$$

Photoprocess type II

$$^3PS^* + {}^3O_2 \rightarrow {}^1PS + {}^1O_2 \quad (2)$$

Photoprocess type I

$$^3PS^* + {}^1PS \rightarrow PS^{-\bullet} + PS^{+\bullet} \quad (3)$$
$$^3PS^* + D \rightarrow PS^{-\bullet} + D^+ \quad (4)$$
$$PS^{-\bullet} + O_2 \rightarrow {}^1PS + O_2^{-\bullet} \quad (5)$$
$$^3PS^* + O_2 \rightarrow PS^{+\bullet} + O_2^{-\bullet} \quad (6)$$

$$2O_2^{-\bullet} + 2H^+ \rightarrow O_2 + H_2O_2 \quad (7)$$
$$Fe^{3+} + O_2^{-\bullet} \rightarrow Fe^{2+} + O_2 \quad (8)$$
$$Fe^{2+} + H_2O_2 \rightarrow O_2 + OH^- + OH^{\bullet} \quad (9)$$

Figure 2. Basic reactions occurring during PDT.

The emission of photon in the form of fluorescence can be utilized for detection purposes. It helps to observe the distribution of photosensitizer both *in vitro* and *in vivo* and enables monitoring of its pharmacokinetic after *in vivo* application. The emitted fluorescence can be also useful diagnostic tool in approach called photodetection or photodiagnosis [37,

38]. The final effect of the photosensitizer is not to kill the cancer cells but to visualize them only and therefore high fluorescence quantum yields (Φ_F) are advantageous in this application. On the other hand, the fluorescence and intersystem crossing are competitive ways of excited singlet state relaxation. Very strong fluorescence of photosensitizer decreases its feasibility to be transformed to the excited triplet state which is the most important for production of cytotoxic species and consequently for photodynamic action. That is why some strong fluorescent dyes were structurally modified to improve their photodynamic properties and they were introduced to PDT trials. An addition of heavy atoms such as bromine to rhodamines [39], dyes with high Φ_F, serves as typical example. The "heavy atom effect" increased their singlet oxygen quantum yield (Φ_Δ) on the account of Φ_F.

The collisions of photosensitizer with solvent molecules result in deactivation of the excited singlet state and the energy is lost in the form of heat (internal conversion). As it is also a competitive process to intersystem crossing, it decreases the photodynamic effect. This relaxation way was, however, also studied as a cancer treatment possibility and termed photothermal therapy [40]. The temperature in local environment of the sensitized cells can reach very high values for short time causing disruption and death of targeted cells.

Despite the fact that the intersystem crossing to T_1 state is a spin-forbidden pathway, the efficient photosensitizers undergo this process with high probability. Energy from this state can be released through a triplet-singlet emission of the photon known as phosphorescence or through energy transfer to surrounding molecules in triplet state. Once the photosensitizer gets into the triplet state, its deactivation is relatively long, again due to spin-forbidden transitions $T_1 \rightarrow S_0$ with lifetimes in the micro- to millisecond range. A long time of triplet state relaxation enables interaction of excited photosensitizer with other molecules in the triplet state and allows energy transfer to them. The quenching of triplet excited state can be distinguished to be photoprocess type I or photoprocess type II (Figure 1). A type I mechanism involves hydrogen atom extraction or electron transfer between excited state of photosensitizer and some surrounding molecules leading to production of radicals. The energy transfer between triplet states of photosensitizer and oxygen results in the type II mechanism and formation of singlet oxygen. Both photoprocesses occur usually simultaneously and it depends on oxygen concentration, type of PS and polarity of the environment which of them prevails in the photooxidative damage of the cells. However, the photoprocess type II that produces highly reactive singlet oxygen is generally accepted to be the main reason for cells destruction.

Photoprocess Type II

Singlet oxygen produced by photoprocess type II (Figure 2, Eq. 2) is highly reactive species and most of the effects of PDT are related to oxidative damage caused by this active molecule. Good overview of its properties and characteristic can be found e.g. in the work of Lang *et al.* [41]. Ground state oxygen is in the triplet state ($^3O_2$)(Figure 3). This is not very common feature for molecules and that is why only limited number of them (e.g. also vitamin A and nitric oxide) can also react in type II photoreactions [42] because the energy transfer proceeds only between species of the same multiplicity. Excitation of ground state triplet oxygen leads to change of the spin of one of the outermost electrons and thus to singlet oxygen ($^1O_2$)(Figure 3). One of the important characteristics of photosensitizers is therefore

their singlet oxygen quantum yield (Φ_Δ) that can be defined as number of singlet oxygen molecules formed per absorbed energy quantum. Typical values for PS range from 0.2 to 0.8, the higher the better.

Singlet oxygen is short-lived species with lifetime in water 3-4 μs [43, 44] which even decreases to approximately 0.2 μs in cells due to its high reactivity with biological substrates [45]. However, the observed low lifetimes in biological media may be more or less caused by problems with detection of $^1O_2$ in this environment. Recently, a lifetime 3 μs which is very close to $^1O_2$ lifetime in water was measured in viable cells [46]. The singlet oxygen lifetime increases in organic solvents and reaches value e.g. 19 μs in octanol [44] or 50-100 μs in lipids [47]. As a consequence of its general short lifetime it can diffuse to distance only about 10 nm [47] (or according to other authors to 45 nm [48]). For comparison, plasma membrane thickness is 7-10 nm, human cells diameter ranges from 10 to 100 μm. It is therefore obvious that the effect of singlet oxygen is strictly limited to the place of origin and shall not affect any surrounding cells.

Photoprocess Type I

Photoprocess type I (Figure 2) is based on electron transfer to excited photosensitizer and involves production of reactive oxygen species (ROS) including mainly superoxide anion ($O_2^{-\bullet}$), hydrogen peroxide (H_2O_2) and hydroxyl radical ($OH^\bullet$). The excited photosensitizer ($^3PS^*$) can react with photosensitizer in the ground state (^1PS) producing reduced anion ($PS^{-\bullet}$) and oxidized cation ($PS^{+\bullet}$) radicals (Eq. 3). Many surrounding electron-donating molecules (D) (e.g. NADH, vitamin C, cysteine, guanine) can also reduce $^3PS^*$ leading to $PS^{-\bullet}$ and oxidized substrate (D^+) (Eq. 4). Photosensitizer anion radical ($PS^{-\bullet}$) undergoes electron-exchange reaction with oxygen (Eq. 5) to produce superoxide anion ($O_2^{-\bullet}$). Though the excited photosensitizer ($^3PS^*$) can also theoretically yield superoxide anion directly through electron transfer (Eq. 6), it has been shown that competitive energy transfer leading to singlet oxygen (Eq. 2) is more favorable [49]. Superoxide anion is reactive species and can inactivate several enzymes but its most important role is in production of hydrogen peroxide (Eq. 7), reduction of Fe^{3+} (Eq. 8) and subsequent formation of hydroxyl radical in Fenton reaction (Eq. 9). This highly reactive radical can add to an organic substrate (e.g. fatty acids, phenylalanine, nucleic acids) disturbing thus its biological functions.

Despite the predominant influence of type II reaction in the photodynamic action, both reactions usually occur at the same time. Photoprocess type II is favored in oxygenated tissues and due to longer singlet oxygen lifetimes also in more lipophilic environment. On the other hand, the balance shifts toward the type I reactions under hypoxic conditions and these reactions substantially contribute to the photodamage of the membrane components in tissues with low oxygen concentration. They are also preferred in more polar environment where the radicals should be stabilized.

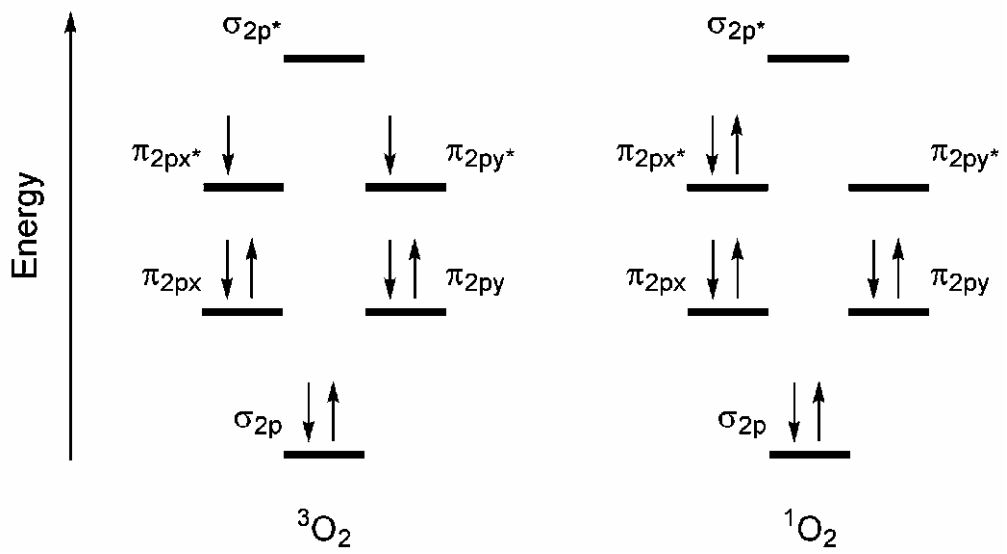

Figure 3. Molecular orbital diagrams of singlet ($^1O_2$) and triplet ($^3O_2$) state of oxygen.

Although some photoreactions can occur under hypoxic conditions, the presence of oxygen is an absolute requirement for successful photodynamic activity. The photodynamic effect is directly proportional to the concentration of oxygen in tissues and no cancer cells are killed under anoxic conditions [50]. The possible oxygen depletion from human tissues may occur due to two main reasons. The first one is a fast consumption of oxygen in photoreactions after illumination of targeted area. It means that the photodynamic effect may limit itself in further cell killing. This problem can be bypassed using lower light fluence rates when the oxygen is not consumed so rapidly. As a consequence, much better clinical results are obtained for the same fluence but lower fluence rates [51]. The second reason arises from low oxygen level in the target tissue. Tumor cells generally are poorly supplied with blood leading to local hypoxia. Moreover, the photodynamic effect causes vascular damage leading to even lower supply. This effect limits the use of PDT in solid tumors where hypoxia must be considered. On the other hand, PDT-induced vascular shutdown is one of the important effects leading to final control over tumor.

BIOLOGICAL RESPONSE

The death of each cell that accumulated enough of the photosensitizer and was illuminated is not the sole effect responsible for regression of the tumor. Three main mechanisms by which PDT mediates the tumor destruction were described. The direct lethal effect of singlet oxygen and other ROS on cells is the first one. PDT-mediated vascular shutdown leading to low nourishment supply and tumor infarction is also very important pathway. Finally, PDT can activate immune response against tumor cells.

Direct Effect

Since the active radius of toxic species produced by PDT is limited, the cell death is a consequence of the damage of subcellular structures. The absorbed photosensitizers are located inside the cell mainly in lysosomes [52-54] and also in mitochondria [55-57]. Some examples are described for photosensitizers (especially temoporfine) present also in endoplasmic reticulum or Golgi apparatus [57-59]. Plasma membrane is a relatively uncommon target in PDT [60]and photosensitizers are localized within it usually only during first minutes of incubation [61]. The fragmentation of DNA after PDT treatment is suggested to be rather a consequence of induced apoptotic response than a contribution of direct PDT effect on cell nucleus [42].

However, it is sometimes impossible to appoint only one target organelle responsible for cell death. The photosensitizer localization can change over time of incubation [61, 62], some of them allocate in various organelles [63], they can redistribute after illumination and thus affect more intracellular targets [64, 65], or they can be found diffused in cytoplasm indicating no distinct subcellular localization [66, 67]. Generally, photosensitizers which are hydrophobic and have two or less negative charges can diffuse across plasma membrane and then relocate to other intracellular membranes. Those which are less hydrophobic and have more than two negative charges tend to be too polar to cross the membrane by passive diffusion and therefore are taken up by endocytosis and they are found in lysosomes [68]. Endocytosis is also important uptake mechanism for aggregated photosensitizers. The cationic dyes are known to accumulate in mitochondria [55, 69, 70] and belong to the most phototoxic ones. Mitochondria are the source of ATP production therefore their injury will lead to energy imbalance. The membrane-bound mitochondrial proteins were found to be more susceptible to photodamage than those located in their matrix or in cytosol [71] due to longer singlet oxygen lifetime in hydrophobic environment. Moreover, mitochondrial way is believed to be the most important in induction of apoptosis after PDT [42, 72, 73].

Vascular Effects

Damage of vasculature of targeted area strongly contributes to final control over the tumor. The viability of tumor depends on the supply of oxygen and other nutrients by blood vessels. The destruction of delivery ways will lead to local hypoxia, anoxia and lack of available nutrients. The basic mechanism of action depends on the photosensitizer used. Porfimer sodium and hydrophobic phthalocyanines induces vessel constriction [74-76], trombus formation was observed after treatment with talaporfin [77] and disulfonated phthalocyanines caused only vascular leakage [74]. The vessel constriction is connected with release of eicosanoids and can be inhibited using indomethacin (inhibitor of cyclooxygenase) [78]. The mechanism may have also a biphasic character as shown for indium pyropheorbide [79]. The acute vascular effects were characteristic of vasoconstriction; however, the long-term vascular shutdown was mediated by thrombus formation.

The highest vascular effect of PDT occurs usually when activation is performed shortly after photosensitizer injection, while direct effect becomes more important when delayed times are used. Vascular targeting of PDT may be of higher effectiveness or even higher selectivity than direct effect and that is why this regimen is currently used for age-related

macular degeneration (AMD) treatment in clinic [80] and experimentally for tumor destruction [81, 82]. Especially for drugs with low selectivity to tumor cells or which are rapidly excreted from the body, this approach may be the primary effect responsible for the cure [77, 83, 84].

Immune Response

Activation of immune response in the targeted area after PDT is perhaps not the primary reason leading to cells death but it may help in long-term control over the tumor. In experiments with normal and immunodeficient mice, the long-term control has been observed only for normal mice although the short-term effects were comparable [85]. The mechanism of activation comprises release of cytokines, inflammatory and chemotactic signals from treated tissues followed by invasions of neutrophiles, mast cells, monocytes and macrophages [86]. Several other studies confirmed that tumor-specific response may be developed [42, 87] and on this ground the pretreatment with immunostimulants seems to bring benefits for PDT [88]. Suggestion that tumor-specific immunity is developed after PDT can be considered in development of vaccination using PDT-influenced tumor cell lysates [89].

PHOTOSENSITIZERS' PROPERTIES

Photosensitizers (PS) are the main components of PDT treatment. Their structure determines the photophysical as well as pharmacokinetic properties and as a consequence leads to different efficacy, tumor selectivity, application methods, irradiation schemes and side effects (especially long-term phototoxicity).

UV-vis absorption spectrum of each photosensitizer is perhaps the most important photophysical property. The transmittance of biological tissues is relatively low at lower wavelengths and increases at longer wavelengths. Endogenous chromophores in human body (hemoglobin, oxyhemoglobin and melanin) are responsible for light absorption up to approximately 630 nm and light penetration through tissues in range of only millimeters. Melanin absorption is important even at wavelengths around 700 nm and that is why especially highly melanotic tumors require photosensitizers with absorption at longer wavelengths. The IR radiation at wavelengths higher than 1000 nm is absorbed by water. The optical window of tissues opens therefore between 630 and 1000 nm. Nevertheless, absorption above 800 nm may not be suitable for singlet oxygen production. The energy difference between $^1O_2$ and $^3O_2$ (ΔE_Δ) is 94 kJ mol^{-1} so the energy of the photosensitizers excited triplet state (ΔE_t) must be larger. As ΔE_t decreases with increasing wavelength it may not be sufficient for excitation of $^3O_2$ to $^1O_2$. The optimal range of absorption for ideal photosensitizer is therefore 680-800 nm.

Similarly to all dyes, the photosensitizers undergo also a photobleaching. This is a process when the macrocycle loses its absorption as a result of self-destruction after illumination. The stability of photosensitizer on light decreases generally with absorption at higher wavelengths. Such low stability may be a limitation during use in therapy but also an

advantage, since the photosensitizer is then excreted from the body faster and it may reduce long-term photosensitivity.

The ideal photosensitizer for PDT would have the following characteristics:

- *Be chemically pure and of known composition*. The porfimer sodium (a hematoporphyrin derivative), which was the first compound approved in clinical practice, consists of a number of different dimers, trimers and other oligomers. Also sulfonated aluminium phthalocyanine (known as Photosens) is a mixture of several phthalocyanine macrocycles with different degree of sulfonation and position of sulfo group.
- *Have low dark toxicity of both photosensitizer and its degradation products*.
- *Be preferentially retained in target tissues*. High tumor-to-healthy tissues ratio is advantage and decreases the systemic toxicity. However, the low selectivity can be bypassed by special irradiation schemes as in the case of talaporfin.
- *Be rapidly excreted from the body*. As the photosensitizer tends to cumulate in skin, it causes prolonged photosensitivity (almost 2 months for porfimer) and patients must avoid the contact with direct sunlight for several weeks. Therefore the use of hydrophilic, rapidly eliminated PS seems to be more advantageous even at the expense of lower selectivity.
- *Have the high singlet oxygen quantum yields*. Since the production of singlet oxygen is crucial for PDT, the quantum yields should be as high as possible. For PS in clinical practice or in trials it ranges from 0.2 to 0.8.
- *Absorb strongly at longer wavelengths.* As mentioned above, the optimal wavelengths for absorption ranges from 680 nm to 800 nm. Moreover, high extinction coefficients (ε) at illumination wavelength allow reduction of PS dose while preserving the amount of produced toxic species.
- *Be available*.

According to above mentioned criteria, the available photosensitizers can be divided into three generations. Compounds involved in the first generation absorb usually at low wavelengths (about 630 nm) with low extinction coefficient (ε~3000 M^{-1} cm^{-1}), have low tumor/skin ratio and are retained in cutaneous tissues for several months. Actually, the only representatives of this generation are porfimer sodium and similar hematoporphyrin derivatives.

The second generation of PS is excited using light at longer wavelengths, mainly from 670 to 800 nm, which penetrates up to 2-3 cm. Also their absorption is much stronger (ε~ 50000-300000 M^{-1} cm^{-1}) which allows reduction of PS amount required for certain therapeutic effect. The interpretations of dose-response relationships are easier because they are not mixtures of compounds as in the case of porfimer. The selectivity of tumor targeting is, however, still not fully satisfying. That is why, the combination of the second generation PS with targeting moieties (monoclonal antibodies, steroids, nucleotides etc.) is under development and sometimes called the third generation of PS.

STRUCTURES OF PHOTOSENSITIZERS

Tetrapyrrolic compounds based on [18]annulene structure are among the most useful PS for PDT. The basic structure of porphyrin consists of four pyrrol units linked by methine bridges to make a ring. The porphyrin ring is an aromatic system containing 22 π-electrons, but only 18 of them are involved in delocalization (Figure 4). It obeys Huckel's rule of aromaticity 4n+2 π-electrons. The pyrrol rings in porphyrin are named A, B, C and D, the carbons forming methine bridges (position 5, 10, 15 and 20) are called *meso* carbons. Reduction of one double bond not involved in [18]annulene ring leads to chlorins, reduction of another double bond gives rise to bacteriochlorins. Pheophorbides and bacteriopheophorbides can be considered as members of chlorin or bacteriochlorin family, respectively, with ethylene bridge between *meso* carbon and adjacent pyrrol unit. [18]annulene ring can be found also in the structure of compounds derived from porphyrin – texaphyrins and porphycenes. Isosteric replacement of *meso* carbons in porphyrin with nitrogens and condensation of benzene rings to each of pyrrol units leads to well known group of synthetic dyes phthalocyanines.

All porphyrin-like compounds have two important absorption bands – Soret band (known as B-band) around 400 nm and a Q-band in area 600-800 nm. The Q-band is important for PDT since it lays in area used for excitation. Porphyrins absorb at λ_{max}~630 nm with only weak extinction coefficient. Reduction of double bonds in porphyrin's pyrrol rings causes bathochromic shift and strengthens the absorption at Q-band. Thus, chlorins absorb at λ_{max}~650-690 nm with ε~40000 M^{-1} cm^{-1} and bacteriochlorins at λ_{max}~740-800 nm with ε~50000 M^{-1} cm^{-1} depending on the substitution of the ring (see Figure 5[1] for comparison [90]).

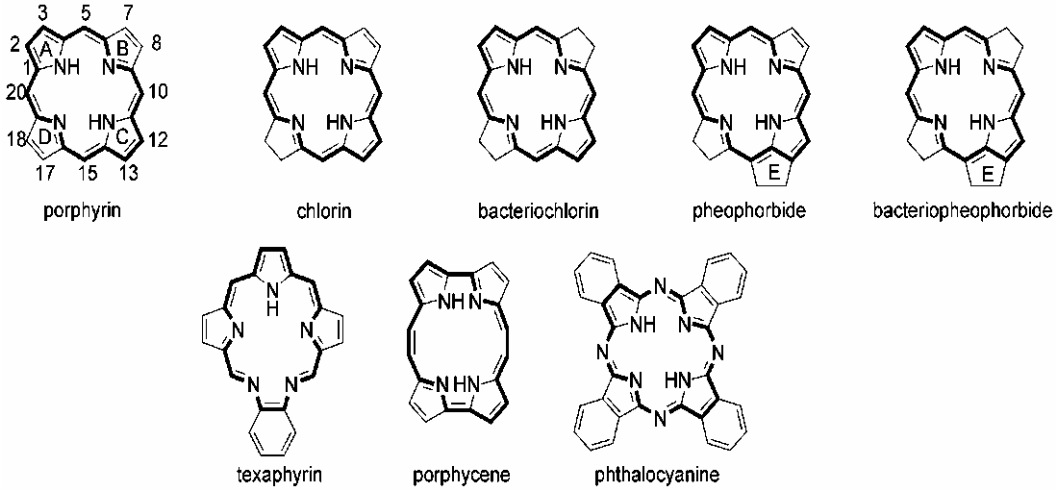

Figure 4. Basic structures of porphyrinoid photosensitizers.

[1] Reprinted with permission from ref [90]. Copyright (2006) American Chemical Society.

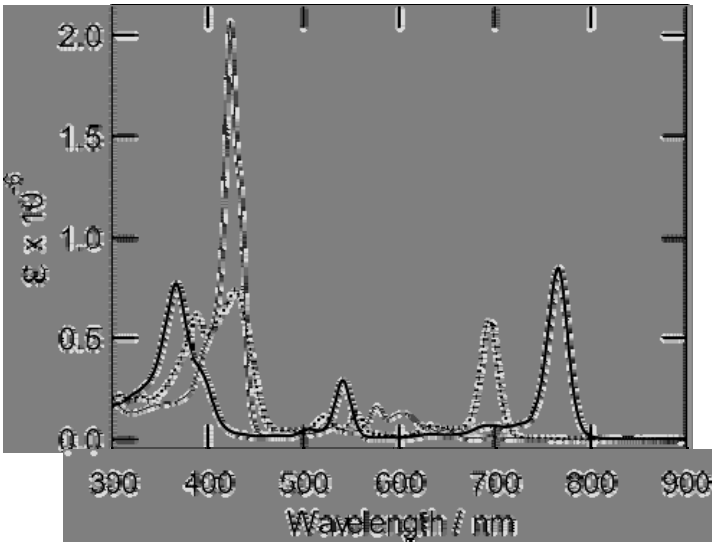

Figure 5. UV-vis absorption spectra of porphyrin (thin line), chlorin (dotted line) and bacteriochlorin (thick line) of the same peripheral substitution and at the same concentration.

Whole macrocyclic system of phthalocyanines is aromatic and conjugated and this substantially changes photophysical properties especially in the Q-band area. The band is shifted to higher wavelengths (λ_{max}=650-700 nm) and is very strong (ε up to 200000 M^{-1} cm^{-1}). B-band absorption, on the other hand, is only weak. Enlargement of phthalocyanine ring for next benzene rings lead to naphthalocyanines (Nc) with even more red-shifted Q-band (λ_{max}=760-810 nm) and ε over 250000 M^{-1} cm^{-1}.

In following paragraphs, we will concentrate on the photosensitizers which have been already approved in clinical practice, are undergoing clinical trials or are prospective in future PDT treatment. The compounds are divided according to their structures into porphyrins, chlorins and bacteriochlorins, phthalocyanines, tricyclic dyes and other photosensitizers. Since the compounds were developed or investigated often by different research groups, they received a lot of names including several abbreviations. For instance, mono-*L*-aspartyl chlorin e6 is also known as talaporfin, Npe6, LS11, MACE or Laserphyrin® and can be also mentioned as a part of Litx™ technology. Where possible, we will prefer use of the international nonproprietary names (INN) which are recommended by WHO for drugs.

PORPHYRINS

Porfimer Sodium

Other names used: hematoporphyrin derivative, HpD, Photofrin, Photogem, Photosan.

Porfimer sodium is an INN name for mix of compounds which are named hematoporphyrin derivative (HpD). In fact, this is not a single compound but a mixture of monomers, dimers and oligomers with not exactly defined proportions of the constituents. Hematoporphyrin (Hp) itself is a potent photosensitizers but it is lack of selectivity to tumor tissues. It was found that oligomeric fractions that arise during isolation of Hp from blood

[91] are responsible for the selective accumulation and therefore these fractions were synthetically enriched to form HpD and later concentrated using gel permeation chromatography.

Heme is a red blood dye responsible for oxygen transport *in vivo* and is photodynamically inactive. It is demetallated using HBr in acetic acid (Scheme 1), the vinyl groups are hydrobrominated at the same time and subsequently hydrolyzed in water medium to yield Hp [92]. Treatment of Hp with sulphuric acid in acetic acid leads to acetylation of free hydroxy groups. Their subsequent hydrolysis with NaOH and neutralization gives a mixture known as HpD. During this process a lot of linkages either ether, ester or direct C-C bonds arises and oligomer fraction is enriched. The removal of acetyl group by NaOH may lead also to elimination and some vinyl groups on periphery may be restored [93]. An example of tetramer combining some of the possible connections and peripheral substitutions in HpD is shown on (Figure 6). The crude mixture was purified by HPLC or gel permeation chromatography to enrich the oligomeric fractions which are responsible for increased tumor uptake and such HpD was used in clinical tests and later introduced to clinical practice as porfimer sodium.

The maximum wavelength of HpD absorption is at 630 nm, its ε at this wavelength reaches only 3000 M^{-1} cm^{-1} and as a consequence large doses of photosensitizer and light are needed for therapeutic effect. Porfimer sodium is water soluble and applied in the form of *i.v.* injections at the dose 2 mg/kg. Its half-life ranges from 17-22 days. The best tumor uptake is reached after 45-50 hours when the targeted area is irradiated. Next irradiation can be done after 90-120 hours. If necessary, second PDT-cycle (including drug administration) can be performed after 30 days. Porfimer is retained in skin for at least 6-8 weeks causing long-term phototoxicity.

The HpD enriched for its oligomeric fractions is approved as porfimer sodium. However, a lot of other HpD of different origin were prepared and the composition may vary. For example, three different HpD forms from a various manufacturers are investigated in China (BeijingHpD, YangzhouHpD, Photocarcinorin) and they have been shown to be of different composition [94]. HpD developed by different technology has been investigated also in Russia and approved for clinical use under the name Photogem® in 1996 [95]. The clinical results obtained for such preparations are therefore very hard to correlate correctly.

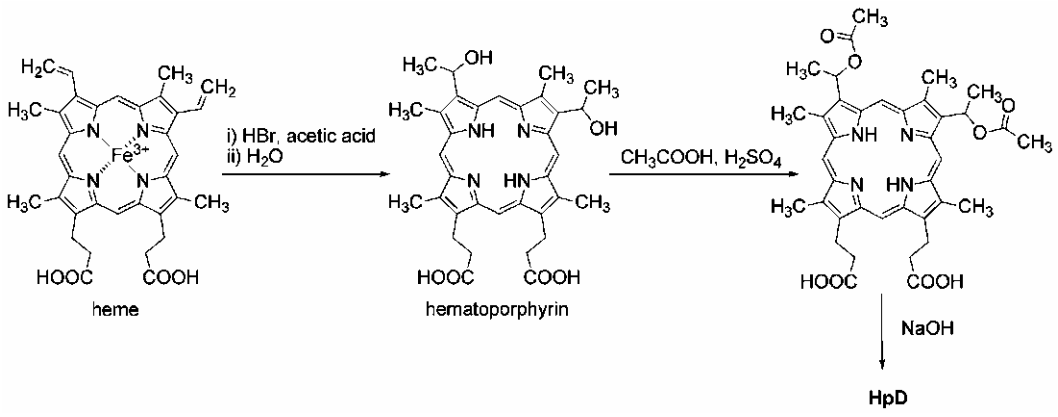

Scheme 1. Preparation of HpD.

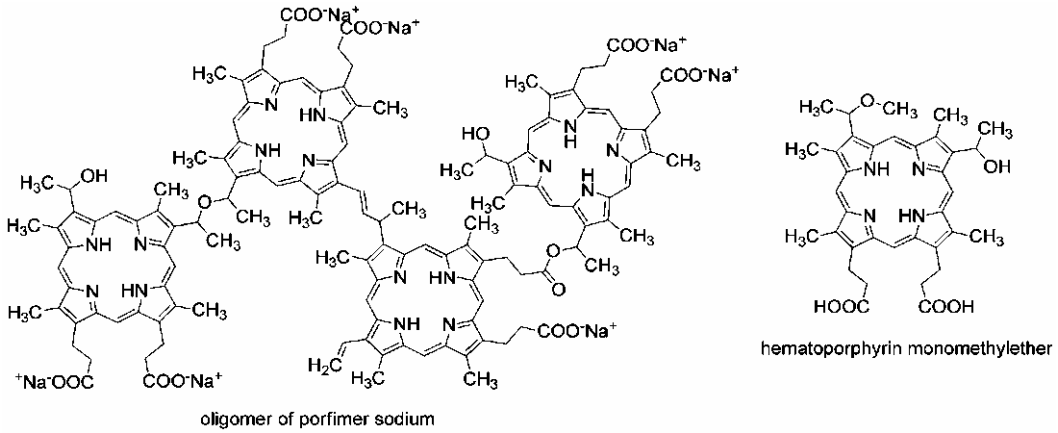

Figure 6. Example of one of porfimer oligomers and structure of hematoporphyrin monomethylether.

Porfimer sodium was developed by QLT, Inc. and as the first photosensitizer approved in clinical practice for PDT in Canada (Photofrin®) in 1993 for the treatment of superficial bladder cancer. A lot of other approvals have been received since that time also in other countries for treatment of advanced stage esophageal cancer, advanced non-small-cell lung cancer, early-stage lung cancer, cervical cancer, gastric cancer and Barret's esophagus [96]. However, since the porfimer sodium is the first and the best known photosensitizer, a lot of other clinical trials for new cancer treatment are under run [97]. For instance, head and neck cancers [98] brain and central nervous system tumors [99, 100] and cholangiocarcinoma [101, 102] have been shown to respond to the porfimer sodium-PDT treatment. The worldwide rights to Photofrin® were sold to Axcan Pharma, Inc. in 2000.

Hematoporphyrin Monomethylether

Other names: HMME, Herimether, PsD-044.

Hematoporphyrin monomethyl ether (Figure 6) is a name for two positional isomers – 3- or 8-methoxyethyl-8- or 3-hydroxyethyldeuteroporphyrin IX. It was synthesized in China and clinical studies have demonstrated that, compared to HpD, it has advantages of stronger photodynamic effect, higher tumor selectivity, lower toxicity and shorter skin photosensitivity [94]. It has been successfully used for treatment of port-wine stains, cancer of gastrointestinal tract and gliomas [103].

5-aminolevulinic Acid

Chemical name: 5-amino-4-oxo-pentanoic acid

Other names: δ-aminolevulinic acid, 5-aminolaevulinic acid, ALA, 5-ALA

5-aminolevulinic acid (5-ALA) is the first compound in the porphyrin synthesis pathway (Scheme 2), leading in the end to hemoglobin in mammals. In eukaryotic cells it is produced by the enzyme ALA synthetase from glycine and succinyl CoA. 5-ALA biosynthesis in plants, algae and most of bacteria starts from glutamic acid and glutamate-1-semialdehyde.

There are two rate-limiting steps in the heme biosynthesis in eukaryotic cells: synthesis of 5-ALA and conversion of PpIX to heme by the enzyme ferrochelatase [104].

As a PDT tool, 5-ALA is a prodrug in the sense of Albert´s [105] concept. The 5-ALA molecule itself is non-active. If produced naturally in cells, it is fluently converted to porphobilinogen (PBG), and then up to heme through several biosynthetic steps. The concentration of heme works as a feedback control mechanism, inhibiting the endogenous 5-ALA formation, so no biosynthesis intermediate is accumulated under physiological conditions. When exogenous 5-ALA is supplied, the biosynthesis runs relatively quickly to the protoporphyrin IX (PpIX), the last intermediate, which normally incorporates an iron ion to form the heme molecule. However, since this step is a bottleneck of the heme biosynthesis, in the case of exogenous 5-ALA supply the PpIX is accumulated in cells in high concentration depending on the 5-ALA availability, because of limited capacity of the ferrochelatase [106, 107]. In contrast to heme, which is not photoactive, the PpIX oxygen quantum yield is about 0.56, which is quite sufficient for effective PDT [108].

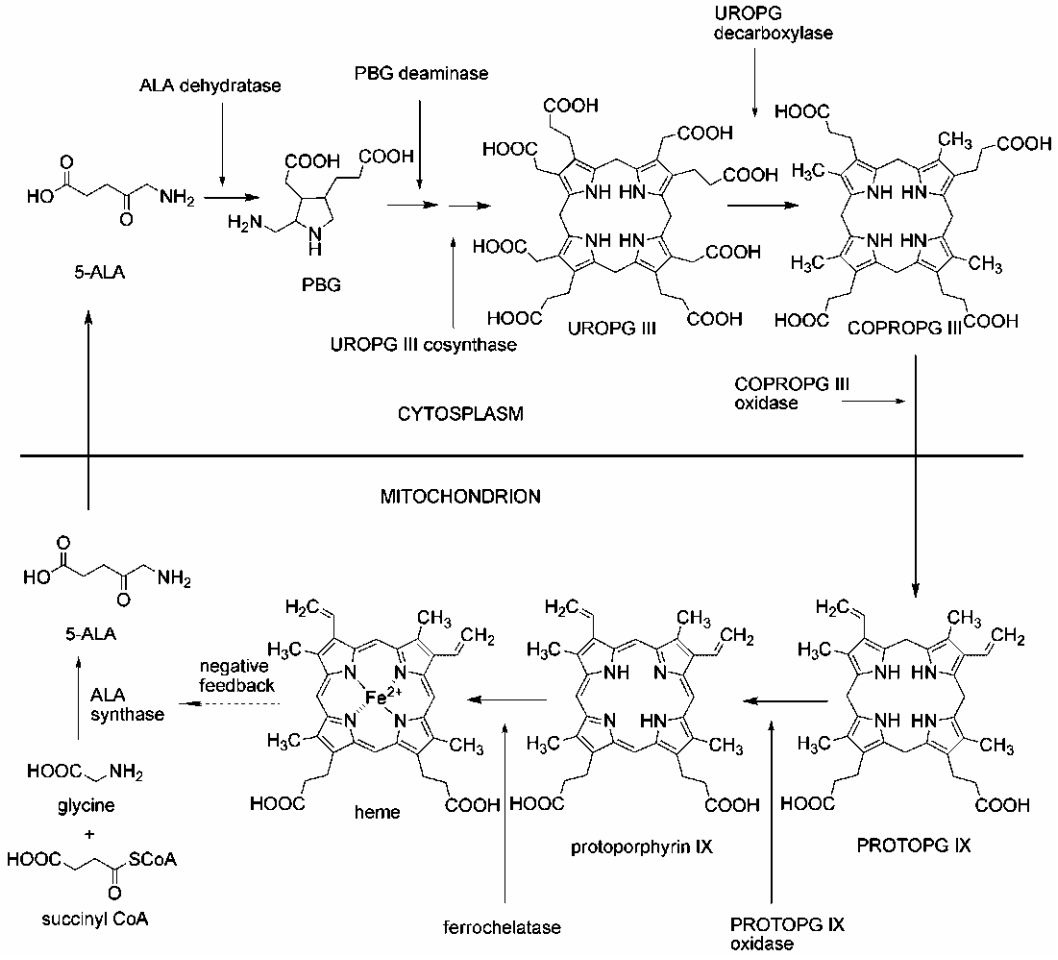

Scheme 2. Pathway of heme biosythesis.

The fundamentals for employment of 5-ALA in photodynamic therapy were put in 1987 by Malik and Lugaci [109], who first used 5-ALA induced PpIX and light for *in vitro* cells inactivation, and by Peng et al. [110, 111], who described endogenous porphyrin synthesis 24 hr after intra-peritoneal injection of 5-ALA in tumor-bearing mice. However, for these successful 5-ALA applications, previous improvements in knowledge about porphyrin biosynthesis and metabolism were necessary. Research of porphyria brought important new information in this field in 1980s, when e.g. Sandberg and Romslo found the phototoxic efficacy of protoporphyrin IX was much higher than that of coproporphyrin and uroporphyrin [112]. In another important finding the same authors revealed the efficiency of PpIX was strongly dependent on subcellular localization of the porphyrins. While PpIX was localized and exerted its damaging power mainly in the mitochondria, uroporphyrin was concentrated in lysosomes and after irradiation it caused release and inactivation of lysosomal enzymes. The higher efficacy of PpIX localized in mitochondria corresponded with the previously described importance of oxygen in the PDT [113, 114].

5-ALA was introduced into human PDT by Kennedy and Pottier in 1990-1992 [115, 116]. They described photosensitivity at patients with superficial skin disorders after exogenous administration of 5-ALA in an aqueous solution and they confirmed that the photosensitivity was caused by PpIX.

Considering the routine human applications of PDT, 5-ALA and its derivatives perform majority of the clinical cases nowadays. Of them, vast majority is realized in dermatology as topical PDT. Beyond the officially approved applications (Bowen´s disease, actinic keratosis and basal cell carcinoma) [117, 118], both 5-ALA and its ester derivatives are examined in many other experimental topical therapeutic and diagnostic applications, e.g. superficial fungal infections [119, 120], acne [121-123], psoriasis [124, 125], warts [126] and other skin viral infections [127, 128]. For these applications, 5-ALA possesses both excellent advantages but also some drawbacks.

The main advantages of the 5-ALA PDT include:

1. The natural character of both the (pro)drug and active metabolite is a good premise for low toxicity of this photodynamic therapeutic system.
2. Relatively short and low skin photosensitization, since the PpIX is not too much accumulated in the skin and the tissue levels are at the standard value in about 24 to 48 hrs [129].
3. The relative selectivity caused by various reasons, e.g.:
    - more expressed porphobilinogen deaminase at some types of tumors enhances the PpIX biosynthesis in tumor cells compared to the normal cells [130-132]
    - lower ferrochelatase activity at some cancer cells [131-134] decreases the PpIX to heme conversion and increases the PpIX accumulation
    - limited availability of iron atoms in rapidly proliferating cancer tissues also contributes to slowered PpIX to heme conversion [135].

The main drawbacks of the 5-ALA mediated PDT are:

1. The strong hydrophilicity of the 5-ALA, which considerably limits its penetration especially through the upper layer of skin, stratum corneum, and through cell membranes. Therefore, only very superficial changes can be treated [136, 137].
2. The instability of 5-ALA, especially in solutions buffered to the physiological pH value.
3. Absorption maximum of the highest PpIX Q-band at approx. 630 nm, which also limits the use of 5-ALA mediated PDT to superficial skin disorders only and disables it from use on pigmented skin defects, because of the endogenous porphyrins and melanins absorption, reaching up to approx. 700 nm.

Despite of these problems, 5-ALA itself is used relatively frequently in human PDT. Officially it is approved for topical treatment of actinic keratoses of head and scalp since 1999 (USA, Levulan® Kerastick®, DUSA Pharmaceuticals). Since 2000 it is also registered as the medicinal preparation Alasens [138] in Russia, as the hydrochloride in powder form for dissolution before application.

A big effort exists in the scientific community to resolve the above mentioned 5-ALA drawbacks, and in some cases this effort was at least partially successful. The 5-ALA hydrophilicity can be overwhelmed to some extent by either chemical modifications or technological formulation methods.

Chemical modifications intended to enhance the 5-ALA penetration through skin and membranes should consider the mechanism of its action, i.e. the amino and carbonyl groups of its molecule are included in the subsequent steps of the hem biosynthesis cycle. Therefore, to maintain its biological activity, these moieties usually should stay free and available for enzymatic condensation. Several studies described formation of *N*-derivatives of 5-ALA, mainly of simple amide or peptide type. Simple amide derivatives were usually not active, probably because of low ability of cells to cleave the amide bond [139-143]. Some peptide derivatives were more successful [141, 142], however, the doses of such compounds to achieve equivalent PpIX biosynthesis compared to 5-ALA were high.

Even if the carboxy group is not directly included in the metabolic bio-condensation, only carboxylic acid precursors are usually considered to be suitable for PDT. Of the chemical modifications described until now, the esterification has shown to be the most successful in enhancing the lipophilicity and penetration while maintaining the activity [137, 144]. A number of 5-ALA esters was synthesized, including both non-branched and branched aliphatic esters [139, 145], alicyclic and aromatic esters (all of them including halogenated derivatives [146]), ethylene glycol esters, nitrophenyl esters, thioesters [147], dendron and dendrimer esters. Despite of the number of compounds, only two ester derivatives were introduced into clinical use until now. The methyl ester (Metvix®, Photocure ASA, Oslo, Norway) is officially approved for treatment of actinic keratoses and hexyl ester (Hexvix®, Photocure ASA, Oslo, Norway) for photodiagnostic use.

Even if the esterification of 5-ALA has shown to enhance penetration through cell membranes and the influx into the cells, the positive effect on the PpIX formation in cells compared to free 5-ALA occurs only in low concentrations. Another factors, especially the rate of the ester hydrolysis and the porphobilinogen deaminase and uroporphyrinogen II cosynthase activity seem to be the limiting for PpIX synthesis [135, 140, 148, 149] in the concentrations above approx. 3-5 mM. Since the concentrations currently used in the dermatologic therapeutic applications are in the range of 16-20 per cent (w/w) (about 1M or

more), the formation of 5-ALA esters as pro-prodrugs with enhanced penetration is probably not the main advantage of this modification. Nevertheless, until now there seems to be no clear evidence that 5-ALA esters are biologically active only after the hydrolysis, since in some cases formation of PpIX esters and diesters was observed and they shown spectral properties analogous to the ones of PpIX itself [150-152]. Taylor et al. also showed that exposition of 5-ALA and its ethyl ester mixture to the 5-ALA dehydratase, the second enzyme in the hem biosynthesis pathway, resulted in a mixture of porphobilinogen as the main product and its ester as the by-product [153].

Unlike the topical use, the concentrations of 5-ALA and its derivatives in body fluids and tissues after systemic administration are much lower and enhanced cell influx enabled by esterification may play an important role. For example, the porphyrin synthesis from 5-ALA hexyl ester was found to be several times higher than that from 5-ALA at 0.05 mM concentration in experiments performed at the murine mammary adenocarcinoma M3 derived LM3 cell line [154]. The low plasmatic concentrations sufficient for high PpIX fluorescence localized with relatively high selectivity in cancer tissue favor the 5-ALA hexylester as the photodiagnostic tool (Hexvix®, Photocure ASA, Oslo, Norway), actually approved for detection of bladder cancer.

For the topical applications, the advantage of ester derivatives seems to be more important as a factor influencing the selectivity of subsequent photodynamic treatment. It was shown that the porphyrin synthesis from 5-ALA esters is much more localized in the cancer tissue than in the surrounding normal cells [155-157]. The reason could be the higher activity of esterases in some cancer or another abnormal cells, as already noted above. The differences in PpIX ratio in normal skin and actinic keratoses were observed by Fritsch et al. [158] also in isolated human skin. Another condition contributing to the higher ratio of PpIX concentrations between the place of application and surrounding tissue at 5-ALA esters could be the higher partitioning and subsequent sequestration of the esters within the stratum corneum, while the free 5-ALA can diffuse to surrounding tissues trough vascular networks more easily thanks to its hydrophilicity [159].

Another advantage of 5-ALA methyl ester mediated topical PDT over the 5-ALA treatment is less pain accompanying the treatment procedure. This phenomenon is probably attributable to different cell uptake mechanisms of these two 5-ALA application forms. While 5-ALA cellular uptake very probably at least partly employs a Na^+ and Cl^- dependent active transport mechanism [160, 161], the uptake mechanism of its methyl ester is independent on the Cl^-. On the other hand, it can be inhibited by amino acids of low polarity (e.g. alanine, methionine, tryptophan) [162].

The second main shortage of the 5-ALA mediated PDT is the drug isufficient stability. It depends strongly on the pH value, on the drug concentration, and temperature of the solution. The main reaction causing the decrease of free 5-ALA molecules number available for PDT is dimerization. 5- ALA belongs among the α-amino ketones which under neutral and alkaline condition readily dimerize and subsequently cyclize to dihydropyrazine derivatives [163](Scheme 3). In the case of 5-ALA, the formation of mainly 2,5-dicarboxyethyl-3,6-dihydropyrazine [164-166] *via* an open-chain ketimine 5-ALA dimer was observed. Porphobilinogen [167] and pseudoporphobilinogen [165, 167] were described to arise as minor side-products. Similarly to biosynthetic steps to subsequent hem intermediates, the amino and carbonyl groups are included in the dimerization reaction [167]. In the presence of oxygen, the dihydropyrazine derivative is further oxidized to the 2,5-dicarboxyethylpyrazine

[165, 168]. The speed of dimerization reaction depends mainly on the pH value. While solutions of 5-ALA with pH under 2 are stable, at pH 7.4 almost complete degradation could occur in several hours. Similarly, at 0.3 g/ml solution the decrease of concentration is more than four times higher during 45 min test period than at a 0.1 g/ml solution at pH 5.5 [167].

Since the 5-ALA instability is caused by similar mechanism, as are the ones which 5-ALA undergoes in the first steps of hem biosynthesis, it is not easy to stabilize the molecule against these undesirable changes. Some attempts to protect the amino moiety via formation of amides were performed, however, they usually resulted in biologically inactive derivatives, as already mentioned above. As a result, a theoretically possible way to stabilize the 5-ALA solutions is to keep the pH at very low value, which is unfortunately unsuitable for clinical human application. The other way is to prepare the solution *in-situ* just before application. This approach is employed at the both the clinically used preparations Levulan® Kerastick® (DUSA Pharmaceuticals, Inc.) and Alasens. Another possible approach is a development of formulations avoiding direct contact of 5-ALA or its derivatives with water. The literature concerning such formulations is outside the scope of this review.

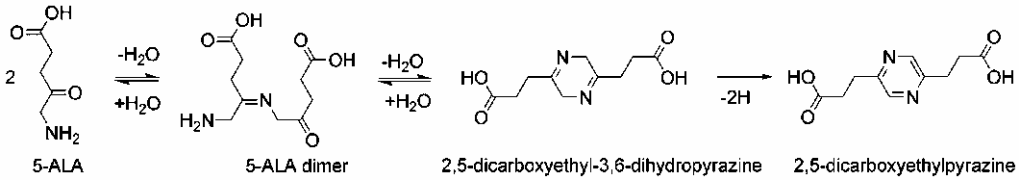

Scheme 3. Reaction mechanism of 5-ALA instability.

CHLORINS

Verteporfin

Other names: benzoporphyrin derivative mono acid ring A, BPD-MA, Visudyne®

In spite of its name benzoporphyrin, verteporfin (developed by QLT, Inc.) is a member of chlorin family. It is a derivative obtained semisynthetically from protoporphyrin (Scheme 4). Protoporphyrin dimethyl ester undergoes a Diels-Alder reaction with dimethyl acetylenedicarboxylate. The adduct double bonds are then rearranged by treatment with base to obtain the benzoporphyrin derivative modified on both A and B rings. Chromatographic separation and partial hydrolysis gives desired benzoporphyrin derivative mono acid ring A [93].

Being a chlorin, the photophysical properties of verteporfin are improved – it absorbs at 690 nm with ε~35000 M^{-1} cm^{-1}. Verteporfin is only sparingly water soluble, so it must be administered in the form of liposomal formulations at dose 6 mg/m^2. It is rapidly cleared from body, its plasma half-life ranges from 5 to 6 hours. The irradiation is performed 15 minutes after start of infusion. The skin photosensitivity is usually developed only for 48 hours.

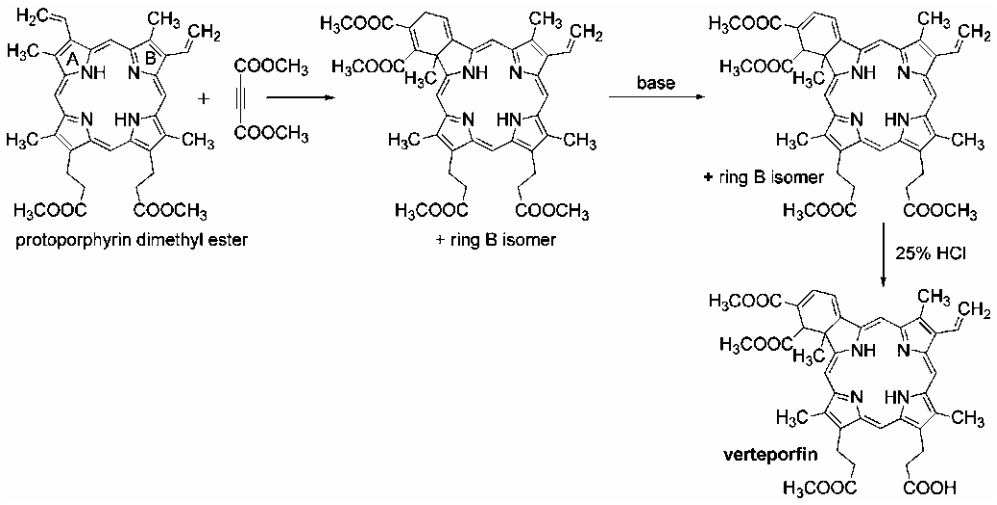

Scheme 4. Synthesis of verteporfin.

Though verteporfin has been tested also for cancer treatment, it received the highest attention in ophthalmic applications for the treatment of age-related macular degeneration (AMD). AMD is the leading cause of severe vision loss among the elderly in western world. It appears in two forms: wet and dry. The wet one is developed from dry one and is characterized by abnormal, leaky blood vessels in the macula, which may create scar tissue, causing permanent blind spots [169]. Verteporfin causes usually vascular shutdown so it is optimal for treatment of neovasculature. It is approved in several countries for treatment of chorioidal neovascularization caused by AMD but also due to other macular disease (pathologic myopia, ocular histoplasmosis). Verteporfin is effective in therapy solely [170], but it is investigated also in combination therapy with other drugs used for treatment of chorioidal neovascularization. It may be administered together with antiangiogenic drugs (ranibizumab, pegaptinib or bevacizumab) or steroids (dexamethasone, triamcinolone acetonide or anecortave acetonide). Although several clinical trials are still running [97] the first results suggest a possible synergistic effect of combination therapy [171, 172]. Verteporfin showed benefit also in dermatology for treatment of non-melanoma skin cancers [173] and port-wine stains [174].

Lemuteporfin

Other names: QLT0074, diethylene glycol benzoporphyrin derivative.

Lemuteporfin, another photosensitizing drug developed by QLT, Inc., can be considered as a derivative of verteporfin. It is prepared by esterification of benzoporphyrin derivative diacid ring A with ethylene glycol (Scheme 5). Its photophysical properties are close to parent molecule of verteporfin (λ_{max} 690 nm) but its pharmacokinetic is much faster. In tests on DBA/2 mice lemuteporfin showed good uptake within first 15-20 minutes, very rapid clearance from whole body and lack of accumulation in skin [175, 176]. It did not show any prolonged photosensitivity.

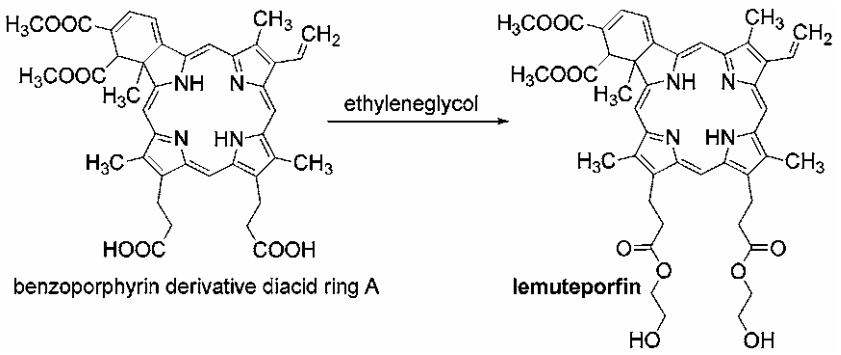

Scheme 5. Synthesis of lemuteporfin.

In test on cells, lemuteporfin showed possibility of immunomodulatory answer. Sublethal doses may result in the modification of cell surface receptor expression levels and cytokine release and consequently influence cell behavior [177]. It seems to affect mainly activated T-lymphocytes [178]. Several studies, including clinical trials phase I/II [97, 179], have been performed also for treatment of benign prostate hyperplasia [180].

Temoporfin

Other names: *m*-tetrahydroxyphenylchlorin, *m*THPC, Foscan®.

Temoporfin is a completely synthetic chlorin prepared by diimide reduction of double bond in 5,10,15,20-tetrakis(*m*-hydroxyphenyl)porphyrin (*m*THPP) which is fully built up from pyrrol and protected 3-hydroxybenzaldehyde [93] (Scheme 6). In a series of positional isomers, *ortho* substituted THPP caused skin photosensitization [181]and that is why it was not even introduced to studies with chlorins. Comparing *meta* and *para* substituted hydroxyphenylchlorins, the *meta* isomer showed much better cost/benefit ratio (expressed as damage to normal and tumor tissue, respectively) [182]. That is why 5,10,15,20-tetrakis(*m*-hydroxyphenyl)chlorin was chosen as the most suitable for clinical evaluation.

Temoporfin absorption is shifted to only 652 nm with ε~30000 M^{-1} cm^{-1}. Its solubility in water is not excellent, so it is administered in a mixture of water, ethanol and PEG. The best selectivity to tumor is achieved after 4 days and that is why it takes a long time between administration and irradiation protocol. However, recently a liposomal formulation of temoporfin showed the same efficacy [183] and high tumor/muscle or tumor/skin ratio were observed within few hours after administration [184]. It is very efficient photosensitizer, which enables administration in dose of only 0.15 mg/kg. Temoporfin has a low clearance with terminal plasma half-life 65 hours. Skin photosensitivity lasts for at least 15 days.

Biolitec Pharma has received the first approval for temoporfin in 2001 for treatment of head and neck cancer and it is still the only PDT-drug approved for this kind of cancer [185]. Good cosmetic results were obtained using this drug also for basal cell carcinoma (BCC) in clinical trials [186, 187]. The advantage of temoporfin over ALA-mediated PDT treatment of BCC is deeper penetration of activating light. Several other clinical trials were performed using this photosensitizer with satisfying results, including photodetection of brain tumors [188] and prostate cancer [189, 190].

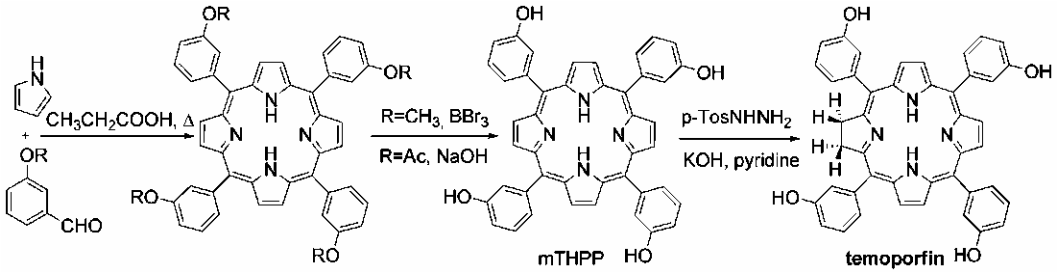

Scheme 6. Synthesis of temoporfin.

Talaporfin

Other names: mono-*L*-aspartyl chlorin e6, Npe6, LS11, MACE or Laserphyrin®, Litx™.

Talaporfin is a semisynthetic derivative of chlorin e6. Chlorin e6 is available directly from chlorophyll a (isolated from certain *Spirulina* species) under vigorous basic conditions [93]. Coupling of chlorin e6 with aspartic acid gives rise to mono-*L*-aspartyl chlorin e6 [191] (Scheme 7). However, three possible carboxy groups can be substituted during the reaction. In the beginning, the structure was attributed to 17^3-aspartyl derivative mainly based on theoretical predictions of reactivity and sterical hindrance. Later, 2D NMR studies [192] and more recently also single crystal X-ray diffraction [193] confirmed unequivocally that the structure corresponds to 15^2-aspartyl derivative. It was also accepted by WHO and INN name for talaporfin is attributed to 15^2-regioisomer.

Q-band position of talaporfin occurs at 664 nm with ε~40000 M^{-1} cm^{-1}. Talaporfin in the form of tetra sodium salt is well water-soluble and can be administered at dose 40 mg/m^2 by *i.v.* injection without the need for any special solubilizing agent. Irradiation of tumors starts in 15-60 minutes after application of the drug because animal models have shown that the response corresponds rather to plasma levels of photosensitizer than to accumulation in tumor tissue [194]. It shows two compartment pharmacokinetic with alpha, beta and terminal half-lives to be 9 h, 106-136 h and 168 h, respectively [195, 196]. It causes only minimal skin photosensitivity, usually within 3-7 days [195, 197] with complete disappearance after 2 weeks [198].

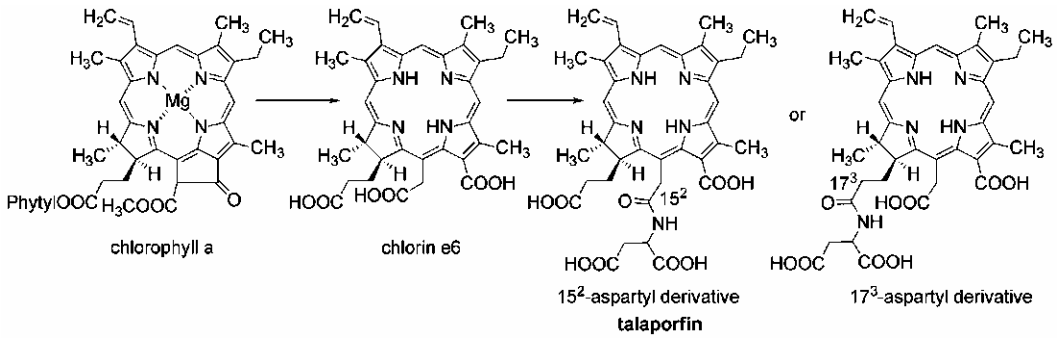

Scheme 7. Synthesis of talaporfin.

Talaporfin sodium, under the name Laserphyrin®, has been approved in Japan for treatment of early-stage bronchopulmonary cancer and is sold for that indication by Meiji Seika Kaisha, Ltd. It is also investigated by Light Sciences Oncology using Litx™ technology for the treatment of liver cancer – both hepatoma (primary liver cancer) and liver metastasis of colorectal carcinoma [199]. They perform also clinical trials on treatment of glioma (brain tumor). Other performed clinical trials involve cutaneous diseases of various cancers [200], superficial squamous cell carcinoma of the lung [198] and showed future promise for the use of talaporfin as efficient and safe photosensitizer. Recent *in vitro* tests with HL-60 cells were performed using this drug in combination with ultrasound (sonodynamic therapy). These results suggest that it sonochemically induces apoptosis as well as necrosis in HL-60 cells [201].

Rostaporfin

Other names: tin etiopurpurin, SnEt2, Purlytin™, Photrex®.

The purpurins are semisythetic derivatives obtained by intramolecular cyclization of porphyrins *meso*-substituted with derivatives of acrylic acid [93]. Tin etiopurpurin has been prepared in 1988 by insertion of metal into corresponding purpurin derivative using $SnCl_2$ in acetic acid (Scheme 8) [202]. Although insertion of metal into purpurin macrocycle shifts its absorption hypsochromically for almost 30 nm, their tumoricidal activity was significantly greater [202] and that is why they were more suitable for PDT applications. From Ag, Ni, Sn and Zn, the most suitable metals were found to be Zn and Sn [202] and in following study on mice tin etiopurpurin showed the best results [203].

Rostaporfin absorbs at 659 nm with ε~30000 M^{-1} cm^{-1}. The compound is hydrophobic and has to be administered in emulsifying agent. The dose is usually 1.2 mg/kg, irradiation starts 24 h after administration.

The drug was developed by Miravant for treatment of AMD (wet form). The drug finished the phase III clinical trials and approval to FDA has been submitted. However, FDA required more trials to confirm efficacy and safety. Miravant has started the confirmation studies in late 2005 [97] but no information have been available since that time. Positive results were obtained with rostaporfin also for treatment of cutaneous metastatic cancers of various origin [204, 205] and treatment of canine prostate [206].

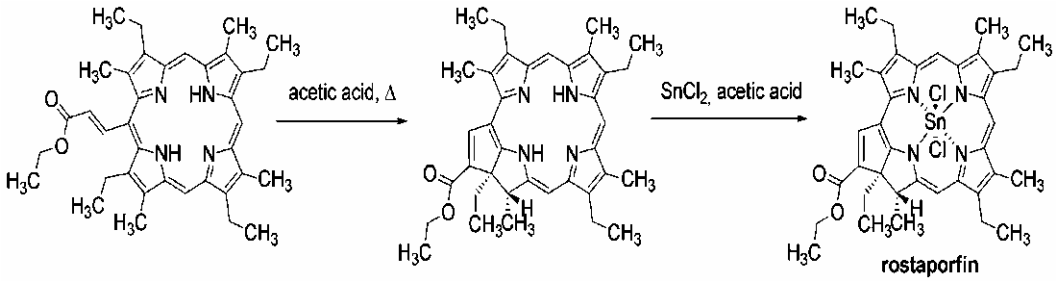

Scheme 8. Synthesis of rostaporfin.

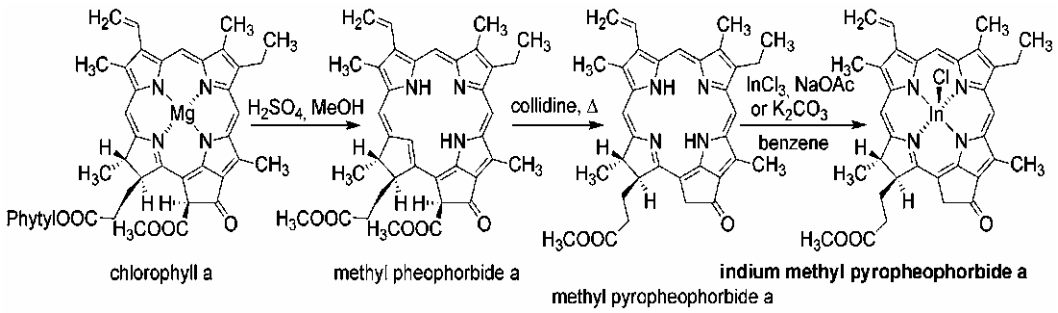

Scheme 9. Preparation of indium methyl pyropheophorbide a.

Indium Methyl Pyropheophorbide A

Other names: MV6401, InCh

Indium methyl pyropheophorbide a is another lipophilic photosensitizer developed by Miravant. Methyl pyropheophorbide a is prepared using standard conditions. Chlorophyll a is isolated from *Spirulina* and demetalated using sulfuric acid in methanol. Thus prepared methyl pheophorbide a is thermally decarboxalated in collidine to yield methyl pyropheophorbide a and subsequently converted in benzene under basic conditions (sodium acetate or potassium carbonate) in the presence of $InCl_3$ to desired indium methyl pyropheophorbide a (Scheme 9) [207]. Due to low solubility in water it must be administered using delivery systems, in this case based on liposomes of egg yolk phosphatidylcholines. It absorbs at 664 nm, usual dosage in animal models is only about 0.1 mg/kg and it has plasma half-life about 20 min [208]. It has been tested for chorioidal neovascularization on animal models with positive results. The best selectivity for this application was achieved when the drug was activated short times after administration (from 10 min to 90 min) [209, 210] indicating importance of vascular targeting. On the other hand, tumor treatment responds better using new approach of fractionated photosensitizer dosing when both tumor tissue and tumor vasculature are affected [208].

2-(1-hexyloxyethyl)-2-devinyl Pyropheophorbide a

Other names: HPPH, Photochlor.

This photosensitizer is example of semisynthetic improvement of naturally occurring porphyrinoids developed in Roswell Park Cancer Institute [211]. HPPH is an extremely hydrophobic compound that was found, in a quantitative structure-activity relationship study that addressed the general property of lipophilicity, to be the most effective photosensitizer against murine tumors amongst a series of homologues with different numbers of methylene groups on the ether function [212]. The original 5-step method of synthesis starts from precursor methyl pheophorbide a which is isolated from *Spirulina maxima* and converted to methyl pyropheophorbide a by refluxing in collidine. Its vinyl group is hydrobrominated in next step and immediately reacted with hexanol. The methyl ester is then hydrolyzed using LiOH (Scheme 10-A) [213]. The older method was recently replaced using much simpler

and faster procedure (Scheme 10-B) [214]. It involves Dieckmann condesation and subsequent thermal decarboxylation of easily obtainable trimethylester chlorin e6 and allows preparation of this promising photosensitizer in large scale.

This second generation photosensitizer absorbs at 665 nm with ε~47000 M^{-1} cm^{-1}. Low solubility in water requires presence of solubilizers and therefore the drug is formulated in 5% dextrose in sterile water containing 2% ethanol and 1% polyoxyethylene sorbitan monooleate (Tween 80). However, a new nanocrystal suspension of HPPH without the need of any stabilizers was successfully tested recently and its *in vitro* and *in vivo* efficacy was comparable with above mentioned application form [215]. The tests of HPPH on patients are performed usually at doses 2-6 mg/m^2. Due to its high hydrophobicity, its pharmacokinetic is slow with plasma half-lives 7.7 h and 596 h and the drug can be detected in plasma even several month after single infusion [216]. In spite of such slow excretion, no or only minimal skin photosensitivity appears [217].

HPPH has been entered into phase I trials at Roswell Park Cancer Institute for early and late stage lung cancer [218]. Clinical trials for treatment of esophageal, head and neck and nonmelanomatous skin cancers are also under run [97].

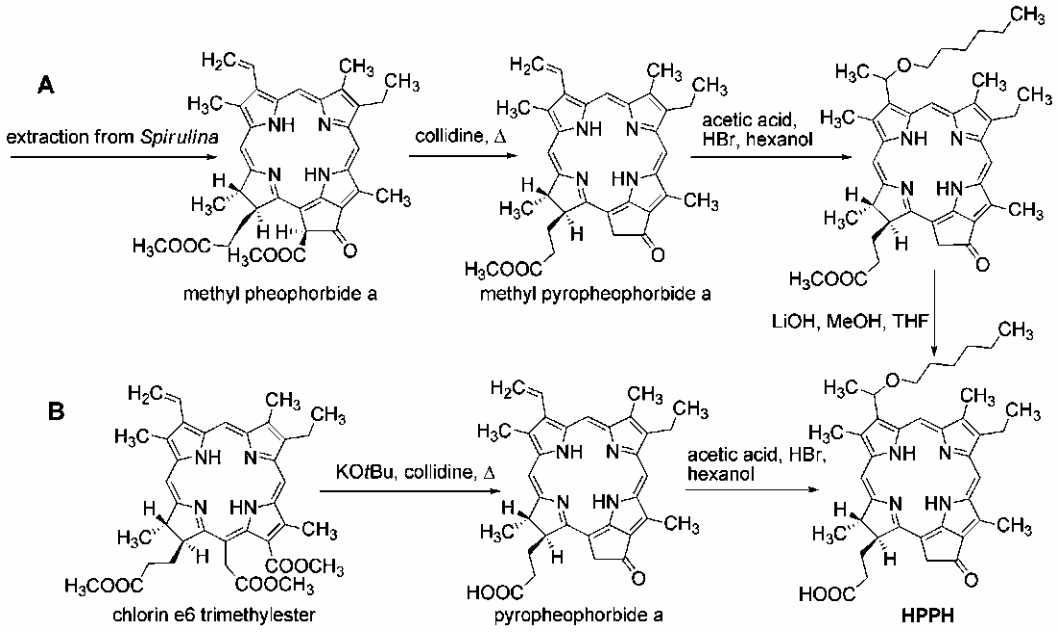

Scheme 10. Methods of preparation of HPPH.

Padoporfin

Other names: WST09, palladium bacteriopheophorbide a, Pd-BPheid, Tookad®.

Padoporfin is example of semisynthetic modification of naturally occuring photosensitizers of bacteriochlorin family. In the first step, bacteriochlorophyll a is isolated from lyophilized bacteria *Rhodovolum sulfidophilum.* Transformation to bacteriopheophorbide a can be done either by direct treatment in trifluoroacetic acid (provides

both hydrolysis of phytyl esters and demetallation) or phytyls are hydrolyzed using enzyme chlorophyllase with subsequent acidic demetallation. Palladium is usually inserted using palladium acetate in the presence of ascorbic acid (Scheme 11) [219].

As padoporfin is a member of bacteriochlorin family, both double bonds out of the [18]annulene ring are reduced and its absorption is red-shifted to 763 nm and also strengthened (ε~88000 M^{-1} cm^{-1}). Padoporfin is not water soluble, so that it must be administered in a Cremophor-based vehicle, in which a fraction of the drug is aggregated upon administration but disaggregates rapidly *in vivo*. Typical dose in human and animal models is 2 mg/kg. It is rapidly excreted from the body with no important accumulation. Plasma half-life in humans is about 20 minutes. Using mouse models, it was not detected in skin or muscles at all and plasma was cleared from the drug within 3 hours [220]. As a probable consequence of no skin accumulation, no photosensitivity was observed on patients in phase I clinical trials [221]. Due to fast clearance from the body, the irradiation usually starts during administration and the effects are contributed almost exclusively to vascular targeted PDT [84].

Padoporfin is tested as possible PDT-drug for prostate cancer and clinical trials phase II/III are under run [97]. Its efficacy and safety have been already confirmed both on human [84] and dogs [222, 223]. Based on vascular effects, it has also high potential to treat chorioidal neovascularization [224].

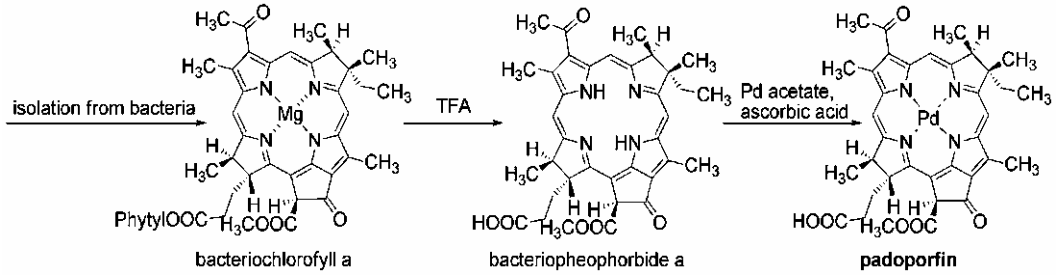

Scheme 11. Synthesis of padoporfin.

PHTHALOCYANINES

Phthalocyanines (Pc) are synthetic dyes used in many industrial applications [225]. They are structurally related to tetraazaporphyrins, with the four bridging carbon atoms at the *meso*-positions replaced by nitrogen atoms. Moreover, Pcs have benzene rings fused to the β-positions of each of the four pyrrolic subunits. This benzene ring addition strengthens the absorption of the chromophore in the near infrared region and shifts the maximum more to the red region [226]. Their high extinction coefficients and appearance of the absorption spectra Q-bands in 670–700 nm region suggest them as potentially suitable molecules for PDT [227]. Unlike of the HpD and some other porphyrin-type dyes, the presence of a suitable chelated metal atom (preferentially Zn, Al, Si) is essential for their photodynamic activity [226]. Comparative advantage of the Pcs considering the PDT is their high singlet oxygen quantum yield. However, they have also some unfavorable properties, which limit their

photodynamic applications. Owing to the extended π-electron system, they exhibit a strong tendency to aggregation resulting in dimeric and oligomeric species formation in solutions [228]. It has been shown that such association of the Pc molecules greatly influences their spectroscopic [229], photophysical [230], electrochemical [231], and conducting properties [232], and it decreases solubility in both water and organic solvents. The aggregation makes the purification and characterization of the Pc problematic and shortens their triplet-state lifetime so reducing the singlet oxygen quantum yield.

Apart from the considerable influence of the solvent and concentration of the Pc in solution [233], the aggregation can be suppressed by several structure modifications: chelatation of central atoms with more coordinating sites with following central atom substitution [234], introduction of aliphatic bulky substituents to the periphery of the Pc macrocycle [235-237], introduction of eight anionic [238] or eight cationic [239] ionized moieties or eight quarternary ammonium substituents [240] on the periphery, which causes a complete monomerization especially in water environment. The use of less than four cationic [241, 242] or anionic [243] peripheral substituents suppresses the aggregation only partially. There are three Pcs in clinical trials or clinical PDT (Figure 7).

Zinc Phthalocyanine CGP55847

Other names: ZnPc

It is the simplest Pc in clinical trials. Because of its very low solubility a liposomal formulation has been developed by QLT Phototherapeutics (Vancouver, Canada) and it has undergone clinical trials phase I/II in Switzerland (sponsored by Ciba Geigy, Novartis, Basel, Switzerland) for treatment of squamous cell carcinomas of the upper aerodigestive tract [244, 245].

Photosens

Other names: Aluminium tetrasulfophthalocyanine, Al-PcTs, AlPcS4, Aluminium phthalocyanine tetrasulfonate

Considerable attention has been paid to the sulfonated phthalocyanines. This type of peripheral substitution both decreases the aggregation and increases the water solubility of Pc. The sodium salts of a mixture of peripherally di- to tetrasulfonated chloro aluminium phthalocyanines (absorption maximum of Q-band in water at 676 nm) is used in Russia since 2001 for human PDT as Photosens [246]. It is approved and used for treatment of cancer of stomach, skin [247], lips, oral cavity, tongue [248, 249], and multidrug resistant skin and subcutaneous metastases of breast cancer [250]. The drug is administered as a 0.2% solution in the isotonic sodium chloride/water solution, in doses of 0.5-0.8 mg/kg of body weight in the case of a systemic administration. Because of relatively long term photosensitization, the patient should avoid intense day light exposition for a period of 4 to 6 weeks.

Another sulfonated phthalocyanine, zinc phthalocyanine tetrasulfonate, finished in 2007 Phase I clinical trial of the use as a photosensitizer for photodynamic therapy in dogs [251].

Pc4

Other names: SiPc IV.

The third Pc on the way to clinical PDT is a silicon complex Pc4. Its ability to kill HIV viruses in red blood cells concentrates was examined by V.I. Technologies, Melville, NY, USA. Currently, the Pc4 starts two Phase I clinical trials for the topical treatment of malignant and pre-malignant skin conditions [97, 252].

Naphthalocyanines (Ncs) are Pc derivatives with additional benzene rings attached to each isoindole subunit on the periphery of the Pc structure. Thanks to the extended chromophore system, the Ncs exhibit strong absorption maxima at wavelengths of approx. 740-800 nm, which predisposes them as good potential PS with two outstanding advantages: possibility of employment of high wavelength light with deeper tissue penetration and especially application on highly pigmented skin lesions [253-255], since they absorb above the absorption region of the melanins, reaching only slightly over 700 nm. They have been investigated also for effectiveness against other types of cancer [256-260]. However, there are some problems to be resolved at the Nc as photosensitizers: comparatively low both chemical and photochemical stability, even higher tendency to aggregation than Pcs and consequently also even worse solubility [226]. Relatively big molecule can also limits their ability to cross biological membranes.

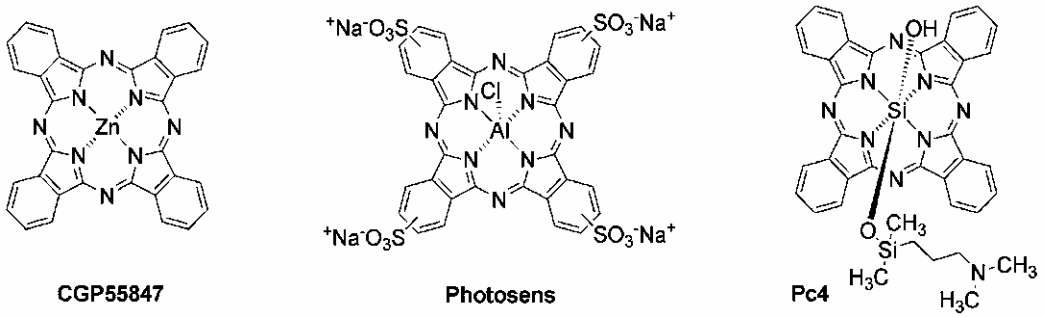

Figure 7. Phthalocyanines that entered clinical trials.

TRICYCLIC DYES

Although vast majority of examined and used photosensitizers is of the porphyrin structure, there are some additional chromophores exhibiting photodynamic activity after irradiation by red light. Among the most important belong the phenothiazinium dyes [261] and xanthenes. Their use as photosensitizers is supported by several reasons, including good water solubility, satisfactory singlet oxygen production at the best of them, main absorption peak in the "phototherapeutic window" and relatively low price and good availability.

The main drawback of the phenothiazinum structure is its metabolic instability. It undergoes relatively quick enzymatic reduction to its leuco-form, which is photodynamically inactive. Therefore, their use in PDT is limited mainly to topical application in dermatology or local treatment after intratumoral injection. The strongly polar character caused by ionic

structure of their molecules also limits ability of the phenothiazinum salts to cross the cell membranes and other lipophilic biological barriers. Considerable dark toxicity of the main commercially available phenothiazinium dyes found at some cell lines could be also a disadvantage for systemic clinical use [262].

Some attempts to improve the phototherapeutic properties of phenothiazinium salts and their analogues were done in effort to obtain compound absorbing at higher wavelengths, compounds with increased singlet oxygen production, or with moderately enhanced lipophilicity [263, 264]. These targets could be achieved by some ring system substitutions, e.g. halogenation, which is known to enhance the singlet oxygen quantum yield [261]. Even better results can be achieved by isosteric replacement of heteroatom in basic structure by an another one with extended electron system (O→S→Se) [261, 265, 266]. On the other hand, the expanded aromatic system of benzo [a]phenothiazinium salts or their benzo [a]phenoxazinium analogues with red-shifted absorption maxima usually resulted in decreased singlet oxygen production [265, 267]. Although some of the newly prepared compound exhibited improved some of the photodynamic properties, until now the well-known dyes stay the only used in human clinical treatment.

As already mentioned above, the phenothiazinum photosensitizers could be successfully used especially in external topical or internal local application. In such cases they can considerably spread the scope of photodynamic therapy to involve antimicrobial [268] and antifungal [269] PDT and melanoma [270]. Methylene blue and toluidine blue O have been the most frequently explored, even if also some other dyes have been tested for their photodynamic activity.

Methylene Blue

Chemical name and synonyma: 3,7-bis(dimethylamino)phenothiazinylium chloride, methylthioninium chloride.

Methylene blue (MB) (Figure 8) is the most common phenothiazinium dye, primarily used in histology for staining. It shows a strong absorption band in range of 550-700 nm with maximum at 664 nm. In high concentrated solutions and in acidic environment, the arising dimers show shift of the absorption maximum to 590 nm.

A comprehensive review of photophysical, photochemical, and biological properties as well as of the experimental clinical use of MB was done by Tardivo *et al*. The authors describe the main human clinical applications including basal cell carcinoma, Kaposi´s sarcoma, melanoma, and some non-cancerous skin conditions like onychomycosis, skin HSV infections and warts [271]. MB mediated PDT of melanoma seems to be more effective than in the case of 5-ALA or HpD. The latter compounds shown low efficiency [272], while MB treatment exhibited complete response of the tumor in more than 60% [270, 271]. Important photodynamic application of MB is the photodynamic inactivation of pathogens in blood *ex vivo* [273, 274].

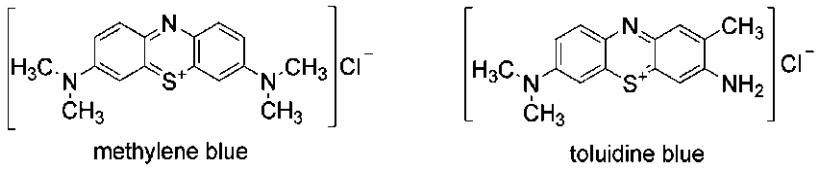

Figure 8. Structures of methylene blue and toluidine blue.

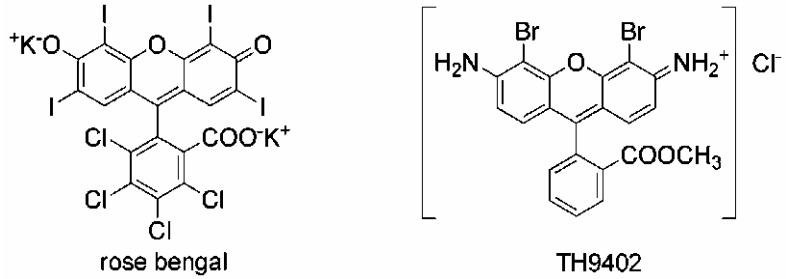

Figure 9. Structures of rose bengal and brominated rhodamin TH9402.

Toluidine Blue

Chemical name and synonyma: 3-amino-7-dimethylamino-2-methylphenothiazinylium chloride, tolonium chloride.

Toluidine blue (TB) (Figure 8) is a second important phenothiazinium dye in PDT. Its absorption maximum is only about 625 nm and the singlet oxygen quantum yield is also somewhat lower than in the case of methylene blue [261, 275, 276]. TB has been also tested for various photodynamic application, e.g. for treatment of cystic fibrosis [277] and in a mucoadhesive patch formulation in topical photodynamic treatment of fungal infections of the mouth [278]. However, the best results were achieved in inactivation of human mouth plaque bacteria [279-284] or in animal model of peridontitis [285]. This was the reason for introduction the dye as photosensitizer in photoactivated oral disinfection technique. It is used by the PerioWave™ system [286], which finished phase III clinical study in December 2006 [97] and approached clinical praxis. It is marketed by Ondine Biopharma Corporation (Canada) [287]. Another photoactivated oral disinfection technique system was introduced by Denfotex Ltd (UK) [288].

Rose Bengal

Another tricyclic dyes known to have photodynamic properties are xanthene structure based photosensitizers. While the non-substituted xanthene dye fluoresceine shows excellent fluorescence but negligible singlet oxygen production, the halogenation of the xanthenes structure results in good singlet oxygen quantum yields. The photodynamic potential of rose bengal (RB) (Figure 9) was confirmed in both physico-chemical [289] and cell culture experiments [290, 291] as well as against viruses [292]. Since the relatively selective uptake of the RB by tumor cells unlike of normal cells, the dye was selected by the Provectus

Pharmaceuticals Inc. (USA) as promising candidate for treatment of some cancer and other lesions [293]. Currently it is in the phase I study for treatment of recurrent breast carcinoma, phase II study for treatment of metastatic melanoma and phase II study in form of topical aqueous gel for photodynamic therapy of psoriasis [97].

Rhodamines

Properly substituted iminoxanthene dyes – rhodamines – also exhibited potential for PDT. Rhodamine dyes frequently used in microbiology and molecular biology for staining and as fluorescent tools showed highly selective uptake into neoplastic unlike normal hematopoetic progenitor cells [294]. This phenomenon suggested possibility of selective neoplastic cells photoeradication via *ex-vivo* photodynamic treatment [295].

Since the basic rhodamine derivatives exhibit only low singlet oxygen production, halogenation of their molecule analogously to fluoresceine was performed, because it was described to increase the efficiency of the intersystem crossing to the triplet state and consequently to increase the singlet oxygen quantum yield [39]. The 4,5-dibromorhodamine methyl ester (TH9402, Theratechnologies, Montreal, QC, Canada) (Figure 9) was selected as the most promising, with low dark toxicity and satisfactory stability. Its absorption maximum in water solution is 504 nm. Preparations with this brominated rhodamine are under development by Kiadis Pharma (The Netherlands) [97, 296]. TH9402 under name Reviroc™ starts phase II clinical trial on autologous stem cells transplantation at patients with blood cancer [97]. The same dye has finished phase II clinical trial for prevention (as ATIR™) and treatment (as Rhitol™) of Graft Versus Host Disease (GVHD).

OTHER PHOTOSENSITIZERS

Motexafin Lutetium

Other names: Lu-Tex, Optrin, Antrin, Lutrin, PCI-0123.

Motexafin lutetium is a member of texaphyrin group, a Texas shape macrocycles with pentaaza core [297]. Texaphyrins are completely synthetic dyes prepared for the first time in 1987 [298]. The core is built by condensation reaction of substituted *o*-phenylendiamine with diformyltripyrrane, which is obtained using condensation of three suitably substituted pyrrol rings. The macrocyclic ligand is then oxidatively metallated using lutetium(III) acetate and triethylamine in air-saturated methanol (Scheme 12) [299].

Thanks to presence of polar peripheral groups, motexafin lutetium is a water soluble photosensitizer. It absorbs at 732 nm with ε~42000 M^{-1} cm^{-1}. Dose is approximately 2-3 mg/kg, however, the optimal times of illumination vary with the treatment target. For example, the prostate cancer is illuminated 3 h postinjection, while coronary artery disease and breast cancer treatment use 18-24 h illumination delay. The drug is retained in neoplastic tissues and neovascularization. It binds well to lipoproteins so it may have activity against atherosclerotic plaques [300]. The drug is rapidly excreted from the body with half-life in tens of hours (13-39 h) [300].

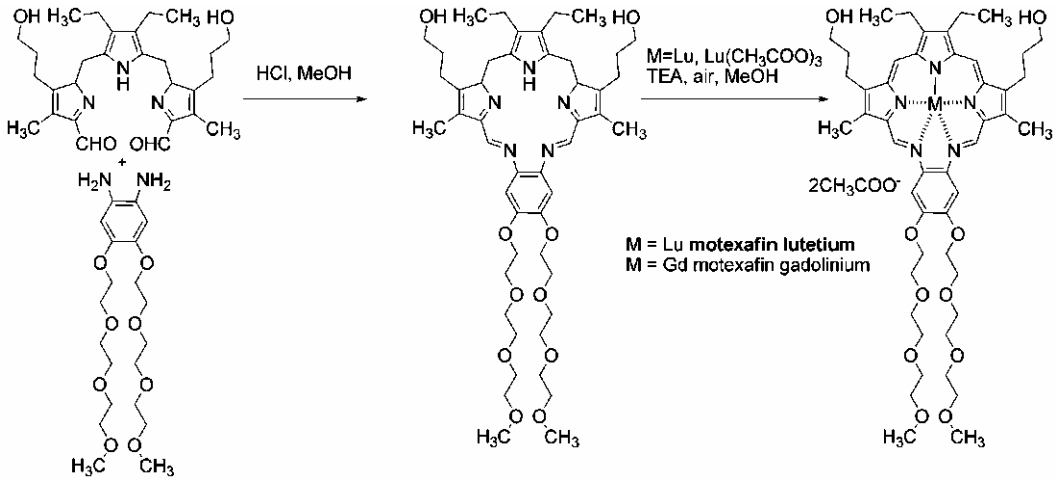

Scheme 12. Synthesis of motexafin lutetium.

Motexafin lutetium is a prospective treatment for human prostate adenocarcinoma. However, the observed variation in PDT dose distribution translates into uncertain therapeutic reproducibility [301] and suggests the use of individualized treatment planning for prostate PDT [302]. Other neoplastic conditions treated with motexafin lutetium include recurrent breast cancer [303] and due to absorption at higher wavelengths it allows also treatment of melanoma [304]. As the drug specifically localizes also within atheromatous plaque, it may be used in a novel therapeutic approach for atherosclerosis – photoangioplasty [300, 305].

The motexafin ligand can bind also other lanthanide metals, the most important being gadolinium. Complexation with gadolinium does not form a photosensitizer for PDT but the drug can be used for cancer treatment based on different mechanism of action. It accumulates selectively in cancer cells due to their increased rates of metabolism. Once inside the cell, it induces apoptosis (programmed cell death) by disrupting redox-dependent pathways. Motexafin gadolinium inhibits the enzyme thioredoxin reductase, which is a tumor growth promoter. This mechanism provides the opportunity to use the drug in a wide range of cancers. Gadolinium is paramagnetic, and therefore is detectable by magnetic resonance imaging (MRI), allowing the visualization of the drug in tumors [306].

Porphycenes are fully synthetic constitutional isomers of porphyrins [307]. Porphycene derivatives show higher absorption than porphyrins in the red spectral region (λ> 600 nm, ε> 50000 M^{-1} cm^{-1}) owing to the lower molecular symmetry. Photophysical and photobiological properties of porphycenes make them suitable candidates as photosensitizers, showing fast uptake and diverse subcellular localizations (mainly membranous organelles) [308]. The most studied porphycene for PDT application is perhaps acetoxy-2,7,12,17-tetrakis-(β-methoxyethyl)-porphycene (ATMPn) absorbing at 640 nm which has been evaluated for PDT application both *in vitro* [309, 310] and *in vivo* [311].

Hypericin, an aromatic dianthraquinone originating from the herb *Hypericum perforatum*, exhibits photodynamic action too [312]. It absorbs at 590 nm with ε~44000 M^{-1} cm^{-1}. Several *in vitro* and *in vivo* tests have evaluated this photosensitizer for treatment of various cancers using PDT [313]. Clinical trials were performed on patients with squamous cell carcinoma and basal cell carcinoma [314].

Also mixtures of different photosensitizers isolated from natural sources are used in therapy. Thus, *Radachlorin*® developed in Russia is a *Spirulina* extract containing purpurin 5, chlorin e6 and purpurin 18 as alkali metal salts [315]. On the other hand, its manufacturer states slightly different composition: chlorin e6 (90-95 %), chlorin p6 (5-7%) and the third chlorin which is not preferred to be disclosed (1-5%) [316]. It is administered at dose from 0.2 to 1 mg/kg and irradiated using light of wavelength 662 nm, irradiation starts usually 2-5 hours after administration. Photosensitivity is very short; patient should avoid direct sunlight for about 24 hours.

NEW APPROACHES CONNECTED WITH PDT

PDT is not the only one new approach to treat cancer. Several new techniques took some advantages of PDT to find new mechanisms of better selectivity to tumors, simpler administration, higher efficiency or they are trying to remove some limitations concerned with PDT. They include e.g. catalytic therapy, photothermal therapy, photochemical internalization and sonodynamic therapy.

Catalytic Therapy (CT)

Catalytic therapy (CT) is a cancer treatment modality based on the generation of reactive oxygen species (ROS) using a combination of substrate molecules and a catalyst. Contrary to PDT, it does not require activation by light that limits the PDT treatment only to tissues and areas accessible to light or light-producing devices. The radicals are formed after the oxidation of substrate (most often ascorbic acid) with oxygen catalyzed by phthalocyanine metal (cobalt or iron) complexes (Figure 10). Recently, also porphyrins were found to be effective in CT [317].

The mechanism involves formation of the superoxide anion in the first step which is followed by the production of hydrogen peroxide and hydroxyl radical [318, 319]. The most promising compound for CT is a sodium salt of cobalt(II)-2,3,9,10,16,17,23,24-octacarboxyphthalocyanine, developed under the name Theraphthal® (Figure 10).

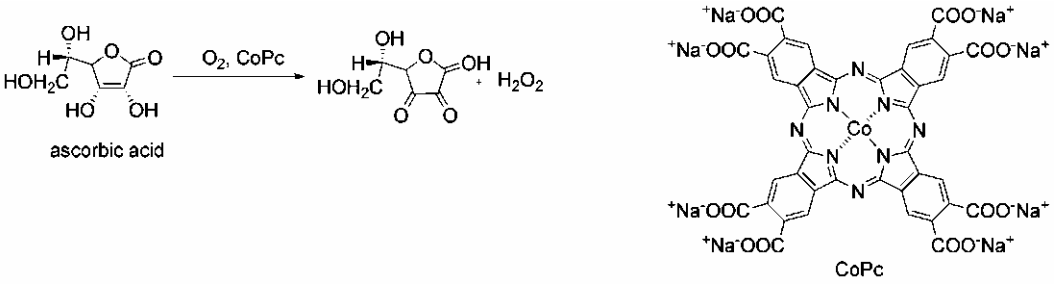

Figure 10. Mechanism of hydrogen peroxide formation in catalytic therapy and structure of the most studied compound Theraphthal® (CoPc).

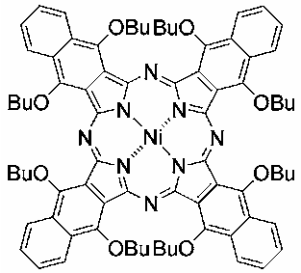

Figure 11. Structure of Ni(II)-5,9,14,18,23,27,32,36-octabutoxy-2,3-naphthalocyanine used in photothermal therapy.

Photothermal Therapy (PTT)

This new approach is based on the promotion of photothermally sensitized processes in tumor cells or tissues. Photothermal processes reflect the tendency of a light-absorbing species to dissipate electronic excitation energy through heating the local environment [320]. The temperature rise can reach 130 °C above the basal value [320]. The consequent sudden expansion of the proximate water shell generates a shock wave which leads to extensive mechanical (*e.g.* ultrasonic shock) and chemical (*e.g.* bond cleavage) damage. This method does not require presence of oxygen and efficiently works in its absence [321]. Similar compounds (phthalocyanines, porphyrins) as in the PDT can be used for therapy and the effect of both methods is considered to be synergistic. The aggregation of sensitizers which is often a problem in PDT, because it strongly decreases singlet oxygen production, is on the other hand an advantage in PTT since the energy is then released preferentially in the form of heat. Therefore, PTT allows the use of sensitizers with enlarged hydrophobic macrocycles (e.g. naphthalocyanines) which often tend to strong aggregation in biological media. Also their absorption at wavelength far behind 800 nm cannot be used for efficient production of singlet oxygen due to possible low energy of triplet state. Irradiation of the targets is performed by strong laser pulses.

Several *in vitro* [40] and *in vivo* [320, 322] tests confirmed efficiency of this approach which is oxygen independent and uses wavelength which penetrates deeper through human tissues. The most studied sensitizer in PTT is Ni(II)-5,9,14,18,23,27,32,36-octabutoxy-2,3-naphthalocyanine (Figure 11) absorbing at wavelength 850 nm with ε~280000 M^{-1} cm^{-1}.

Photochemical Internalization (PCI)

Photochemical internalization (PCI) is a technology for light-directed drug delivery and was developed to introduce therapeutic molecules in a biologically active form specifically into diseased cells [323]. In this case, photosensitizers do not serve as therapeutic agents but only as delivery enhancers.

It is widely acknowledged that macromolecules have great potential as therapeutic agents. However, their use is often limited because they do not leave the endosomes within cells after endocytosis. Adjacently substituted photosensitizers (e.g. disulfonated phthalocyanines and

meso-phenylporphyrins (Figure 12)) localize primarily into membranes of lysosomes and endosomes of cells. After irradiation, these subcellular structures rupture and release their content. So, the PCI principle is based on common administration of photosensitizer and the macromolecule drug into blood stream. They are both taken up into endosomes of targeted cells and macromolecules are released into cytosol after irradiation [324, 325] (Figure 12). This approach showed *in vitro* increased uptake for several types of molecules, e.g. protein toxins [326], oligonucleotides [327], nanoparticles [328] and many others. It also proved to be efficient *in vivo* in improvement of tumor therapy using protein toxins [329], gene therapy [330] and delivery of bleomycin [331]. The most studied photosensitizers are disulfonated aluminium phthalocyanine and disulfonated tetraphenylporphyrin where sulfonation takes place on adjacent benzene (or phenyl) rings. Clinical trials on patients treated with bleomycine-PCI shall start soon [325].

Sonodynamic Therapy

Sonodynamic therapy (SDT) is a treatment employing combination of ultrasound in doses which are normally non-destructive to tissues and a chemical called sonosensitizer, which is non-toxic without the exposition to the ultrasound. The idea is similar to the one of photodynamic therapy, replacing the light by ultrasound, which brings an advantage of much deeper penetration of the activating agent into the tissues. Often similar types of sensitizers are used. Also in some studies an improved effectiveness was observed using the PDT and *SDT in combination.*

Ultrasound is a mechanical wave realized by vibrations of particles of medium, where the ultrasound is spread, at frequencies equal to or higher than 20 kHz. It is generally considered as safe and used commonly in medical diagnostic methods. However, it can interact with biological media and the interactions can be amplified in presence of the sonosensitizers. Unlike of the photosensitizers, the mechanism of ultrasound enhanced cytotoxicity is probably different at various types of molecules tested as sonosensitizers [332].

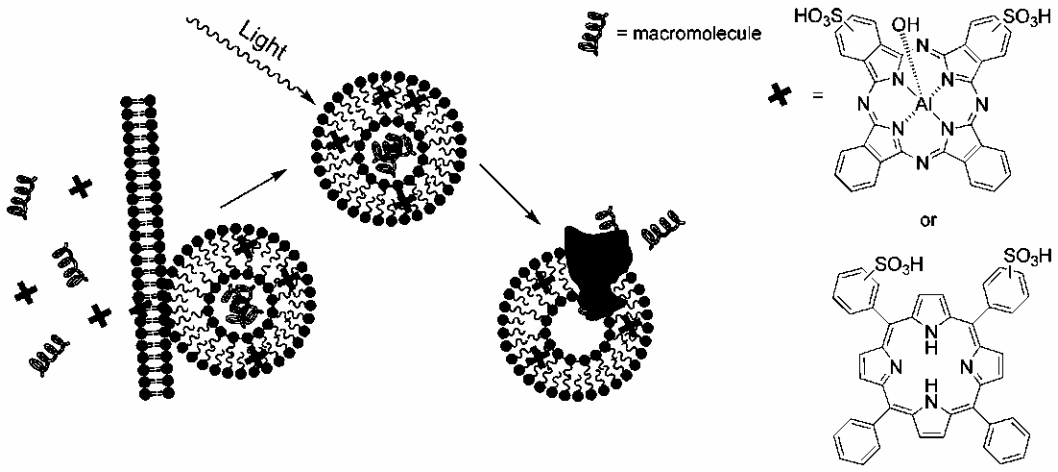

Figure 12. Mechanism of action of photochemical internalization and structures of two most studied photosensitizers in this application.

Among suggested mechanisms of sonodynamic therapy belong:

(1) hydrodynamic stress caused by fast moving bubbles in the tissue, where sonosensitizers work probably as membrane destabilizing molecules physically reducing the strength of the cell membrane, as described e.g. at extracellular localized porphyrins [333, 334];
(2) generation of sonosensitizer derived peroxyl, alkoxyl and/or other free radicals resulting in peroxidation of membrane lipids chains or similar radical damage of cells [335];
(3) the sonosensitizer attributed physical destabilization of the cell membrane rendering the cell more susceptible to shear forces or ultrasound enhanced drug transport across the cell membrane (sonoporation) [336];
(4) singlet oxygen formation as a result of sonoluminiscence caused by the ultrasound in tissue, which was observed e.g. at hematoporphyrin [337, 338], porfimer [339, 340], gallium-porphyrin complex [341], pheophorbide a [342], rose bengal [343], and some other compounds.

The mechanism of mutual potentiation of PDT and SDT when used in combination can be attributed to a combination of different mechanisms of action and also to the ability of the ultrasound to monomerize aggregated photosensitizers [344].

Until now, various types of compounds have been tested in combination with ultrasound in order to find possible increased toxicity of the combined treatment unlike of the sole components. We would like to concentrate more on the compounds possessing both the photo- and sonosensitizing activities, while the “pure” sonosensitizers we mention only marginally, since their mechanisms of action usually does not include photodynamic components. Among sonosensitizing compounds without photodynamic activity or with potential of singlet oxygen formation, but not absorbing in the “phototerapeutic window” belong some alkylating anticancer drugs [345-347], anthracycline anticancer antibiotics, especially to adriamycin or its derivatives [348-352], oxicam-type non-steroidal anti-inflammatory drugs piroxicam and tenoxicam [353, 354] and some azo-dyes [355, 356].

Unlike the alkylating agents and anthracyclines the *porphyrins* are non-toxic when administered without additional treatment. The combined use of the hematoporphyrin and ultrasound was tested in several studies. In most of the cases, the enhanced cell killing was observed. The results of the studies suggest that the cell damage enhancement is probably mediated *via* singlet oxygen generated by ultrasonically activated hematoporphyrin [357-360].

On the other hand, no significant ultrasound mediated cytotoxicity of hematoporphyrin was observed in the cases when extracellular fraction of the sensitizer was removed or missing [333, 334]. Therefore it seems to be probable that only the extracellular porphyrin sensitizer participates in the ultrasound-induced interactions. Similar findings were described also at some other porphyrins tested for their sonodynamic activity [332]. The sonodynamically induced antitumor effect was also confirmed at porfimer sodium against mammary tumor grow in rats [361], at protoporphyrin IX against sarcoma 180 cells grow [362, 363] and at Photofrin II in several various studies. The effect were dose dependent [339, 364-366]. Another porphyrin derivative tested for its sonodynamic activity is 7,12-bis(1-decyloxyethyl)-Ga(III)-3,8,13,17-tetramethylporphyrin-2,18-dipropionyl-diaspartic acid

(ATX-70). Similarly to Photofrin II, a dose dependent ultrasound mediated cytotoxicity was observed [333, 334, 367-369].

A *chlorin* derivative 4-formyloxymethylidene-3-hydroxy-2-vinyl-deuterioporphynyl (IX)-6,7-diaspartic acid (ATX-S10) was successfully tested on both cells and animal model for its sonodynamic activity, with more than two-fold increase of cytotoxicity after combined application compared to ultrasound alone [370]. Sonodynamically induced apoptosis, caspase-3 activation and nitroxide generation were observed after application of ultrasound in the presence of talaporfin on HL-60 cells [201]. Up to a twice enhanced sonodynamically induced antitumor effect of pheophorbide-a was observed both *in vitro* and *in vivo* on sarcoma 180 cells or tumors [342].

A second-generation photosensitizer, chloroaluminium *phthalocyanine* tetrasulfonate (Photosens) was subjected to activation by ultrasound 24 hr after intravenous application to mice bearing subcutaneously localized colon 26 carcinoma. The combined treatment showed significant effect, although total eradication of the tumor was not achieved [371]. Simple zinc and chloroaluminum phthalocyanines were effective as potential sonosensitizers as well [372].

The xanthene structure based photosensitizing compounds rose bengal and erythrosine B has been successfully tested for its sonosensitizing effectiveness on sarcoma 180 cells. The application of ultrasound increased the dye cytotoxicity up to three times and five times, respectively [343, 373].

CONCLUSION

PDT generally is a very effective treatment, almost without any developed resistance to drugs and perfectly targets the diseased tissues. The great advantage of PDT in targeting the chosen area is, at the same time, the major drawback. PDT is a localized therapy; it means you treat only what you see, the metastases disseminated through the whole body, unfortunately, are not treatable.

Since the times of Raab and von Tappeiner, the photodynamic therapy has come a long way. Scientists have uncovered the mechanisms of this procedure, developed several compounds accepted in clinical practice for treatment of various diseases and still are searching for more suitable photosensitizers. Similarly to development of every new group of drugs, the first accepted compound (porfimer, 1993, Canada) is of course not lacking side effects. However, the newest compounds seem to get very close to the “optimal” photosensitizer for therapy. Their photophysical, photochemical, and sometimes also pharmacokinetic properties were optimized for chosen treatments, although there is still a long way to go before they will be accepted in practice.

ACKNOWLEDGEMENT

The work was supported by Research Project MSM 002160822.

REFERENCES

[1] Ackroyd, R., Kelty, C., Brown, N. and Reed, M. (2001). The history of photodetection and photodynamic therapy. *Photochem. Photobiol., 74*, 656-669.

[2] Moan, J. and Peng, Q. (2003). An outline of the hundred-year history of PDT. *Anticancer Res., 23*, 3591-3600.

[3] Manniche, L.: Egyptian Luxuries: Fragrance, aromatherapy, and cosmetics in pharaonic times. Cairo: American University in Cairo Press; 1999.

[4] Shaat, M. and Shaat, N.: Ancient Egyptian cosmetics, toiletries and essentials oils. In: *IFSCC 23rd Congress: 2004*; Orlando, Florida; 2004: paper 7.

[5] Boulos, L.: Flora of Egypt. vol. 1 and 2: Egypt: Al Hadra Publishing; 2000.

[6] American Academy of Dermatology (1994). Guidelines of care for phototherapy and photochemotherapy. Practice management information. *J. Am. Acad. Dermatol., 31*, 643-648.

[7] Ledo, E. and Ledo, A. (2000). Phototherapy, photochemotherapy, and photodynamic therapy: Unapproved uses or indications. *Clin. Dermatol., 18*, 77-86.

[8] Fitzpatrick, T. B. and Pathak, M. A. (1959). Historical Aspects of Methoxsalen and Other Furocoumarins. *J. Invest. Dermatol., 32*, 229-231.

[9] Daniell, M. D. and Hill, J. S. (1991). A History of Photodynamic Therapy. *Aust. N. Z. J. Surg., 61*, 340-348.

[10] Parrish, J. A., Fitzpatrick, T. B., Tanenbau., L and Pathak, M. A. (1974). Photochemotherapy of Psoriasis with Oral Methoxsalen and Longwave Ultraviolet-Light. *N. Engl. J. Med., 291*, 1207-1211.

[11] Scherer, H. (1841). Chemisch-physiologische untersuchungen. *Ann. Chem. Pharm., 40*, 1.

[12] Thudichum, J. L. W.: Report on researches intended to promote an improved chemical identification of disease.London: HMSO; 1867; 152-233.

[13] Hoppe-Seyler, F. (1871). The haematins. *Tubinger Med. Chem. Untersuchungen, 4*, 523-533.

[14] Finsen, N.: Phototherapy. London: Arnold; 1901.

[15] Raab, O. (1900). Uber die Wirkung fluoreszierender Stoffe auf Infusorien. *Z. Biol., 39*, 524-546.

[16] Prime, J.: Les accidentes toxiques par l'eosinate de sodium. Paris: Jouve and Boyer; 1900.

[17] von Tappeiner, H. and Jesionek, A. (1903). Therapeutische Versuche mit fluoreszierenden Stoffen. *Münch. Med. Wochenschr., 47*, 2042-2044.

[18] von Trappeiner, H. and Jodlbauer, A. (1904). Uber Wirkung der photodynamischen (fluorieszierenden) Stoffe auf Protozan und Enzyme. *Dtsch. Arch. Klin. Med., 80*, 427-487.

[19] von Tappeiner, H. and Jodlbauer, A.: Die Sensibilisierende Wirkung fluorieszierender Substanzer. Gesammte Untersuchungen uber die photodynamische Erscheinung. Leipzig: F. C. W. Vogel; 1907.

[20] Hausmann, W. (1908). Uber die sensibilisierende Wirkung tiericher Farbstoffe und ihre physiologische Bedeutung. *Biochem. Z., 14*, 275-278.

[21] Hausmann, W. (1911). The sensitizing action of haematoporphyrin. *Biochem. Z.*, *30*, 276-316.

[22] Fisher, H. and Meyer-Betz, F. (1912). Formation of porphyrins. *Z. Physiol. Chem.*, *82*, 96-108.

[23] Meyer-Betz, F. (1913). Untersuchungen uber die Biologische (photodynamische) Wirkung des Haematoporphyrins und anderer Derivative des Blut- und Galenfarbstoffs. *Dtsch. Arch. Klin. Med. 112*, 476-503.

[24] Policard, A. (1924). Etudes sur les aspects offerts par des tumeurs experimentales examinee a la lumiere de Woods. *Compt. Rend. Soc. Biol.*, *91*, 1423-1424.

[25] Figge, F. H. J., Weiland, G. S. and Mangeniello, L. O. J. (1948). Affinity of neoplastic, embryonic and traumatized regenerating tissue for porphyrins and metalloporphyrins. *Proc. Soc. Exp. Biol. Med..*, *68*, 143-146.

[26] Rasmussen-Taxdal, D.S., Ward, G. E. and Figge, F. H. (1954). Fluorescence of human lymphatic and cancer tissues following high doses of intravenous hematoporphyrin. *Surg. Forum*, *5*, 619-624.

[27] Lipson, R. L., Baldes, E. J. and Olsen, A. M. (1961). Use of a Derivative of Hematoporphyrin in Tumor Detection. *J. Natl. Cancer Inst.*, *26*, 1-11.

[28] Lipson, R. L., Baldes, E. J. and Olsen, A. M. (1964). Further Evaluation of the Use of Hematoporphyrin Derivative as a New Aid for the Endoscopic Detection of Malignant Disease. *Dis. Chest*, *46*, 676-679.

[29] Gray, M. J., Lipson, R., Maeck, J. V., Parker, L. and Romeyn, D. (1967). Use of Hematoporphyrin Derivative in Detection and Management of Cervical Cancer - a Preliminary Report. *Am. J. Obstet. Gynecol.*, *99*, 766-771.

[30] Weishaupt, K.R., Gomer, C. J.and Dougherty, T. J. (1976). Identification of singlet oxygen as the cytotoxic agent in photoinactivation of a murine tumor *Cancer Res*, *36*, 2326-2329.

[31] Dougherty, T. J., Kaufman, J. E., Goldfarb, A., Weishaupt, K. R., Boyle, D. and Mittleman, A. (1978). Photoradiation Therapy for Treatment of Malignant-Tumors. *Cancer Res.*, *38*, 2628-2635.

[32] Hayata, Y., Konaka, C., Takizawa, N. and Kato, H. (1982). Hematoporphyrin Derivative and Laser Photoradiation in the Treatment of Lung-Cancer. *Chest*, *81*, 269-277.

[33] McCaughan, J. S., Hicks, W., Laufman, L., May, E. and Roach, R. (1984). Palliation of Esophageal Malignancy with Photoradiation Therapy. *Cancer*, *54*, 2905-2910.

[34] Barr, H., Krasner, N., Boulos, P. B., Chatlani, P. and Bown, S. G. (1990). Photodynamic Therapy for Colorectal-Cancer - a Quantitative Pilot-Study. *Br. J. Surg.*, *77*, 93-96.

[35] Kaye, A. H., Morstyn, G. and Brownbill, D. (1987). Adjuvant High-Dose Photoradiation Therapy in the Treatment of Cerebral Glioma - a Phase 1-2 Study. *J. Neurosurg.*, *67*, 500-505.

[36] Laws, E. R., Cortese, D. A., Kinsey, J. H., Eagan, R. T. and Anderson, R. E. (1981). Photoradiation Therapy in the Treatment of Malignant Brain-Tumors - a Phase-I (Feasibility) Study. *Neurosurgery*, *9*, 672-678.

[37] Fritsch, C., Lang, K., Neuse, W., Ruzicka, T. and Lehmann, P. (1998). Photodynamic diagnosis and therapy in dermatology. *Skin Pharmacol. Appl. Skin Physiol.*, *11*, 358-373.

[38] Jichlinski, P., Guillou, L., Karlsen, S. J., Malmstrom, P. U., Jocham, D., Brennhovd, B., Johansson, E., Gartner, T., Lange, N., van den Bergh, H. *et al* (2003). Hexyl aminolevulinate fluorescence cystoscopy: A new diagnostic tool for the photodiagnosis of superficial bladder cancer - A multicenter study. *J. Urol., 170*, 226-229.

[39] Pal, P., Zeng, H., Durocher, G., Girard, D., Li, T., Gupta, A. K., Giasson, R., Blanchard, L., Gaboury, L., Balassy, A. *et al* (1996). Phototoxicity of Some Bromine-Substituted Rhodamine Dyes: Synthesis, Photophysical Properties and Application as Photosensitizers. *Photochem. Photobiol., 63*, 161-168.

[40] Soncin, M., Busetti, A., Fusi, F., Jori, G. and Rodgers, M. A. J. (1999). Irradiation of Amelanotic Melanoma Cells with 532 nm High Peak Power Pulsed Laser Radiation in the Presence of the Photothermal Sensitizer Cu(II)-Hematoporphyrin: A New Approach to Cell Photoinactivation. *Photochem. Photobiol., 69*, 708-712.

[41] Lang, K., Mosinger, J. and Wagnerová, D. M. (2004). Photophysical properties of porphyrinoid sensitizers non-covalently bound to host molecules; models for photodynamic therapy. *Coord. Chem. Rev., 248*, 321-350.

[42] MacDonald, I. J. and Dougherty, T. J. (2001). Basic principles of photodynamic therapy. *J. Porphyr. Phthalocyanines, 5*, 105-129.

[43] Egorov, S. Y., Kamalov, V. F., Koroteev, N. I., Krasnovsky, A. A., Toleutaev, B. N. and Zinukov, S. V. (1989). Rise and Decay Kinetics of Photosensitized Singlet Oxygen Luminescence in Water - Measurements with Nanosecond Time-Correlated Single Photon-Counting Technique. *Chem. Phys. Lett., 163*, 421-424.

[44] Rodgers, M. A. J. (1983). Solvent-Induced Deactivation of Singlet Oxygen - Additivity Relationships in Non-Aromatic Solvents. *J. Am. Chem. Soc., 105*, 6201-6205.

[45] Baker, A. and Kanofsky, J. R. (1992). Quenching of Singlet Oxygen by Biomolecules from L1210 Leukemia-Cells. *Photochemistry and Photobiology, 55*, 523-528.

[46] Hatz, S., Lambert, J. D. C. and Ogilby, P. R. (2007). Measuring the lifetime of singlet oxygen in a single cell: addressing the issue of cell viability. *Photochem. Photobiol. Sci., 6*, 1106-1116.

[47] Henderson, B. W. and Dougherty, T. J. (1992). How Does Photodynamic Therapy Work. *Photochem. Photobiol., 55*, 145-157.

[48] Moan, J. and Boye, E. (1981). Photodynamic Effect on DNA and Cell-Survival of Human-Cells Sensitized by Hematoporphyrin. *Photobiochem. Photobiophys., 2*, 301-307.

[49] Lee, P. C. C. and Rodgers, M. A. J. (1987). Laser Flash Photokinetic Studies of Rose-Bengal Sensitized Photodynamic Interactions of Nucleotides and DNA. *Photochem. Photobiol., 45*, 79-86.

[50] Henderson, B. W. and Fingar, V. H. (1987). Relationship of Tumor Hypoxia and Response to Photodynamic Treatment in an Experimental Mouse-Tumor. *Cancer Res., 47*, 3110-3114.

[51] Sitnik, T. M., Hampton, J. A. and Henderson, B. W. (1998). Reduction of tumour oxygenation during and after photodynamic therapy in vivo: effects of fluence rate. *Br. J. Cancer, 77*, 1386-1394.

[52] Berg, K. and Moan, J. (1994). Lysosomes as Photochemical Targets. *International Journal of Cancer, 59*, 814-822.

[53] Lo, P. C., Chan, C. M. H., Liu, J. Y., Fong, W. P. and Ng, D. K. P. (2007). Highly photocytotoxic glucosylated silicon(IV) phthalocyanines. Effects of peripheral chloro

substitution on the photophysical and photodynamic properties. *J. Med. Chem.*, *50*, 2100-2107.

[54] Sibrian-Vazquez, M., Ortiz, J., Nesterova, I. V., Fernandez-Lazaro, F., Sastre-Santos, A., Soper, S. A. and Vicente, M. G. H. (2007). Synthesis and properties of cell-targeted Zn(II)-phthalocyanine-peptide conjugates. *Bioconjugate Chem.*, *18*, 410-420.

[55] Dummin, H., Cernay, T. and Zimmermann, H. W. (1997). Selective photosensitization of mitochondria in HeLa cells by cationic Zn(II) phthalocyanines with lipophilic side-chains. *J. Photochem. Photobiol. B-Biol.*, *37*, 219-229.

[56] Trivedi, N. S., Wang, H. W., Nieminen, A. L., Oleinick, N. L. and Izatt, J. A. (2000). Quantitative analysis of Pc 4 localization in mouse lymphoma (LY-R) cells via double-label confocal fluorescence microscopy. *Photochem. Photobiol.*, *71*, 634-639.

[57] Kessel, D. and Reiners, J. J. (2007). Apoptosis and autophagy after mitochondrial or endoplasmic reticulum photodamage. *Photochem. Photobiol.*, *83*, 1024-1028.

[58] Teiten, M. H., Bezdetnaya, L., Morliere, P., Santus, R. and Guillemin, F. (2003). Endoplasmic reticulum and Golgi apparatus are the preferential sites of Foscan(R) localisation in cultured tumour cells. *Br. J. Cancer*, *88*, 146-152.

[59] Marchal, S., Francois, A., Dumas, D., Guillemin, F. and Bezdetnaya, L. (2007). Relationship between subcellular localisation of Foscan (R) and caspase activation in photosensitised MCF-7 cells. *Br. J. Cancer*, *96*, 944-951.

[60] Aveline, B. M. and Redmond, R. W. (1999). Can Cellular Phototoxicity be Accurately Predicted on the Basis of Sensitizer Photophysics? *Photochem. Photobiol.*, *69*, 306-316.

[61] Hsieh, Y. J., Wu, C. C., Chang, C. J. and Yu, J. S. (2003). Subcellular localization of Photofrin (R) determines the death phenotype of human epidermoid carcinoma A431 cells triggered by photodynamic therapy: When plasma membranes are the main targets. *J. Cell. Physiol.*, *194*, 363-375.

[62] Nilsson, R., Swanbeck, G. and Wennersten, G. (1975). Primary Mechanisms of Erythrocyte Photolysis Induced by Biological Sensitizers and Phototoxic Drugs. *Photochem. Photobiol.*, *22*, 183-186.

[63] Sun, X. and Leung, W. N. (2002). Photodynamic therapy with pyropheophorbide-a methyl ester in human lung carcinoma cancer cell: Efficacy, localization and apoptosis. *Photochem. Photobiol.*, *75*, 644-651.

[64] Berg, K., Madslien, K., Bommer, J. C., Oftebro, R., Winkelman, J. W. and Moan, J. (1991). Light-Induced Relocalization of Sulfonated Meso-Tetraphenylporphines in Nhik 3025 Cells and Effects of Dose Fractionation. *Photochem. Photobiol.*, *53*, 203-210.

[65] Moan, J., Berg, K., Anholt, H. and Madslien, K. (1994). Sulfonated Aluminum Phthalocyanines as Sensitizers for Photochemotherapy - Effects of Small Light Doses on Localization, Dye Fluorescence and Photosensitivity in V79 Cells. *Int. J. Cancer*, *58*, 865-870.

[66] Melnikova, V. O., Bezdetnaya, L. N., Bour, C., Festor, E., Gramain, M. P., Merlin, J. L., Potapenko, A. Y. and Guillemin, F. (1999). Subcellular localization of meta-tetra(hydroxyphenyl) chlorin in human tumor cells subjected to photodynamic treatment. *J. Photochem. Photobiol. B-Biol.*, *49*, 96-103.

[67] Chen, J. Y., Mak, N. K., Wen, J. M., Leung, W. N., Chen, S. C., Fung, M. C. and Cheung, N. H. (1998). A comparison of the photodynamic effects of temoporfin

(mTHPC) and MC540 on leukemia cells: Efficacy and apoptosis. *Photochem. Photobiol., 68*, 545-554.

[68] Castano, A. P., Demidova, T. N. and Hamblin, M. R. (2004). Mechanisms in photodynamic therapy: part one--photosensitizers, photochemistry and cellular localization. *Photodiagn. Photodyn. Ther., 1*, 279-293.

[69] Rashid, F. and Horobin, R. W. (1990). Interaction of Molecular Probes with Living Cells and Tissues .2. a Structure-Activity Analysis of Mitochondrial Staining by Cationic Probes, and a Discussion of the Synergistic Nature of Image-Based and Biochemical Approaches. *Histochemistry*, *94*, 303-308.

[70] Woodburn, K. W., Vardaxis, N. J., Hill, J. S., Kaye, A. H. and Phillips, D. R. (1991). Subcellular-Localization of Porphyrins Using Confocal Laser Scanning Microscopy. *Photochem. Photobiol.*, *54*, 725-732.

[71] Hilf, R., Warne, N. W., Smail, D. B. and Gibson, S. L. (1984). Photodynamic inactivation of selected intracellular enzymes by hematoporphyrin derivative and their relationship to tumor cell viability in vitro. *Cancer Lett., 24*, 165-172.

[72] Castano, A. P., Demidova, T. N. and Hamblin, M. R. (2005). Mechanisms in photodynamic therapy: part two--cellular signaling, cell metabolism and modes of cell death. *Photodiagn. Photodyn. Ther., 2*, 1-23.

[73] Hilf, R. (2007). Mitochondria are targets of photodynamic therapy. *J. Bioenerg. Biomembr., 39*, 85-89.

[74] Fingar, V. H., Wieman, T. J., Karavolos, P. S., Doak, K. W., Ouellet, R. and Vanlier, J. E. (1993). The Effects of Photodynamic Therapy Using Differently Substituted Zinc Phthalocyanines on Vessel Constriction, Vessel Leakage and Tumor Response. *Photochem. Photobiol., 58*, 251-258.

[75] Fingar, V. H., Wieman, T. J. and Haydon, P. S. (1997). The effects of thrombocytopenia on vessel stasis and macromolecular leakage after photodynamic therapy using photofrin. *Photochem. Photobiol., 66*, 513-517.

[76] Fingar, V. H., Wieman, T. J., Wiehle, S. A. and Cerrito, P. B. (1992). The Role of Microvascular Damage in Photodynamic Therapy - the Effect of Treatment on Vessel Constriction, Permeability, and Leukocyte Adhesion. *Cancer Res., 52*, 4914-4921.

[77] McMahon, K. S., Wieman, T. J., Moore, P. H. and Fingar, V. H. (1994). Effects of Photodynamic Therapy Using Mono-L-Aspartyl Chlorin E(6) on Vessel Constriction, Vessel Leakage, and Tumor Response. *Cancer Res., 54*, 5374-5379.

[78] Fingar, V. H., Wieman, T. J. and Doak, K. W. (1990). Role of Thromboxane and Prostacyclin Release on Photodynamic Therapy-Induced Tumor Destruction. *Cancer Res., 50*, 2599-2603.

[79] Dolmans, D., Kadambi, A., Hill, J. S., Waters, C. A., Robinson, B. C., Walker, J. P., Fukumura, D. and Jain, R. K. (2002). Vascular accumulation of a novel photosensitizer, MV6401, causes selective thrombosis in tumor vessels after photodynamic therapy. *Cancer Res., 62*, 2151-2156.

[80] Brown, S. B. and Mellish, K. J. (2001). Verteporfin: a milestone in opthalmology and photodynamic therapy. *Expert Opin. Pharmacother., 2*, 351-361.

[81] Chen, B., Pogue, B. W., Hoopes, P. J. and Hasan, T. (2005). Combining vascular and cellular targeting regimens enhances the efficacy of photodynamic therapy. *Int. J. Radiat. Oncol. Biol. Phys., 61*, 1216-1226.

[82] Chen, B., Pogue, B. W., Luna, J. M., Hardman, R. L., Hoopes, P. J. and Hasan, T. (2006). Tumor vascular permeabilization by vascular-targeting photosensitization: Effects, mechanism, and therapeutic implications. *Clin. Cancer Res., 12*, 917-923.

[83] Webber, J., Leeson, B., Fromm, D. and Kessel, D. (2005). Effects of photodynamic therapy using a fractionated dosing of mono-L-aspartyl chlorin e6 in a murine tumor. *J. Photochem. Photobiol. B-Biol., 78*, 135-140.

[84] Trachtenberg, J., Bogaards, A., Weersink, R. A., Haider, M. A., Evans, A., McCluskey, S. A., Scherz, A., Gertner, M. R., Yue, C., Appu, S. *et al* (2007). Vascular targeted photodynamic therapy with palladium-bacteriopheophorbide photosensitizer for recurrent prostate cancer following definitive radiation therapy: Assessment of safety and treatment response. *J. Urol., 178*, 1974-1979.

[85] Korbelik, M., Krosl, G., Krosl, J. and Dougherty, G. J. (1996). The role of host lymphoid populations in the response of mouse EMT6 tumor to photodynamic therapy. *Cancer Res., 56*, 5647-5652.

[86] Korbelik, M. (1996). Induction of tumor immunity by photodynamic therapy. *J. Clin. Laser Med. Surg., 14*, 329-334.

[87] Castano, A. P., Demidova, T. N. and Hamblin, M. R. (2005). Mechanisms in photodynamic therapy: Part three--Photosensitizer pharmacokinetics, biodistribution, tumor localization and modes of tumor destruction. *Photodiagn. Photodyn. Ther., 2*, 91-106.

[88] Krosl, G. and Korbelik, M. (1994). Potentiation of photodynamic therapy by immunotherapy: the effect of schizophyllan (SPG). *Cancer Lett., 84*, 43-49.

[89] Gollnick, S. O., Vaughan, L. and Henderson, B. W. (2002). Generation of effective antitumor vaccines using photodynamic therapy. *Cancer Res., 62*, 1604-1608.

[90] Sasaki, S. and Tamiaki, H. (2006). Synthesis and optical properties of bacteriochlorophyll-a derivatives having various C3 substituents on the bacteriochlorin pi-system. *J. Org. Chem., 71*, 2648-2654.

[91] Sternberg, E. D., Dolphin, D. and Bruckner, C. (1998). Porphyrin-based photosensitizers for use in photodynamic therapy. *Tetrahedron, 54*, 4151-4202.

[92] Labbe, R. F. and Nishida, G. (1957). A new method of hemin isolation. *Biochim. Biophys. Acta, 26*, 437.

[93] Bonnett, R. (1995). Photosensitizers of the Porphyrin and Phthalocyanine Series for Photodynamic Therapy. *Chem. Soc. Rev., 24*, 19-33.

[94] Huang, Z. (2006). Photodynamic therapy in China: Over 25 years of unique clinical experience: Part One--History and domestic photosensitizers. *Photodiagn. Photodyn. Ther., 3*, 3-10.

[95] Anti cancer drug: PDT therapy against cancer growth tumor [online]. 2008 [cited 2008-02-18]. Available from: www.photogem.ru.

[96] Triesscheijn, M., Baas, P., Schellens, J. H. M. and Stewart, F. A. (2006). Photodynamic Therapy in Oncology. *Oncologist, 11*, 1034-1044.

[97] ClinicalTrials.gov [online]. 2008 [cited 2008-02-07]. Available from: www.clinicaltrials.gov.

[98] Schweitzer, V. G. (2001). PHOTOFRIN-mediated photodynamic therapy for treatment of early stage oral cavity and laryngeal malignancies. *Lasers Surg. Med., 29*, 305-313.

[99] Muller, P. J. and Wilson, B. C. (2006). Photodynamic therapy of brain tumors - A work in progress. *Lasers Surg. Med., 38*, 384-389.

[100] Madsen, S. J. and Hirschberg, H. (2006). Photodynamic therapy and detection of high-grade gliomas. *J. Environ. Pathol. Toxicol. Oncol., 25*, 453-465.

[101] Wolfsen, H. C. (2005). Uses of photodynamic therapy in premalignant and malignant lesions of the gastrointestinal tract beyond the esophagus. *J. Clin. Gastroenterol., 39*, 653-664.

[102] Wiedmann, M., Berr, F., Schiefke, I., Witzigmann, H., Kohlhaw, K., Mossner, J. and Caca, K. (2004). Photodynamic therapy in patients with non-resectable hilar cholangiocarcinoma: 5-year follow-up of a prospective phase II study. *Gastrointest. Endosc., 60*, 68-75.

[103] Huang, Z. (2006). Photodynamic therapy in China: Over 25 years of unique clinical experience: Part two-Clinical experience. *Photodiagn. Photodyn. Ther., 3*, 71-84.

[104] Martin, D.: Porphyrins. In: Martin D., Mayes, P. and Rodwel, V. editors. *Harper´s Review of Biochemistry*. Los Altos, CA: Lange Medical Publications; 1983: pp. 317-333.

[105] Albert, A. (1958). Chemical Aspects of Selective Toxicity. *Nature, 182*, 421-423.

[106] Peng, Q., Warloe, T., Berg, K., Moan, J., Kongshaug, M., Giercksky, K. E. and Nesland, J. M. (1997). 5-aminolevulinic acid-based photodynamic therapy - Clinical research and future challenges. *Cancer, 79*, 2282-2308.

[107] Peng, Q., Berg, K., Moan, J., Kongshaug, M. and Nesland, J. M. (1997). 5-aminolevulinic acid-based photodynamic therapy: Principles and experimental research. *Photochem. Photobiol., 65*, 235-251.

[108] Redmond, R. W. and Gamlin, J. N. (1999). A compilation of singlet oxygen yields from biologically relevant molecules. *Photochem. Photobiol., 70*, 391-475.

[109] Malik, Z. and Lugaci, H. (1987). Destruction of Erythroleukemic Cells by Photoactivation of Endogenous Porphyrins. *Br. J. Cancer, 56*, 589-595.

[110] Peng, Q., Evensen, J. F., Rimington, C. and Moan, J. (1987). A Comparison of Different Photosensitizing Dyes with Respect to Uptake C3h-Tumors and Tissues of Mice. *Cancer Lett., 36*, 1-10.

[111] Moan, J., Peng, Q., Evensen, J. F., Berg, K., Western, A. and Rimington, C. (1987). Photosensitizing Efficiencies, Tumor-Uptake and Cellular-Uptake of Different Photosensitizing Drugs Relevant for Photodynamic Therapy of Cancer. *Photochem. Photobiol., 46*, 713-721.

[112] Sandberg, S. and Romslo, I. (1980). Porphyrin-Sensitized Photodynamic Damage of Isolated Rat-Liver Mitochondria. *Biochim. Biophys. Acta, 593*, 187-195.

[113] Sandberg, S. and Romslo, I. (1981). Porphyrin-Induced Photodamage at the Cellular and the Subcellular Level as Related to the Solubility of the Porphyrin. *Clin. Chim. Acta, 109*, 193-201.

[114] Sandberg, S., Romslo, I., Hovding, G. and Bjorndal, T. (1982). Porphyrin-Induced Photodamage as Related to the Sub-Cellular Localization of the Porphyrins. *Acta Derm.-Venereol.*, 75-80.

[115] Kennedy, J. C., Pottier, R. H. and Pross, D. C. (1990). Photodynamic Therapy with Endogenous Protoporphyrin .9. Basic Principles and Present Clinical-Experience. *J. Photochem. Photobiol. B-Biol., 6*, 143-148.

[116] Kennedy, J. C. and Pottier, R. H. (1992). Endogenous Protoporphyrin-Ix, a Clinically Useful Photosensitizer for Photodynamic Therapy. *J. Photochem. Photobiol. B-Biol., 14*, 275-292.

[117] Babilas, P., Landthaler, M. and Szeimies, R. M. (2006). Photodynamic therapy in dermatology. *Eur. J. Dermatol.*, *16*, 340-348.

[118] Ettler, K. (2004). Our Clinical Experience with the Use of Photodynamic Therapy in Patients with the Basal Cell Carcinoma and Morbus Bowen (Comparison of Efficacy of Two Photosensitizers). *Cesk. Dermatol.*, *70*, 200-204.

[119] Calzavara-Pinton, P. G., Venturini, M. and Sala, R. (2005). A comprehensive overview of photodynamic therapy in the treatment of superficial fungal infections of the skin. *J. Photochem. Photobiol. B-Biol.*, *78*, 1-6.

[120] Ettler, K. (2006). Photodynamic Therapy Used in Dermatology - Further Method Development. *Cas. Lek. Cesk.*, *145*, 184-187.

[121] Hwang, E. J., Chang, S. H., Kim, B. S. and Cho, M. K. (2008). Treatment of acne vulgaris by photodynamic therapy with aminolevulinic acid: Clinical and histopathologic findings. *J. Am. Acad. Dermatol.*, *58*, AB17-AB17.

[122] Wiegell, S. R. and Wulf, H. C. (2006). Photodynamic therapy of acne vulgaris using 5-aminolevulinic acid versus methyl aminolevulinate. *J. Am. Acad. Dermatol.*, *54*, 647-651.

[123] Niwa, A. B. M., Godoi, L., Torezan, L. and Osorio, N. (2008). Photodynamic therapy for facial acne vulgaris using methyl aminolaevutinate: Six month follow up. *J. Am. Acad. Dermatol.*, *58*, Suppl. 2, AB141-AB141.

[124] Stringer, M. R., Collins, P., Robinson, D. J., Stables, G. I. and SheehanDare, R. A. (1996). The accumulation of protoporphyrin IX in plaque psoriasis after topical application of 5-aminolevulinic acid indicates a potential for superficial photodynamic therapy. *J. Invest. Dermatol.*, *107*, 76-81.

[125] Collins, P., Robinson, D. J., Stringer, M. R., Stables, G. I. and SheehanDare, R. A. (1997). The variable response of plaque psoriasis after a single treatment with topical 5-aminolaevulinic acid photodynamic therapy. *Br. J. Dermatol.*, *137*, 743-749.

[126] Fabbrocini, G., Di Costanzo, M. P., Riccardo, A. M., Quarto, M., Colasanti, A., Roberti, G. and Monfrecola, G. (2001). Photodynamic therapy with topical delta-aminolaevulinic acid for the treatment of plantar warts. *J. Photochem. Photobiol. B-Biol.*, *61*, 30-34.

[127] Smetana, Z., Malik, Z., Orenstein, A., Mendelson, E. and BenHur, E. (1997). Treatment of viral infections with 5-aminolevulinic acid and light. *Lasers Surg. Med.*, *21*, 351-358.

[128] Wainwright, M. (2003). Local treatment of viral disease using photodynamic therapy. *Int. J. Antimicrob. Agents*, *21*, 510-520.

[129] Webber, J., Kessel, D. and Fromm, D. (1997). Plasma levels of protoporphyrin IX in humans after oral administration of 5-aminolevulinic acid. *J. Photochem. Photobiol. B-Biol.*, *37*, 151-153.

[130] Leibovici, L., Schoenfeld, N., Yehoshua, H. A., Mamet, R., Rakowsky, E., Shindel, A. and Atsmon, A. (1988). Activity of Porphobilinogen Deaminase in Peripheral-Blood Mononuclear-Cells of Patients with Metastatic Cancer. *Cancer*, *62*, 2297-2300.

[131] Schoenfeld, N., Epstein, O., Lahav, M., Mamet, R., Shaklai, M. and Atsmon, A. (1988). The Heme Biosynthetic-Pathway in Lymphocytes of Patients with Malignant Lymphoproliferative Disorders. *Cancer Lett.*, *43*, 43-48.

[132] Kondo, M., Hirota, N., Takaoka, T. and Kajiwara, M. (1993). Heme-Biosynthetic Enzyme-Activities and Porphyrin Accumulation in Normal Liver and Hepatoma-Cell Lines of Rat. *Cell Biol. Toxicol.*, *9*, 95-105.

[133] Dailey, H. A. and Smith, A. (1984). Differential Interaction of Porphyrins Used in Photoradiation Therapy with Ferrochelatase. *Biochem. J.*, *223*, 441-445.

[134] Vanhillegersberg, R., Vandenberg, J. W. O., Kort, W. J., Terpstra, O. T. and Wilson, J. H. P. (1992). Selective Accumulation of Endogenously Produced Porphyrins in a Liver Metastasis Model in Rats. *Gastroenterology*, *103*, 647-651.

[135] Fukuda, H., Casas, A. and Batlle, A. (2006). Use of ALA and ALA derivatives for optimizing ALA-based photodynamic therapy: A review of our experience. *J. Environ. Pathol. Toxicol. Oncol.*, *25*, 127-143.

[136] Tunstall, R. G., Barnett, A. A., Schofield, J., Griffiths, J., Vernon, D. I., Brown, S. B. and Roberts, D. J. H. (2002). Porphyrin accumulation induced by 5-aminolaevulinic acid esters in tumour cells growing in vitro and in vivo. *Br. J. Cancer*, *87*, 246-250.

[137] Lopez, R. F. V., Lange, N., Guy, R. and Bentley, M. (2004). Photodynamic therapy of skin cancer: controlled drug delivery of 5-ALA and its esters. *Adv. Drug Deliv. Rev.*, *56*, 77-94.

[138] Alasensum [online]. 2008 [cited 10-04-2008]. Available from: http://www.niopik.ru/products/medicine/alasense/#.

[139] Kloek, J. and vanHenegouwen, G. (1996). Prodrugs of 5-aminolevulinic acid for photodynamic therapy. *Photochem. Photobiol.*, *64*, 994-1000.

[140] Kaliszewski, M., Juzeniene, A., Juzenas, P., Kwasny, M., Kaminski, J., Dabrowski, Z., Golinski, J. and Moan, J. (2005). Formation of protoporphyrin IX from carboxylic- and amino-derivatives of 5-aminolevulinic acid. *Photodiagn. Photodyn. Ther.*, *2*, 129-134.

[141] Berger, Y., Greppi, A., Siri, O., Neier, R. and Juillerat-Jeanneret, L. (2000). Ethylene glycol and amino acid derivatives of 5-aminolevulinic acid as new photosensitizing precursors of protoporphyrin IX in cells. *J. Med. Chem.*, *43*, 4738-4746.

[142] Berger, Y., Ingrassia, L., Neier, R. and Juillerat-Jeanneret, L. (2003). Evaluation of dipeptide-derivatives of 5-aminolevulinic acid as precursors for photosensitizers in photodynamic therapy. *Bioorg. Med. Chem.*, *11*, 1343-1351.

[143] Ninomiya, Y., Itoh, Y., Tajima, S. and Ishibashi, A. (2001). In vitro and in vivo expression of protoporphyrin IX induced by lipophilic 5-aminolevulinic acid derivatives. *J. Dermatol. Sci.*, *27*, 114-120.

[144] Zenzen, V. and Zankl, H. (2003). Protoporphyrin IX-accumulation in human tumor cells following topical ALA- and h-ALA-application in vivo. *Cancer Lett.*, *202*, 35-42.

[145] Whitaker, C. J., Battah, S. H., Forsyth, M. J., Edwards, C., Boyle, R. W. and Matthews, E. K. (2000). Photosensitization of pancreatic tumour cells by delta-aminolaevulinic acid esters. *Anticancer Drug Des.*, *15*, 161-170.

[146] Uehlinger, P., Zellweger, M., Wagnieres, G., Juillerat-Jeanneret, L., van den Bergh, H. and Lange, N. (2000). 5-Aminolevulinic acid and its derivatives: physical chemical properties and protoporphyrin IX formation in cultured cells. *J. Photochem. Photobiol. B-Biol.*, *54*, 72-80.

[147] Brunner, H., Hausmann, F. and Knuechel, R. (2003). New 5-aminolevulinic acid esters - Efficient protoporphyrin precursors for photodetection and photodynamic therapy. *Photochem. Photobiol.*, *78*, 481-486.

[148] Di Venosa, G., Batlle, A., Fukuda, H., MacRobert, A. and Casas, A. (2006). Distribution of 5-aminolevulinic acid derivatives and induced porphyrin kinetics in mice tissues. *Cancer Chemother. Pharmacol.*, *58*, 478-486.

[149] Di Venosa, G., Fukuda, H., Batlle, A., MacRobert, A. and Casas, A. (2006). Photodynamic therapy: Regulation of porphyrin synthesis and hydrolysis from ALA esters. *J. Photochem. Photobiol. B-Biol.*, *83*, 129-136.

[150] Fotinos, N., Campo, M. A., Popowycz, F., Gurny, R. and Lange, N. (2006). 5-aminolevulinic acid derivatives in photomedicine: Characteristics, application and perspectives. *Photochem. Photobiol.*, *82*, 994-1015.

[151] Gaullier, J. M., Berg, K., Peng, Q., Anholt, H., Selbo, P. K., Ma, L. W. and Moan, J. (1997). Use of 5-aminolevulinic acid esters to improve photodynamic therapy on cells in culture. *Cancer Res.*, *57*, 1481-1486.

[152] Vena, F. C. B., Turchiello, R. F., Laville, I., Pigaglio, S., Blais, J. and Tedesco, A. C. (2004). 5-Aminolevulinic acid ester-induced protoporphyrin IX in a murine melanoma cell line. *Lasers Med. Sci.*, *19*, 119-126.

[153] Taylor, E. L., Vernon, D. I. and Brown, S. B.: Mechanism of protoporphyrin IX formation from ALA esters. In: *Program and Abstracts of the 9th Congress of European Society for Photobiology.* Aix-les-bains; 2005; 178.

[154] Di Venosa, G., Fukuda, H., Batlle, A., MacRobert, A. and Casas, A. (2006). Photodynamic therapy: Regulation of porphyrin synthesis and hydrolysis from ALA esters. *J. Photochem. Photobiol. B-Biol.*, *83*, 129-136.

[155] Moan, J., Ma, L. W. and Iani, V. (2001). On the pharmacokinetics of topically applied 5-aminolevulinic acid and two of its esters. *Int. J. Cancer*, *92*, 139-143.

[156] Perotti, C., Casas, A., Fukuda, H., Sacca, P. and Batlle, A. (2003). Topical application of ALA and ALA hexyl ester on a subcutaneous murine mammary adenocarcinoma: tissue distribution. *Br. J. Cancer*, *88*, 432-437.

[157] Casas, A., Perotti, C., Fukuda, H., Rogers, L., Butler, A. R. and Batlle, A. (2001). ALA and ALA hexyl ester-induced porphyrin synthesis in chemically induced skin tumours: the role of different vehicles on improving photosensitization. *Br. J. Cancer*, *85*, 1794-1800.

[158] Fritsch, C., Homey, B., Stahl, W., Lehmann, P., Ruzicka, T. and Sies, H. (1998). Preferential relative porphyrin enrichment in solar keratoses upon topical application of delta-aminolevulinic acid methylester. *Photochem. Photobiol.*, *68*, 218-221.

[159] Donnelly, R. F., McCarron, P. A. and Woolfson, A. D. (2005). Drug delivery of aminolevulinic acid from topical formulations intended for photodynamic therapy. *Photochem. Photobiol.*, *81*, 750-767.

[160] Rud, E., Gederaas, O., Hogset, A. and Berg, K. (2000). 5-aminolevulinic acid, but not 5-aminolevulinic acid esters, is transported into adenocarcinoma cells by system BETA transporters. *Photochem. Photobiol.*, *71*, 640-647.

[161] Doring, F., Walter, J., Will, J., Focking, M., Boll, M., Amasheh, S., Clauss, W. and Daniel, H. (1998). Delta-aminolevulinic acid transport by intestinal and renal peptide transporters and its physiological and clinical implications. *J. Clin. Invest.*, *101*, 2761-2767.

[162] Gederaas, O. A., Holroyd, A., Brown, S. B., Vernon, D., Moan, J. and Berg, K. (2001). 5-aminolaevulinic acid methyl ester transport on amino acid carriers in a human colon adenocarcinoma cell line. *Photochem. Photobiol.*, *73*, 164-169.

[163] I.J., K. and E., S. P. (1947). The pyrazines. *Chem. Rev.*, *40*, 290-358.
[164] Granick, S. and Mauzerall, D. (1958). Porphyrin Biosynthesis in Erythrocytes .2. Enzymes Converting Delta-Aminolevulinic Acid to Coproporphyrinogen. *J. Biol. Chem.*, *232*, 1119-1140.
[165] Butler, A. R. and George, S. (1992). The Nonenzymatic Cyclic Dimerization of 5-Aminolevulinic Acid. *Tetrahedron*, *48*, 7879-7886.
[166] Novo, M., Huttmann, G. and Diddens, H. (1996). Chemical instability of 5-aminolevulinic acid used in the fluorescence diagnosis of bladder tumours. *J. Photochem. Photobiol. B-Biol.*, *34*, 143-148.
[167] Bunke, A., Zerbe, O., Schmid, H., Burmeister, G., Merkle, H. P. and Gander, B. (2000). Degradation mechanism and stability of 5-aminolevulinic acid. *J. Pharm. Sci.*, *89*, 1335-1341.
[168] Dalton, J. T., Zhou, D. S., Mukherjee, A., Young, D., Tolley, E. A., Golub, A. L. and Meyer, M. C. (1999). Pharmacokinetics of aminolevulinic acid after intravesical administration to dogs. *Pharm. Res.*, *16*, 288-295.
[169] Visudyne.com [online]. 2008 [cited 2008-02-11]. Available from: www.visudyne.com.
[170] Wickens, J. and Blinder, K. J. (2006). A preliminary benefit-risk assessment of verteporfin in age-related macular degeneration. *Drug Saf.*, *29*, 189-199.
[171] Costa, R. A., Jorge, R., Calucci, D., Melo, L. A. S., Cardillo, J. A. and Scott, I. U. (2007). Intravitreal bevacizumab (Avastin) in combination with verteporfin photodynamic therapy for choroidal neovascularization associated with age-related macular degeneration (IBeVe Study). *Graefes Arch. Clin. Exp. Ophthalmol.*, *245*, 1273-1280.
[172] Donati, G. (2007). Emerging therapies for Neovascular age-related macular degeneration: State of the art. *Ophthalmologica*, *221*, 366-377.
[173] Lui, H., Hobbs, L., Tope, W. D., Lee, P. K., Elmets, C., Provost, N., Chan, A., Neyndorff, H., Su, X. Y., Jain, H. *et al* (2004). Photodynamic therapy of multiple nonmelanoma skin cancers with verteporfin and red light-emitting diodes - Two-year results evaluating tumor response and cosmetic outcomes. *Arch. Dermatol.*, *140*, 26-32.
[174] Mordon, S. (2007). Vascular-Targeted Photodynamic Therapy: a new technique for port wine stain treatment. *Ann. Dermatol. Venereol.*, *134*, 281-286.
[175] Boch, R., Canaan, A. J., Cho, A., Dolphin, D. D., Hong, L., Jain, A. K., North, J. R., Richter, A. M., Smits, C. and Sternberg, E. D. (2006). Cellular and antitumor activity of a new diethylene glycol benzoporphyrin derivative (lemuteporfin). *Photochem. Photobiol.*, *82*, 219-224.
[176] Boch, R. E., Sternberg, E., Dolphin, D., Levy, J. G., Richter, A. M., Hunt, D. W. C., Jain, A., Waterfield, E. M. and Tovey, A. N. (2002). Use of ethylene glycol esters of monohydrobenzoporphyrin derivatives as photoactive agents. European Patent EP1177795. Available also from: www.freepatentsonline.com.
[177] Ratkay, L. G., Waterfield, J. D. and Hunt, D. W. C. (2000). Photodynamic therapy in immune (non-oncological) disorders - Focus on benzoporphyrin derivatives. *Biodrugs*, *14*, 127-135.
[178] Jiang, H. J., Granville, D. J., North, J. R., Richter, A. M. and Hunt, D. W. C. (2002). Selective action of the photosensitizer QLT0074 on activated human T lymphocytes. *Photochem. Photobiol.*, *76*, 224-231.

[179] Perez-Marrero, R., Goldenberg, S. L., Shore, N., Benaim, E., Fay, R., Manyak, M. J. and Elhilali, M. (2005). A phase I/II dose-escalation study to assess the safety, tolerability, and preliminary efficacy of transurethral photodynamic therapy with lemuteporfin in men with lower urinary tract symptoms due to benign prostatic hyperplasia. *J. Urol.*, *173*, Suppl. S, 421-422.

[180] Xiao, Z. W., Dickey, D., Owen, R. J., Tulip, J. and Moore, R. (2007). Interstitial photodynamic therapy of the canine prostate using intra-arterial administration of photosensitizer and computerized pulsed light delivery. *J. Urol.*, *178*, 308-313.

[181] Berenbaum, M. C., Akande, S. L., Bonnett, R., Kaur, H., Ioannou, S., White, R. D. and Winfield, U. J. (1986). Meso-Tetra(Hydroxyphenyl)Porphyrins, a New Class of Potent Tumor Photosensitizers with Favorable Selectivity. *Br. J. Cancer*, *54*, 717-725.

[182] Berenbaum, M. C., Bonnett, R., Chevretton, E. B., Akandeadebakin, S. L. and Ruston, M. (1993). Selectivity of Meso-Tetra(Hydroxyphenyl)Porphyrins and Chlorins and of Photofrin-Ii in Causing Photodamage in Tumor, Skin, Muscle and Bladder - the Concept of Cost-Benefit in Analyzing the Results. *Lasers Med. Sci.*, *8*, 235-243.

[183] Kiesslich, T., Berlanda, J., Plaetzer, K., Krammer, B. and Berr, F. (2007). Comparative characterization of the efficiency and cellular pharmacokinetics of Foscan (R) and Foslip (R)-based photodynamic treatment in human biliary tract cancer cell lines. *Photochem. Photobiol. Sci.*, *6*, 619-627.

[184] Svensson, J., Johansson, A., Grafe, S., Gitter, B., Trebst, T., Bendsoe, N., Andersson-Engels, S. and Svanberg, K. (2007). Tumor selectivity at short times following systemic administration of a liposomal temoporfin formulation in a murine tumor model. *Photochem. Photobiol.*, *83*, 1211-1219.

[185] Biel, M. A. (2007). Photodynamic therapy treatment of early oral and laryngeal cancers. *Photochem. Photobiol.*, *83*, 1063-1068.

[186] Baas, P., Saarnak, A. E., Oppelaar, H., Neering, H. and Stewart, F. A. (2001). Photodynamic therapy with meta-tetrahydroxyphenylchlorin for basal cell carcinoma: a phase I/II study. *Br. J. Dermatol.*, *145*, 75-78.

[187] Triesscheijn, M., Ruevekamp, M., Antonini, N., Neering, H., Stewart, F. A. and Baas, P. (2006). Optimizing meso-tetra-hydroxyphenyl-chlorin-mediated photodynamic therapy for basal cell carcinoma. *Photochem. Photobiol.*, *82*, 1686-1690.

[188] Zimmermann, A., Ritsch-Marte, M. and Kostron, H. (2001). mTHPC-mediated photodynamic diagnosis of malignant brain tumors. *Photochem. Photobiol.*, *74*, 611-616.

[189] Moore, C. M., Nathan, T. R., Lees, W. R., Mosse, C. A., Freeman, A., Emberton, M. and Bown, S. G. (2006). Photodynamic therapy using meso tetra hydroxy phenyl chlorin (mTHPC) in early prostate cancer. *Lasers Surg. Med.*, *38*, 356-363.

[190] Nathan, T. R., Whitelaw, D. E., Chang, S. C., Lees, W. R., Ripley, P. M., Payne, H., Jones, L., Parkinson, M. C., Emberton, M., Gillams, A. R. *et al* (2002). Photodynamic therapy for prostate cancer recurrence after radiotherapy: a phase I study. *J. Urol.*, *168*, 1427-1432.

[191] Bommer, J. C. and Burnham, B. F. (1987). Tetrapyrrole therapeutic agents. United States Patent US4693885. Available also from: www.freepantentsonline.com.

[192] Gomi, S., Nishizuka, T., Ushiroda, O., Uchida, N., Takahashi, H. and Sumi, S. (1998). The structures of mono-L-aspartyl chlorin e6 and its related compounds. *Heterocycles*, *48*, 2231-2243.

[193] Hargus, J. A., Fronczek, F. R., Vicente, M. G. H. and Smith, K. M. (2007). Mono-(l)-aspartylchlorin-e6. *Photochem. Photobiol.*, *83*, 1006-1015.

[194] Saito, K., Mikuniya, N. and Aizawa, K. (2000). Effects of photodynamic therapy using mono-L-aspartyl chlorin e6 on vessels and its contribution to the antitumor effect. *Jpn. J. Cancer Res.*, *91*, 560-565.

[195] Chan, A. L., Juarez, M., Allen, R., Volz, W. and Albertson, T. (2005). Pharmacokinetics and clinical effects of mono-L-aspartyl chlorin e6 (NPe6) photodynamic therapy in adult patients with primary or secondary cancer of the skin and mucosal surfaces. *Photodermatol. Photoimmunol. Photomed.*, *21*, 72-78.

[196] Kessel, D. (1997). Pharmacokinetics of N-aspartyl chlorin e6 in cancer patients. *J. Photochem. Photobiol. B-Biol.*, *39*, 81-83.

[197] Kujund, M., zcaron, cacute, Rustemovi, T. J. V. D. S. N., cacute, Kati, R. A. H. M. R. M., ccaron, cacute and Wang, R. C. R. A. L. S. (2007). A Phase II safety and effect on time to tumor progression study of intratumoral light infusion technology using talaporfin sodium in patients with metastatic colorectal cancer. *J. Surg. Oncol.*, *96*, 518-524.

[198] Kato, H., Furukawa, K., Sato, M., Okunaka, T., Kusunoki, Y., Kawahara, M., Fukuoka, M., Miyazawa, T., Yana, T., Matsui, K. *et al* (2003). Phase II clinical study of photodynamic therapy using mono-L-aspartyl chlorin e6 and diode laser for early superficial squamous cell carcinoma of the lung. *Lung Cancer*, *42*, 103-111.

[199] Light Science Oncology, Inc. [online]. 2008 [cited 2008-02-13]. Available from: www.lightsciences.com.

[200] Taber, S. W., Fingar, V. H., Coots, C. T. and Wieman, T. J. (1998). Photodynamic therapy using mono-L-aspartyl chlorin e6 (Npe6) for the treatment of cutaneous disease: a Phase I clinical study. *Clin. Cancer Res.*, *4*, 2741-2746.

[201] Yumita, N., Han, Q. S., Kitazumi, I. and Umemura, S. (2008). Sonodynamically-induced apoptosis, necrosis, and active oxygen generation by mono-l-aspartyl chlorin e6. *Cancer Sci.*, *99*, 166-172.

[202] Morgan, A. R., Garbo, G. M., Keck, R. W. and Selman, S. H. (1988). New Photosensitizers for Photodynamic Therapy: Combined Effect of Metallopurpurin Derivatives and Light on Transplantable Bladder Tumors. *Cancer Res., 48,* 194-198.

[203] Morgan, A. R., Garbo, G. M., Keck, R. W., Eriksen, L. D. and Selman, S. H. (1990). Metallopurpurins and light: effect on transplantable rat bladder tumors and murine skin. *Photochem. Photobiol., 51,* 589-592.

[204] Mang, T. S., Allison, R., Hewson, G., Snider, W. and Moskowitz, R. (1998). A phase II/III clinical study of tin ethyl etiopurpurin (Purlytin)-induced photodynamic therapy for the treatment of recurrent cutaneous metastatic breast cancer. *Cancer J.*, *4*, 378-384.

[205] Kaplan, M. J., Somers, R. G., Greenberg, R. H. and Ackler, J. (1998). Photodynamic therapy in the management of metastatic cutaneous adenocarcinomas: Case reports from phase 1/2 studies using tin ethyl etiopurpurin (SnET2). *J. Surg. Oncol.*, *67*, 121-125.

[206] Selman, S. H., Albrecht, D., Keck, R. W., Brennan, P. and Kondo, S. (2001). Studies of tin ethyl etiopurpurin photodynamic therapy of the canine prostate. *J. Urol.*, *165*, 1795-1801.

[207] Chen, Y., Zheng, X., Dobhal, M. P., Gryshuk, A., Morgan, J., Dougherty, T. J., Oseroff, A. and Pandey, R. K. (2005). Methyl Pyropheophorbide-a Analogues:

Potential Fluorescent Probes for the Peripheral-Type Benzodiazepine Receptor. Effect of Central Metal in Photosensitizing Efficacy. *J. Med. Chem.*, *48*, 3692-3695.

[208] Dolmans, D. E. J. G. J., Kadambi, A., Hill, J. S., Flores, K. R., Gerber, J. N., Walker, J. P., Rinkes, I. H. M. B., Jain, R. K. and Fukumura, D. (2002). Targeting Tumor Vasculature and Cancer Cells in Orthotopic Breast Tumor by Fractionated Photosensitizer Dosing Photodynamic Therapy. *Cancer Res.*, *62*, 4289-4294.

[209] Ciulla, T. A., Criswell, M. H., Danis, R. P., Snyder, W. J. and Small, W. (2004). Evaluation of photopoint photosensitizer MV6401, indium chloride methyl pyropheophorbide, as a photodynamic therapy agent in primate choriocapillaris and laser-induced choroidal neovascularization. *Retin.-J. Retin. Vitr. Dis.*, *24*, 521-529.

[210] Ciulla, T. A., Criswell, M. H., Snyder, W. J. and Small, W. (2005). Photodynamic therapy with PhotoPoint photosensitiser MV6401, indium chloride methyl pyropheophorbide, achieves selective closure of rat corneal neovascularisation and rabbit choriocapillaris. *Br. J. Ophthalmol.*, *89*, 113-119.

[211] Pandey, R. K., Bellnier, D. A., Smith, K. M. and Dougherty, T. J. (1991). Chlorin and Porphyrin Derivatives as Potential Photosensitizers in Photodynamic Therapy. *Photochem. Photobiol.*, *53*, 65-72.

[212] Henderson, B. W., Bellnier, D. A., Greco, W. R., Sharma, A., Pandey, R. K., Vaughan, L. A., Weishaupt, K. R. and Dougherty, T. J. (1997). An in Vivo Quantitative Structure-Activity Relationship for a Congeneric Series of Pyropheophorbide Derivatives as Photosensitizers for Photodynamic Therapy. *Cancer Res.*, *57*, 4000-4007.

[213] Pandey, R. K., Shiau, F. Y., Sumlin, A. B., Dougherty, T. J. and Smith, K. M. (1992). Structure-Activity-Relationships among Photosensitizers Related to Pheophorbides and Bacteriopheophorbides. *Bioorg. Med. Chem. Lett.*, *2*, 491-496.

[214] Pallenberg, A. J., Dobhal, M. P. and Pandey, R. K. (2004). Efficient synthesis of pyropheophorbide-a and its derivatives. *Org. Process Res. Dev.*, *8*, 287-290.

[215] Baba, K., Pudavar, H. E., Roy, I., Ohulchanskyy, T. Y., Chen, Y. H., Pandey, R. K. and Prasad, P. N. (2007). New method for delivering a hydrophobic drug for photodynamic therapy using pure nanocrystal form of the drug. *Mol. Pharm.*, *4*, 289-297.

[216] Bellnier, D. A., Greco, W. R., Loewen, G. M., Nava, H., Oseroff, A. R., Pandey, R. K., Tsuchida, T. and Dougherty, T. J. (2003). Population pharmacokinetics of the photodynamic therapy agent 2- [1-hexyloxyethyl]-2-devinyl pyropheophorbide-a in cancer patients. *Cancer Res.*, *63*, 1806-1813.

[217] Bellnier, D. A., Greco, W. R., Nava, H., Loewen, G. M., Oseroff, A. R. and Dougherty, T. J. (2006). Mild skin photosensitivity in cancer patients following injection of Photochlor (2- [1-hexyloxyethyl]-2-devinyl pyropheophorbide-a; HPPH) for photodynamic therapy. *Cancer Chemother. Pharmacol.*, *57*, 40-45.

[218] Loewen, G. M., Pandey, R., Bellnier, D., Henderson, B. and Dougherty, T. (2006). Endobronchial photodynamic therapy for lung cancer. *Lasers Surg. Med.*, *38*, 364-370.

[219] Scherz, A., Salomon, Y., Brandis, A. and Scheer, H. (2003). Palladium-substituted bacteriochlorophyll derivatives and use thereof. United States Patent US6569846. Available also from: www.freepatentsonline.com.

[220] Brun, P. H., DeGroot, J. L., Dickson, E. F. G., Farahani, M. and Pottier, R. H. (2004). Determination of the in vivo pharmacokinetics of palladium-bacteriopheophorbide

(WST09) in EMT6 tumour-bearing Balb/c mice using graphite furnace atomic absorption spectroscopy. *Photochem. Photobiol. Sci.*, *3*, 1006-1010.

[221] Weersink, R. A., Forbes, J., Bisland, S., Trachtenberg, J., Elhilali, M., Brun, P. H. and Wilson, B. C. (2005). Assessment of cutaneous photosensitivity of TOOKAD (WST09) in preclinical animal models and in patients. *Photochem. Photobiol.*, *81*, 106-113.

[222] Huang, Z., Chen, Q., Dole, K. C., Barqawi, A. B., Chen, Y. K., Blanc, D. Q., Wilson, B. C. and Hetzel, F. W. (2007). The effect of Tookad-mediated photodynamic ablation of the prostate gland on adjacent tissues - in vivo study in a canine model. *Photochem. Photobiol. Sci.*, *6*, 1318-1324.

[223] Huang, Z., Chen, Q., Luck, D., Beckers, J., Wilson, B. C., Trncic, N., LaRue, S. M., Blanc, D. and Hetzel, F. W. (2005). Studies of a vascular-acting photosensitizer, Pd-bacteriopheophorbide (Tookad), in normal canine prostate and spontaneous canine prostate cancer. *Lasers Surg. Med.*, *36*, 390-397.

[224] Framme, C., Sachs, H. G., Flucke, B., Theisen-Kunde, D. and Birngruber, R. (2006). Evaluation of the new photosensitizer tookad (WST09) for photodynamic vessel occlusion of the choroidal tissue in rabbits. *Invest. Ophthalmol. Vis. Sci.*, *47*, 5437-5446.

[225] Armstrong, N. R. (2000). Phthalocyanines and porphyrins as materials. *J. Porphyr. Phthalocyanines*, *4*, 414-417.

[226] Ali, H. and van Lier, J. E. (1999). Metal complexes as photo- and radiosensitizers. *Chem. Rev.*, *99*, 2379-2450.

[227] Allen, C. M., Sharman, W. M. and Van Lier, J. E. (2001). Current status of phthalocyanines in the photodynamic therapy of cancer. *J. Porphyr. Phthalocyanines*, *5*, 161-169.

[228] Nevin, W. A., Liu, W. and Lever, A. B. P. (1987). Dimerization of Mononuclear and Binuclear Cobalt Phthalocyanines. *Can. J. Chem.*, *65*, 855-858.

[229] Kobayashi, N., Higashi, R., Ishii, K., Hatsusaka, K. and Ohta, K. (1999). Aggregation, complexation with guest molecules, and mesomorphism of amphiphilic phthalocyanines having four- or eight tri(ethylene oxide) chains. *Bull. Chem. Soc. Jpn.*, *72*, 1263-1271.

[230] Lang, K., Kubat, P., Mosinger, J. and Wagnerova, D. M. (1998). Photochemical consequences of porphyrin and phthalocyanine aggregation on nucleoprotein histone. *J. Photochem. Photobiol. A-Chem.*, *119*, 47-52.

[231] Isago, H., Leznoff, C. C., Ryan, M. F., Metcalfe, R. A., Davids, R. and Lever, A. B. P. (1998). Aggregation effects on electrochemical and spectroelectrochemical properties of [2,3,9,10,16,17,23,24-octa(3,3-dimethyl-1-butynyl)phthalocyaninato]cobal t(II) complex. *Bull. Chem. Soc. Jpn.*, *71*, 1039-1047.

[232] Deng, H. H., Mao, H. F., Zhang, H., Lu, Z. H. and Xu, H. J. (1998). Photoelectric effect of tetrasulfonated gallium phthalocyanine on a nanostructured TiO2 electrode. *J. Porphyr. Phthalocyanines*, *2*, 171-175.

[233] Lagorio, M. G., Dicelio, L. E. and Roman, E. S. (1993). Visible and near-Ir Spectroscopic and Photochemical Characterization of Substituted Metallophthalocyanines. *J. Photochem. Photobiol. A-Chem.*, *72*, 153-161.

[234] Maree, M. D., Nyokong, T., Suhling, K. and Phillps, D. (2002). Effects of axial ligands on the photophysical properties of silicon octaphenoxyphthalocyanine. *J. Porphyr. Phthalocyanines*, *6*, 373-376.

[235] Choi, M. T. M., Li, P. P. S. and Ng, D. K. P. (2000). A direct comparison of the aggregation behavior of phthalocyanines and 2,3-naphthalocyanines. *Tetrahedron*, *56*, 3881-3887.

[236] Bench, B. A., Beveridge, A., Sharman, W. M., Diebold, G. J., van Lier, J. E. and Gorun, S. M. (2002). Introduction of bulky perfluoroalkyl groups at the periphery of zinc perfluorophthalocyanine: Chemical, structural, electronic, and preliminary photophysical and biological effects. *Angew. Chem.-Int. Edit.*, *41*, 748-+.

[237] Kostka, M., Zimcik, P., Miletin, M., Klemera, P., Kopecky, K. and Musil, Z. (2006). Comparison of aggregation properties and photodynamic activity of phthalocyanines and azaphthalocyanines. *J. Photochem. Photobiol. A-Chem.*, *178*, 16-25.

[238] Kudrevich, S. V., Galpern, M. G. and Vanlier, J. E. (1994). Synthesis of Octacarboxytetra(2,3-Pyrazino)Porphyrazine - Novel Water-Soluble Photosensitizers for Photodynamic Therapy. *Synthesis (Stuttg.)*, 779-781.

[239] De Filippis, M. P., Dei, D., Fantetti, L. and Roncucci, G. (2000). Synthesis of a new water-soluble octa-cationic phthalocyanine derivative for PDT. *Tetrahedron Lett.*, *41*, 9143-9147.

[240] Zimcik, P., Miletin, M., Musil, Z., Kopecky, K., Kubza, L. and Brault, D. (2006). Cationic azaphthalocyanines bearing aliphatic tertiary amino substituents--Synthesis, singlet oxygen production and spectroscopic studies. *J. Photochem. Photobiol. A-Chem.*, *183*, 59-69.

[241] Sakamoto, K., Kato, T., Ohno-Okumura, E., Watanabe, M. and Cook, M. J. (2005). Synthesis of novel cationic amphiphilic phthalocyanine derivatives for next generation photosensitizer using photodynamic therapy of cancer. *Dyes Pigment.*, *64*, 63-71.

[242] Scalise, I. and Durantini, E. N. (2005). Synthesis, properties, and photodynamic inactivation of Escherichia coli using a cationic and a noncharged Zn(II) pyridyloxyphthalocyanine derivatives. *Bioorg. Med. Chem.*, *13*, 3037-3045.

[243] Abramczyk, H., Szymczyk, I., Waliszewska, G. and Lebioda, A. (2004). Photoinduced redox processes in phthalocyanine derivatives by resonance Raman spectroscopy. *J. Phys. Chem. A*, *108*, 264-274.

[244] Sharman, W. M., Allen, C. M. and van Lier, J. E. (1999). Photodynamic therapeutics: basic principles and clinical applications. *Drug Discov. Today*, *4*, 507-517.

[245] Nyman, E. S. and Hynninen, P. H. (2004). Research advances in the use of tetrapyrrolic photosensitizers for photodynamic therapy. *J. Photochem. Photobiol. B-Biol.*, *73*, 1-28.

[246] Photosense [online]. 2008 [cited 2008-04-10]. Available from: http://www.niopik.ru/products/medicine/photosense/.

[247] Vakulovskaya, E. G. and Shental, V. V. (2002). Combination of photodynamic therapy and cryosurgery in treatment of advanced skin cancer. *Int. J. Cancer*, Suppl. 13, 404-404.

[248] Vakulovskaya, E. G., Shental, V. V. and Kondratjeva, T. T. (2002). Photodynamic therapy and fluorescent diagnostics of head and neck tumors with photosense. *Int. J. Cancer*, Suppl. 13, 262-262.

[249] Vakulovskaya, E. G., Ungiadze, G. V. and Tabolinovskaya, T. D. (2005). PD10. Photodynamic therapy of oral cancer andcancer of oropharynx with second-generation photosensitizers. *Oral Oncology Supplement*, *1*, 68.

[250] Vakulovskaya, E., Shental, V., Letyagin, V., Oumnova, L., Vorozhcsov, V., Philinov, V. and Stranadko, E. (2002). Photodynamic therapy and fluorescent diagnostics of breast cancer with photosense. *Int. J. Cancer*, Suppl. 13, 211-211.

[251] Borgatti-Jeffreys, A., Hooser, S. B., Miller, M. A. and Lucroy, M. D. (2007). Phase I clinical trial of the use of zinc phthalocyanine tetrasulfonate as a photosensitizer for photodynamic therapy in dogs. *Am. J. Vet. Res.*, *68*, 399-404.

[252] Miller, J. D., Nancy, O., Scull, H. M., Hsia, A., Cooper, K. D. and Baron, E. D. (2006). Phase I clinical trial using topical silicon phthalocyanine Pc 4-photodynamic therapy for the treatment of malignant and pre-malignant skin conditions: an update. *J. Invest. Dermatol.*, *126*, 46-46.

[253] Shopova, M., Woehrle, D., Mantareva, V. and Mueller, S. (1999). Naphthalocyanine complexes as potential photosensitizers for photodynamic therapy of tumors. *J. Biomed. Opt.*, *4*, 276-285.

[254] Soncin, M., Busetti, A., Biolo, R., Jori, G., Kwag, G., Li, Y. S., Kenney, M. E. and Rodgers, M. A. J. (1998). Photoinactivation of amelanotic and melanotic melanoma cells sensitized by axially substituted Si-naphthalocyanines. *J. Photochem. Photobiol. B-Biol.*, *42*, 202-210.

[255] Biolo, R., Jori, G., Soncin, M., Pratesi, R., Vanni, U., Rihter, B., Kenney, M. E. and Rodgers, M. A. J. (1994). Photodynamic Therapy of B16 Pigmented Melanoma with Liposome-Delivered Si(Iv)-Naphthalocyanine. *Photochem. Photobiol.*, *59*, 362-365.

[256] Shopova, M., Wohrle, D., Stoichkova, N., Milev, A., Mantareva, V., Muller, S., Kassabov, K. and Georgiev, K. (1994). Hydrophobic Zn(Ii)-Naphthalocyanines as Photodynamic Therapy Agents for Lewis Lung-Carcinoma. *J. Photochem. Photobiol. B-Biol.*, *23*, 35-42.

[257] Muller, S., Mantareva, V., Stoichkova, N., Kliesch, H., Sobbi, A., Wohrle, D. and Shopova, M. (1996). Tetraamido-substituted 2,3-naphthalocyanine zinc(II) complexes as phototherapeutic agents: Synthesis, comparative photochemical and photobiological studies. *Journal of Photochemistry and Photobiology B-Biology*, *35*, 167-174.

[258] Zuk, M. M., Rihter, B. D., Kenney, M. E., Rodgers, M. A. J. and KreimerBirnbaum, M. (1996). Effect of delivery system on the pharmacokinetics and tissue distribution of bis(Di-isobutyl octadecylsiloxy)silicon 2,3-naphthalocyanine (isoBOSINC), a photosensitizer for tumor therapy. *Photochem. Photobiol.*, *63*, 132-140.

[259] Mantareva, V., Shopova, M., Spassova, G., Wohrle, D., Muller, S., Jori, G. and Ricchelli, F. (1997). Si(IV)-methoxyethylene-glycol-naphthalocyanine: synthesis and pharmacokinetic and photosensitizing properties in different tumour models. *J. Photochem. Photobiol. B-Biol.*, *40*, 258-262.

[260] Brasseur, N., Nguyen, T. L., Langlois, R., Ouellet, R., Marengo, S., Houde, D. and Vanlier, J. E. (1994). Synthesis and Photodynamic Activities of Silicon 2,3-Naphthalocyanine Derivatives. *J. Med. Chem.*, *37*, 415-420.

[261] Wainwright, M. and Giddens, R. M. (2003). Phenothiazinium photosensitisers: choices in synthesis and application. *Dyes Pigment.*, *57*, 245-257.

[262] Wainwright, M., Phoenix, D. A., Rice, L., Burrow, S. M. and Waring, J. (1997). Increased cytotoxicity and phototoxicity in the methylene blue series via chromophore methylation. *J. Photochem. Photobiol. B-Biol.*, *40*, 233-239.

[263] Wainwright, M., Grice, N. J. and Pye, L. E. C. (1999). Phenothiazine photosensitizers: part 2. 3,7-Bis(arylamino)phenothiazines. *Dyes Pigment.*, *42*, 45-51.

[264] Wainwright, M. (2007). Phenothiazinium photosensitisers: V. Photobactericidal activities of chromophore-methylated phenothiazinium salts. *Dyes Pigment.*, *73*, 7-12.

[265] Cincotta, L., Foley, J. W. and Cincotta, A. H. (1993). Phototoxicity, Redox Behavior, and Pharmacokinetics of Benzophenoxazine Analogs in Emt-6 Murine Sarcoma-Cells. *Cancer Res.*, *53*, 2571-2580.

[266] Georgakoudi, I. and Foster, T. H. (1998). Effects of the subcellular redistribution of two nile blue derivatives on photodynamic oxygen consumption. *Photochem. Photobiol.*, *68*, 115-122.

[267] Cincotta, L., Foley, J. W. and Cincotta, A. H. (1987). Novel Red Absorbing Benzo [a]Phenoxazinium and Benzo [a]Phenothiazinium Photosensitizers - Invitro Evaluation. *Photochem. Photobiol.*, *46*, 751-758.

[268] Wainwright, M. (2005). The development of phenothiazinium photosensitisers. *Photodiagn. Photodyn. Ther.*, *2*, 263-272.

[269] Donnelly, R. F., McCarron, P. A. and Tunney, M. M. (2008). Antifungal photodynamic therapy. *Microbiol. Res.*, *163*, 1-12.

[270] Tardivo, J. P., Del Giglio, A., Paschoal, L. H. C., Ito, A. S. and Baptista, M. S. (2004). Treatment of melanoma lesions using methylene blue and RL50 light source. *Photodiagn. Photodyn. Ther.*, *1*, 345-346.

[271] Tardivo, J. P., Del Giglio, A., de Oliveira, C. S., Gabrielli, D. S., Junqueira, H. C., Tada, D. B., Severino, D., de Fatima Turchiello, R. and Baptista, M. S. (2005). Methylene blue in photodynamic therapy: From basic mechanisms to clinical applications. *Photodiagn. Photodyn. Ther.*, *2*, 175-191.

[272] Brown, S. B., Brown, E. A. and Walker, I. (2004). The present and future role of photodynamic therapy in cancer treatment. *Lancet Oncol.*, *5*, 497-508.

[273] Mohr, H., Lambrecht, B. and Selz, A. (1995). Photodynamic Virus Inactivation of Blood Components. *Immunol. Invest.*, *24*, 73-85.

[274] Wainwright, M., Mohr, H. and Walker, W. H. (2007). Phenothiazinium derivatives for pathogen inactivation in blood products. *J. Photochem. Photobiol. B-Biol.*, *86*, 45-58.

[275] Usacheva, M. N., Teichert, M. C. and Biel, M. A. (2001). Comparison of the methylene blue and toluidine blue photobactericidal efficacy against gram-positive and gram-negative microorganisms. *Lasers Surg. Med.*, *29*, 165-173.

[276] Pottier, R., Bonneau, R. and Joussotdubien, J. (1975). Ph-Dependence of Singlet Oxygen Production in Aqueous-Solutions Using Toluidine Blue as a Photosensitizer. *Photochem. Photobiol.*, *22*, 59-61.

[277] Donnelly, R. F., McCarron, P. A., Cassidy, C. M., Elborn, J. S. and Tunney, M. M. (2007). Delivery of photosensitisers and light through mucus: Investigations into the potential use of photodynamic therapy for treatment of Pseudomonas aeruginosa cystic fibrosis pulmonary infection. *J. Control. Release*, *117*, 217-226.

[278] Donnelly, R. F., McCarron, P. A., Tunney, M. M. and David Woolfson, A. (2007). Potential of photodynamic therapy in treatment of fungal infections of the mouth.

Design and characterisation of a mucoadhesive patch containing toluidine blue O. *J. Photochem. Photobiol. B-Biol.*, *86*, 59-69.

[279] Qin, Y. L., Luan, X. L., Bi, L. J., He, G. P., Bai, X. F., Zhou, C. N. and Zhang, Z. G. (2008). Toluidine blue-mediated photoinactivation of periodontal pathogens from supragingival plaques. *Lasers Med. Sci.*, *23*, 49-54.

[280] Wilson, M., Burns, T., Pratten, J. and Pearson, G. J. (1995). Bacteria in Supragingival Plaque Samples Can Be Killed by Low-Power Laser-Light in the Presence of a Photosensitizer. *J. Appl. Bacteriol.*, *78*, 569-574.

[281] Williams, J., Wilson, M., Conway-Wallace, H., Pearson, G. and Colles, J. (2003). Action of tolonium chloride against S mutans in a collagen matrix. *J. Dent. Res.*, *82*, 498-498.

[282] Williams, J. A., Pearson, G. J., Colles, M. J. and Wilson, M. (2003). The effect of variable energy input from a novel light source on the photoactivated bactericidal action of toluidine blue O on Streptococcus mutans. *Caries Res.*, *37*, 190-193.

[283] Bonsor, S. J., Nichol, R., Reid, T. M. S. and Pearson, G. J. (2006). Microbiological evaluation of photo-activated disinfection in endodontics (An in vivo study). *Br. Dent. J.*, *200*, 337-341.

[284] Bonsor, S. J., Nichol, R., Reid, T. M. S. and Pearson, G. J. (2006). An alternative regimen for root canal disinfection. *Br. Dent. J.*, *201*, 101-105.

[285] Qin, Y. L., Luan, X. L., Bi, L. J., Sheng, Y. Q., Zhou, C. N. and Zhang, Z. G. (2008). Comparison of toluidine blue-mediated photodynamic therapy and conventional scaling treatment for periodontitis in rats. *J. Periodont. Res.*, *43*, 162-167.

[286] PerioWave.com [online]. 2008 [cited 2008-04-02]. Available from: http://www.periowave.com/

[287] OndineBiopharma.com [online]. 2008 [cited 2008-04-02]. Available from: http://www.ondinebiopharma.com/

[288] Denfotex.com [online]. 2008 [cited 2008-04-02]. Available from: http://www.denfotex.com/

[289] Rozanowska, M., Ciszewska, J., Korytowski, W. and Sarna, T. (1995). Rose-bengal-photosensitized formation of hydrogen peroxide and hydroxyl radicals. *J. Photochem. Photobiol. B-Biol.*, *29*, 71-77.

[290] Carballo, M., Alvarez, S. and Boveris, A. (1993). Cellular stress by light and Rose Bengal in human lymphocytes. *Mutat. Res.-Fundam. Mol. Mech. Mutagen.*, *288*, 215-222.

[291] Matthews, E. K. and Cui, Z. J. (1989). Photodynamic action of rose bengal on isolated rat pancreatic acini: stimulation of amylase release. *FEBS Lett.*, *256*, 29-32.

[292] Stevenson, N. R. and Lenard, J. (1993). Antiretroviral activities of hypericin and rose bengal: Photodynamic effects on Friend leukemia virus infection of mice. *Antiviral Res.*, *21*, 119-127.

[293] ProvectusPharmaceuticals.com [online]. 2008 [cited 2008-04-02]. Available from: http://www.pvct.com/index.html.

[294] Udomsakdi, C., Eaves, C. J., Sutherland, H. J. and Lansdorp, P. M. (1991). Separation of Functionally Distinct Subpopulations of Primitive Human Hematopoietic-Cells Using Rhodamine-123. *Exp. Hematol.*, *19*, 338-342.

[295] Brasseur, N., Menard, I., Forget, A., El Jastimi, R., Hamel, R., Molfino, N. A. and van Lier, J. E. (2000). Eradication of multiple myeloma and breast cancer cells by TH9402-

mediated photodynamic therapy: Implication for clinical ex vivo purging of autologous stem cell transplants. *Photochem. Photobiol.*, *72*, 780-787.

[296] KiadisPharma.com [online]. 2008 [cited 2008-04-02]. Available from: http://www.kiadis.com/home.html.

[297] Sessler, J. L., Hemmi, G., Mody, T. D., Murai, T., Burrell, A. and Young, S. W. (1994). Texaphyrins: Synthesis and Applications. *Acc. Chem. Res.*, *27*, 43-50.

[298] Sessler, J. L., Johnson, M. R. and Lynch, V. (1987). Synthesis and crystal structure of a novel tripyrrane-containing porphyrinogen-like macrocycle. *J. Org. Chem.*, *52*, 4394-4397.

[299] Young, S. W., Woodburn, K. W., Wright, M., Mody, T. D., Fan, Q., Sessler, J. L., Dow, W. C. and Miller, R. A. (1996). Lutetium Texaphyrin (PCI-0123): A Near-Infrared, Water-Soluble Photosensitizer. *Photochem. Photobiol.*, *63*, 892-897.

[300] Kereiakes, D. J., Szyniszewski, A. M., Wahr, D., Herrmann, H. C., Simon, D. I., Rogers, C., Kramer, P., Shear, W., Yeung, A. C., Shunk, K. A. *et al* (2003). Phase I drug and light dose-escalation trial of motexafin lutetium and far red light activation (phototherapy) in subjects with coronary artery disease undergoing percutaneous coronary intervention and stent deployment: procedural and long-term results. *Circulation*, *108*, 1310-1315.

[301] Du, K. L., Mick, R., Busch, T. M., Zhu, T. C., Finlay, J. C., Yu, G., Yodh, A. G., Malkowicz, S. B., Smith, D., Whittington, R. *et al* (2006). Preliminary results of interstitial motexafin lutetium-mediated PDT for prostate cancer. *Lasers Surg. Med.*, *38*, 427-434.

[302] Verigos, K., Stripp, D. C., Mick, R., Zhu, T. C., Whittington, R., Smith, D., Dimofte, A., Finlay, J., Busch, T. M., Tochner, Z. A. *et al* (2006). Updated results of a phase I trial of motexafin lutetium-mediated interstitial photodynamic therapy in patients with locally recurrent prostate cancer. *J. Environ. Pathol. Toxicol. Oncol.*, *25*, 373-387.

[303] Dimofte, A., Zhu, T. C., Hahn, S. M. and Lustig, R. A. (2002). In vivo light dosimetry for motexafin lutetium-mediated PDT of recurrent breast cancer. *Lasers Surg. Med.*, *31*, 305-312.

[304] Woodburn, K. W., Fan, Q., Kessel, D., Luo, Y. and Young, S. W. (1998). Photodynamic Therapy of B16F10 Murine Melanoma with Lutetium Texaphyrin. *J. Invest. Dermatol.*, *110*, 746-751.

[305] Rockson, S. G., Kramer, P., Razavi, M., Szuba, A., Filardo, S., Fitzgerald, P., Cooke, J. P., Yousuf, S., DeVault, A. R., Renschler, M. F. *et al* (2000). Photoangioplasty for Human Peripheral Atherosclerosis : Results of a Phase I Trial of Photodynamic Therapy With Motexafin Lutetium (Antrin). *Circulation*, *102*, 2322-2324.

[306] Pharmacyclics [online]. 2008 [cited 2008-02-18]. Available from: www.pharmacyclics.com.

[307] Sanchez-Garcia, D. and Sessler, J. L. (2008). Porphycenes: synthesis and derivatives. *Chem. Soc. Rev.*, *37*, 215-232.

[308] Stockert, J. C., Canete, M., Juarranz, A., Villanueva, A., Horobin, R. W., Borrell, J., Teixido, J. and Nonell, S. (2007). Porphycenes: Facts and prospects in photodynamic therapy of cancer. *Curr. Med. Chem.*, *14*, 997-1026.

[309] Szeimies, R.-M., Karrer, S., Abels, C., Steinbach, P., Fickweiler, S., Messmann, H., Baumler, W. and Landthaler, M. (1996). 9-Acetoxy-2,7,12,17-tetrakis([beta]-methoxyethyl)-porphycene (ATMPn), a novel photosensitizer for photodynamic

therapy: uptake kinetics and intracellular localization. *J. Photochem. Photobiol. B-Biol.*, *34*, 67-72.

[310] Fickweiler, S., Abels, C., Karrer, S., Baumler, W., Landthaler, M., Hofstadter, F. and Szeimies, R.-M. (1999). Photosensitization of human skin cell lines by ATMPn (9-acetoxy-2,7,12,17-tetrakis-([beta]-methoxyethyl)-porphycene) in vitro: mechanism of action. *J. Photochem. Photobiol. B-Biol.*, *48*, 27-35.

[311] Segalla, A., Fedeli, F., Reddi, E., Jori, G. and Cross, A. (1997). Effect of chemical structure and hydrophobicityon the pharmacokinetic properties of porphycenes in tumour-bearing mice. *Int. J. Cancer*, *72*, 329-336.

[312] Duraan, N. and Song, P.-S. (1986). Hypericine and its photodynamic action. *Photochem. Photobiol.*, *43*, 677-680.

[313] Agostinis, P., Vantieghem, A., Merlevede, W. and de Witte, P. A. M. (2002). Hypericin in cancer treatment: more light on the way. *Int. J. Biochem. Cell Biol.*, *34*, 221-241.

[314] Alecu, M., Ursaciuc, C., Halalau, F., Coman, G., Merlevede, W., Waelkens, E. and de Witte, P. (1998). Photodynamic treatment of basal cell carcinoma and squamous cell carcinoma with hypericin. *Anticancer Res.*, *18*, 4651-4654.

[315] SciFinder Scholar 2007 [database online]. 2008 © American Chemical Society [cited 2008-02-22] Available from: www.cas.org/products/sfacad/index.html.

[316] RadaPharma [online]. 2008 [cited 2008-02-22]. Available from: www.radapharma.ru/radachlorin.

[317] Rozanova, N., Zhang, J. Z. and Heck, D. E. (2007). Catalytic therapy of cancer with porphyrins and ascorbate. *Cancer Lett.*, *252*, 216-224.

[318] Girenko, E. G., Borisenkova, S. A. and Kaliya, O. L. (2002). Oxidation of ascorbic acid in the presence of phthalocyanine metal complexes. Chemical aspects of catalytic anticancer therapy. 1. Catalysis of oxidation by cobalt octacarboxyphthalocyanine. *Russ. Chem. Bull.*, *51*, 1231-1236.

[319] Petrova, E. G., Borisenkova, S. A. and Kaliya, O. L. (2004). Oxidation of ascorbic acid in the presence of phthalocyanine metal complexes. Chemical aspects of catalytic therapy of cancer 2. Catalysis by cobalt octacarboxyphthalocyanine. Reaction products. *Russ. Chem. Bull.*, *53*, 2322-2326.

[320] Camerin, M., Rello, S., Villanueva, A., Ping, X., Kenney, M. E., Rodgers, M. A. J. and Jori, G. (2005). Photothermal sensitisation as a novel therapeutic approach for tumours: Studies at the cellular and animal level. *Eur. J. Cancer*, *41*, 1203-1212.

[321] Camerin, M., Rodgers, M. A. J., Kenney, M. E. and Jori, G. (2005). Photothermal sensitisation: evidence for the lack of oxygen effect on the photosensitising activity. *Photochem. Photobiol. Sci.*, *4*, 251-253.

[322] Busetti, A., Soncin, M., Reddi, E., Rodgers, M. A. J., Kenney, M. E. and Jori, G. (1999). Photothermal sensitization of amelanotic melanoma cells by Ni(II)-octabutoxy-naphthalocyanine. *J. Photochem. Photobiol. B-Biol.*, *53*, 103-109.

[323] Berg, K., Sandvik, K. and Moan, J. (1996). Transfer of molecules into the cytosol of cells. Wipo Patent WO/1996/007432. Available also from: www.freepatentsonline.com.

[324] Berg, K., Kristian Selbo, P., Prasmickaite, L., Tjelle, T. E., Sandvig, K., Moan, J., Gaudernack, G., Fodstad, O., Kjolsrud, S., Anholt, H. *et al* (1999). Photochemical

Internalization: A Novel Technology for Delivery of Macromolecules into Cytosol. *Cancer Res.*, *59*, 1180-1183.

[325] PCI Biotech AS [online]. 2008 [cited 2008-25-02]. Available from: www.pcibiotech.com.

[326] Selbo, P. K., Sandvig, K., Kirveliene, V. and Berg, K. (2000). Release of gelonin from endosomes and lysosomes to cytosol by photochemical internalization. *Biochim. Biophys. Acta-Gen. Subj.*, *1475*, 307-313.

[327] Shiraishi, T. and Nielsen, P. E. (2006). Photochemically enhanced cellular delivery of cell penetrating peptide-PNA conjugates. *FEBS Lett.*, *580*, 1451-1456.

[328] Fretz, M. M., Hogset, A., Koning, G. A., Jiskoot, W. and Storm, G. (2007). Cytosolic delivery of liposomally targeted proteins induced by photochemical internalization. *Pharm. Res.*, *24*, 2040-2047.

[329] Selbo, P. K., Sivam, G., Fodstad, O., Sandvig, K. and Berg, K. (2001). In vivo documentation of photochemical internalization, a novel approach to site specific cancer therapy. *Int. J. Cancer*, *92*, 761-766.

[330] Ndoye, A., Dolivet, G., Hogset, A., Leroux, A., Fifre, A., Erbacher, P., Berg, K., Behr, J. P., Guillemin, F. and Merlin, J. L. (2006). Eradication of p53-mutated head and neck squamous cell carcinoma xenografts using nonviral p53 gene therapy and photochemical internalization. *Mol. Ther.*, *13*, 1156-1162.

[331] Berg, K., Dietze, A., Kaalhus, O. and Hogset, A. (2005). Site-Specific Drug Delivery by Photochemical Internalization Enhances the Antitumor Effect of Bleomycin. *Clin. Cancer Res.*, *11*, 8476-8485.

[332] Rosenthal, I., Sostaric, J. Z. and Riesz, P. (2004). Sonodynamic therapy - a review of the synergistic effects of drugs and ultrasound. *Ultrason. Sonochem.*, *11*, 349-363.

[333] Kessel, D., Jeffers, R., Fowlkes, J. B. and Cain, C. (1994). Porphyrin-Induced Enhancement of Ultrasound Cytotoxicity. *Int. J. Radiat. Biol.*, *66*, 221-228.

[334] Miyoshi, N., Misik, V. and Riesz, P. (1997). Sonodynamic toxicity of gallium-porphyrin analogue ATX-70 in human leukemia cells. *Radiat. Res.*, *148*, 43-47.

[335] Tata, D. B., Biglow, J., Wu, J. R., Tritton, T. R. and Dunn, F. (1996). Ultrasound-enhanced hydroxyl radical production from two clinically employed anticancer drugs, adriamycin and mitomycin C. *Ultrason. Sonochem.*, *3*, 39-45.

[336] Saad, A. H. and Hahn, G. M. (1992). Ultrasound-Enhanced Effects of Adriamycin against Murine Tumors. *Ultrasound Med. Biol.*, *18*, 715-723.

[337] Yumita, N., Nishigaki, R., Umemura, K., Morse, P. D., Swartz, H. M., Cain, C. A. and Umemura, S. (1994). Sonochemical Activation of Hematoporphyrin - an ESR Study. *Radiat. Res.*, *138*, 171-176.

[338] Yumita, N., Umemura, S., Magario, N., Umemura, K. and Nishigaki, R. (1996). Membrane lipid peroxidation as a mechanism of sonodynamically induced erythrocyte lysis. *Int. J. Radiat. Biol.*, *69*, 397-404.

[339] Yumita, N., Nishigaki, R. and Umemura, S. (2000). Sonodynamically induced antitumor effect of Photofrin II on colon 26 carcinoma. *J. Cancer Res. Clin. Oncol.*, *126*, 601-606.

[340] Yumita, N., Umemura, S. and Nishigaki, R. (2000). Ultrasonically induced cell damage enhanced by photofrin II: Mechanism of sonodynamic activation. *In Vivo*, *14*, 425-429.

[341] Umemura, S. I., Yumita, N. and Nishigaki, R. (1993). Enhancement of Ultrasonically Induced Cell-Damage by a Gallium-Porphyrin Complex, Atx-70. *Jpn. J. Cancer Res., 84*, 582-588.

[342] Umemura, K., Yumita, N., Nishigaki, R. and Umemura, S. I. (1996). Sonodynamically induced antitumor effect of pheophorbide a. *Cancer Lett., 102*, 151-157.

[343] Umemura, S., Yumita, N., Umemura, K. and Nishigaki, R. (1999). Sonodynamically induced effect of rose bengal on isolated sarcoma 180 cells. *Cancer Chemother. Pharmacol., 43*, 389-393.

[344] Miyoshi, N., Takeshita, T., Misik, V. and Riesz, P. (2001). Monomerization of photo sensitizers by ultrasound irradiation in surfactant micellar solutions. *Ultrason. Sonochem., 8*, 367-371.

[345] Kremkau, F. W., Kaufmann, J. S., Walker, M. M., Burch, P. G. and Spurr, C. L. (1976). Ultrasonic Enhancement of Nitrogen-Mustard Cytotoxicity in Mouse Leukemia. *Cancer, 37*, 1643-1647.

[346] Longo, F. W., Tomashefsky, P., Rivin, B. D. and Tannenbaum, M. (1983). Interaction of Ultrasonic Hyperthermia with 2 Alkylating-Agents in a Murine Bladder-Tumor. *Cancer Res., 43*, 3231-3235.

[347] Moore, W. E., Lopez, R., Matthews, D. E., Sheets, P. W., Etchison, M. R., Hurwitz, A. S., Chalian, A. A., Fry, F. J., Vane, D. W. and Grosfeld, J. L. (1989). Evaluation of High-Intensity Therapeutic Ultrasound Irradiation in the Treatment of Experimental Hepatoma. *J. Pediatr. Surg., 24*, 30-33.

[348] Saad, A. H. and Hahn, G. M. (1989). Ultrasound Enhanced Drug Toxicity on Chinese-Hamster Ovary Cells-Invitro. *Cancer Res., 49*, 5931-5934.

[349] Harrison, G. H., Balcerkubiczek, E. K. and Eddy, H. A. (1991). Potentiation of Chemotherapy by Low-Level Ultrasound. *Int. J. Radiat. Biol., 59*, 1453-1466.

[350] Harrison, G. H., BalcerKubiczek, E. K. and Gutierrez, P. L. (1996). In vitro action of continuous-wave ultrasound combined with adriamycin, X rays or hyperthermia. *Radiat. Res., 145*, 98-101.

[351] Yumita, N., Umemura, S., Kaneuchi, M., Okano, Y., Magario, N., Ishizaki, M., Shimizu, K., Sano, Y., Umemura, K. and Nishigaki, R. (1998). Sonodynamically-induced cell damage with fluorinated anthracycline derivative, FAD104. *Cancer Lett., 125*, 209-214.

[352] Yumita, N., Kaneuchi, M., Okano, Y., Nishigaki, R., Umemura, K. and Umemura, S. (1999). Sonodynamically induced cell damage with 4 '-O-tetrahydropyranyladriamycin, THP. *Anticancer Res., 19*, 281-284.

[353] Sakusabe, N., Okada, K., Sato, K., Kamada, S., Yoshida, Y. and Suzuki, T. (1999). Enhanced sonodynamic antitumor effect of ultrasound in the presence of nonsteroidal anti-inflammatory drugs. *Jpn. J. Cancer Res., 90*, 1146-1151.

[354] Okada, K., Itoi, E., Miyakoshi, N., Nakajima, M., Suzuki, T. and Nishida, J. (2002). Enhanced antitumor effect of ultrasound in the presence of piroxicam in a mouse air pouch model. *Jpn. J. Cancer Res., 93*, 216-222.

[355] Feril, L. B., Tsuda, Y., Kondo, T., Zhao, Q. L., Ogawa, R., Cui, Z. G., Tsukada, K. and Riesz, P. (2004). Ultrasound-induced killing of monocytic U937 cells enhanced by 2,2 '-azobis(2-amidinopropane) dihydrochloride. *Cancer Sci., 95*, 181-185.

[356] Misik, V., Miyoshi, N. and Riesz, P. (1996). EPR spin trapping study of the decomposition of azo compounds in aqueous solutions by ultrasound: Potential for use as sonodynamic sensitizers for cell killing. *Free Radic. Res.*, *25*, 13-22.

[357] Yumita, N., Nishigaki, R., Umemura, K. and Umemura, S. (1989). Hematoporphyrin as a Sensitizer of Cell-Damaging Effect of Ultrasound. *Jpn. J. Cancer Res.*, *80*, 219-222.

[358] Yumita, N., Nishigaki, R., Umemura, K. and Umemura, S. (1990). Synergistic Effect of Ultrasound and Hematoporphyrin on Sarcoma-180. *Jpn. J. Cancer Res.*, *81*, 304-308.

[359] Umemura, S., Yumita, N., Nishigaki, R. and Umemura, K. (1990). Mechanism of Cell-Damage by Ultrasound in Combination with Hematoporphyrin. *Jpn. J. Cancer Res.*, *81*, 962-966.

[360] Quan-hong, L., Shi-hui, S., Ya-ping, X., Hao, Q., Jin-xuan, Z., Yao-hui, R., Meng, L. and Pan, W. (2004). Synergistic Anti-Tumor Effect of Ultrasound and Hematoporphyrin on Sarcoma180 Cells with Special Reference to the Changes of Morphology and Cytochrome Oxidase Activity of Tumor Cells. *J. Exp. Clin. Cancer Res.*, *23*, 333-341.

[361] Yumita, N., Okuyama, N., Sasaki, K. and Umemura, S. (2004). Sonodynamic therapy on chemically induced mammary tumor: Pharmacokinetics, tissue distribution and sonodynamically induced antitumor effect of porfimer sodium. *Cancer Sci.*, *95*, 765-769.

[362] Umemura, S., Kawabata, K., Sasaki, K., Yumita, N., Umemura, K. and Nishigaki, R. (1996). Recent advances in sonodynamic approach to cancer therapy. *Ultrason. Sonochem.*, *3*, S187-S191.

[363] Liu, Q. H., Wang, X. B., Wang, P., Xiao, L. N. and Hao, Q. (2007). Comparison between sonodynamic effect with protoporphyrin IX and hematoporphyrin on sarcoma 180. *Cancer Chemother. Pharmacol.*, *60*, 671-680.

[364] Tachibana, K., Kimura, N., Okumura, M., Eguchi, H. and Tachibana, S. (1993). Enhancement of Cell-Killing of Hl-60 Cells by Ultrasound in the Presence of the Photosensitizing Drug Photofrin-Ii. *Cancer Lett.*, *72*, 195-199.

[365] Yumita, N. and Umemura, S. (2003). Sonodynamic therapy with photofrin II on AH130 solid tumor - Pharmacokinetics, tissue distribution and sonodynamic antitumoral efficacy of photofrin II. *Cancer Chemother. Pharmacol.*, *51*, 174-178.

[366] Tachibana, K., Sugata, K., Meng, J., Okumura, M. and Tachibana, S. (1994). Liver-Tissue Damage by Ultrasound in Combination with the Photosensitizing Drug, Photofrin-Ii. *Cancer Lett.*, *78*, 177-181.

[367] Yumita, N., Sasaki, K., Umemura, S. and Nishigaki, R. (1996). Sonodynamically induced antitumor effect of a gallium-porphyrin complex, ATX-70. *Jpn. J. Cancer Res.*, *87*, 310-316.

[368] Yumita, N., Sasaki, K., Umemura, S., Yukawa, A. and Nishigaki, R. (1997). Sonodynamically induced antitumor effect of gallium-porphyrin complex by focused ultrasound on experimental kidney tumor. *Cancer Lett.*, *112*, 79-86.

[369] Sasaki, K., Yumita, N., Nishigaki, R. and Umemura, S. (1998). Antitumor effect sonodynamically induced by focused ultrasound in combination with Ga-porphyrin complex. *Jpn. J. Cancer Res.*, *89*, 452-456.

[370] Yumita, N., Nishigaki, R., Sakata, I., Nakajima, S. and Umemura, S. (2000). Sonodynamically induced antitumor effect of 4-formyloximethylidene-3-hydroxy-2-

vinyl-deuterio-porphynyl(IX)-6,7-diaspartic acid (ATX-S10). *Jpn. J. Cancer Res.*, *91*, 255-260.

[371] Yumita, N. and Umemura, S. (2004). Sonodynamic antitumour effect of chloroaluminum phthalocyanine tetrasulfonate on murine solid tumour. *J. Pharm. Pharmacol.*, *56*, 85-90.

[372] Milowska, K. and Gabryelak, T. (2005). Synergistic effect of ultrasound and phthalocyanines on nucleated erythrocytes in vitro. *Ultrasound Med. Biol.*, *31*, 1707-1712.

[373] Yumita, N., Kawabata, K., Sasaki, K. and Umemura, S. (2002). Sonodynamic effect of erythrosin B on sarcoma 180 cells in vitro. *Ultrason. Sonochem.*, *9*, 259-265.

In: Dyes and Pigments: New Research
Editor: Arnold R. Lang
ISBN 978-1-60692-027-5

Chapter 2

PHTHLOCYANINE TO USE PHOTOSENSITIZER FOR PHOTODYNAMIC THERAPY OF CANCER

Keiichi Skamoto[1,*] and Eiko Ohno-Okumura[2]

[1]Department of Applied Molecular Chemistry, College of Industrial Technology, Nihon University, 1-2-1 Izumi-cho, Narashino-shi, Chiba-ken, 275-8575 Japan

[2]Research Institute of Chemical Science, Technology and Education, 8-37-1-104 Narashinodai, Funabashi-shi, Chiba-ken 274-0063 Japan

ABSTRACT

Phthalocyanine analogues containing alkyl-substituted benzenoid rings and pyridine rings are interesting compounds, because quaternation of the pyridine nitrogen is expected to form cationic amphiphilic compounds.

Non peripheral long alkyl substituted zinc phthalocyanine derivatives, zinc bis(1,4-didecylbenzo)-bis(3,4-pyrido)porphyrazine and zinc bis(1,4-didecylbenzo)-bis(2,3-pyrido)porphyrazine were reacted with dimethyl sulfate and monochloroacetic acid to give their quaternary products. Also the zinc phthalocyanine derivatives reacted with diethyl sulfate to afford the sufo-substituted products. All reacted compounds showed amphiphilic character.

Regio isomers of zinc bis(1,4-didecylbenzo)-bis(3,4-pyrido)porphyrazine were also quaternized with dimethyl sulfate.

Identical peaks in cyclic voltammograms appeared for these products before and after quaternization.

Zinc bis(1,4-didecylbenzo)-bis(2,3-pyrido)porphyrazine was evaluated the the photodynamic therapy of cancer efficacy by cancer cell culture.

The light exposed dimethyl sulfate quaternized zinc bis(1,4-didecylbenzo)-bis(2,3-pyrido) porphyrazines in IU-002 cells produces cell disruption that can be detected as a decrease as fluorescence.

* Correspondence should be addressed to Keiici Sakamoto, k5saka@cit.nihon-u.ac.jp

INTRODUCTION

Phthalocyanine was accidentally discovered as a blue colored by-product of the *o*-cyanobenzamide from phthalimide in 1907. The blue colored by-product was named "phthalocynine". Phthalocynine and metal containing derivatives have established as blue and green dystuffs, and are an important industrial commodity since 1942 [1].

Phthalocyanine derivatives have a similar structure to porphyrin. In general, porphyrins consist of four pyrrole units, while phthalocyanine derivatives construct four isoindole and nitrogen atoms at *meso* positions. The central cavity of phthalocyanine derivatives can place 63 different elemental ions include hydrogens (metal-free phthalocyanine). One or two metal ions containing phthalocyanine is called metal phthalocyanine.

Over the last decade, phthalocyanine derivatives have attracted attention as functional chromophores for applications [1–3], especially organic charge carriers in photocopiers [2], as laser light absorbers in data storage systems [4, 5], as photoconductors in photovoltaic cells [6], and in electrochromic displays [7].

Moreover, phthalocyanine derivatives known to have the potential as second-generation photosensitizers for the photodynamic therapy of cancer (PDT) [2], because they show strong absorption of far-red region between 600 and 850 nm wavelength, which has a greater penetration of tissue [3], and photo-sensitization of singlet oxygen [4].

It is well known that aluminum and zinc phthalocyanine derivatives expected to be used as the photosensitizer for PDT [8]. In these days, porphyrin derivatives such as hematoporphyrin derivatives and Photofrin™ have been used as photosensitizers for PDT at medical institutions [9, 10].

In general, the sensitizer for PDT requires a high photostability, high selectivity to tumors, no cytotoxity when no light is irradiated, strong absorption in the region between 600 and 800 nm where penetration of tissue is good, and a long triplet state lifetime [11]. However porphyrin derivatives including hematoporphyrin derivatives and Photofrin™ are known to have a main absorption of around 400 nm where tissue penetration is low and a weak absorption. On the other hand, phthalocyanine derivatives exhibit the maximum absorption in the far-red range between 600 and 850 nm, and have a greater penetration of tissue [12] and a long triplet lifetime, and high singlet oxygen quantum yields [13]. The aggregation properties of phthalocyanine derivatives are a strong influence on the bioavailability, the *in vivo* distribution and the oxygen production efficiency [14].

Unsubstituted phthalocyanine derivatives are known to insoluble or lower soluble in common organic solvents. Insolubility or lower solubility of unsubstituted phthalocyanine derivatives has problems to utilize in many fields including PDT. Insolubility or lower solubility in common organic solvents is improved to introduce substituents such as alkyl groups onto the ring system. Alkyl group substituted phthalocyanine derivatives become soluble in common organic solvents, and have lipophilic property. Lipophilic phthalocyanine derivatives are reported to have a higher tumor affinity [15].

Whereas, introduction of hydrophilic groups into substituted phthalocyanine derivatives were performed in order to soluble in aqueous media. Water solubility of phthalocyanine derivatives has a strong influence on the bioavailability and *in vivo* distribution. Synthesized water-soluble phthalocyanine derivatives possess sulfo-, carboxy- and phosphono-

substituents, which used to compound have been synthesized to use tumor treatment [11, 14, 16-22].

Phthalocyanine analogues in which one or more of benzenoid rings are replaced by pyridine rings are interesting compound because quaternation of the pyridine nitrogen is expected to confer solubility in aqueous media [23]. Tetrapyridoporphyrazines containing four pyridinoid rings in place of four benzenoid ones were first synthesized by Linstead and his co-workers [24]. Tetramethylated tetrapyridoporphyrazines by quaternation were reported to become soluble in water [25, 26], and then these compounds were studied for PDT [27].

The authors reported a fundamental study on PDT by measuring for the triplet state lifetime of non-peripheral substituted phthalocyanine derivatives [27]. We synthesized to use non-peripheral substituted phthalocyanine derivative, zinc bis(1,4-didecylbenzo)-bis(3,4-pyrido)porphyrazine (*5c*), which possesses two didecylbenzenoid and two pyridinoid moieties in the molecule (Scheme 1) [23].

The compound *5c* exhibits solubility in organic solvents and is expected to have a higher tumor affinity than water soluble phthalocyanines such as tetrasulfophthalocyanines. Then, quaternation of the pyridine nitrogen in *5c* is expected to confer solubility in an aqueous media [25, 26], and to have bioavailability and *in vivo* distribution. The amphiphilic phthalocyanine derivatives are considered the best compound for a new generation of photosensitizers for PDT [13, 14, 15, 23]. Thus, the quaternation of *5c* will provide to be amphiphilic phthalocyanine derivatives.

Another type novel non-peripheral substituted phthalocyanine derivative, zinc bis(1,4-didecylbenzo)-bis(2,3-pyrido)porphyrazine (*6*) was synthesized (Scheme 2).

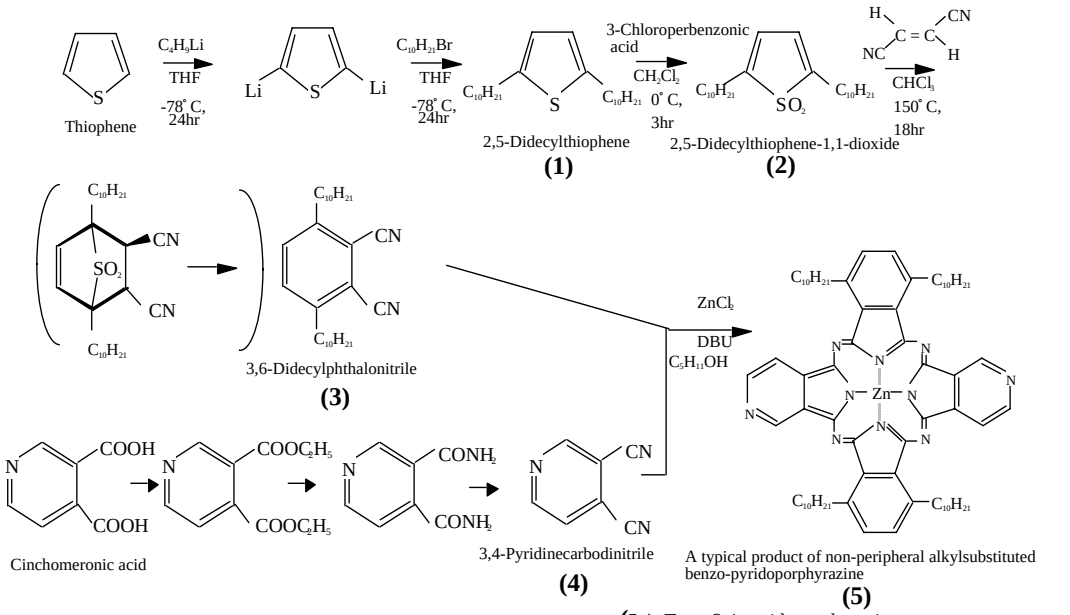

Scheme 1

Scheme 1.

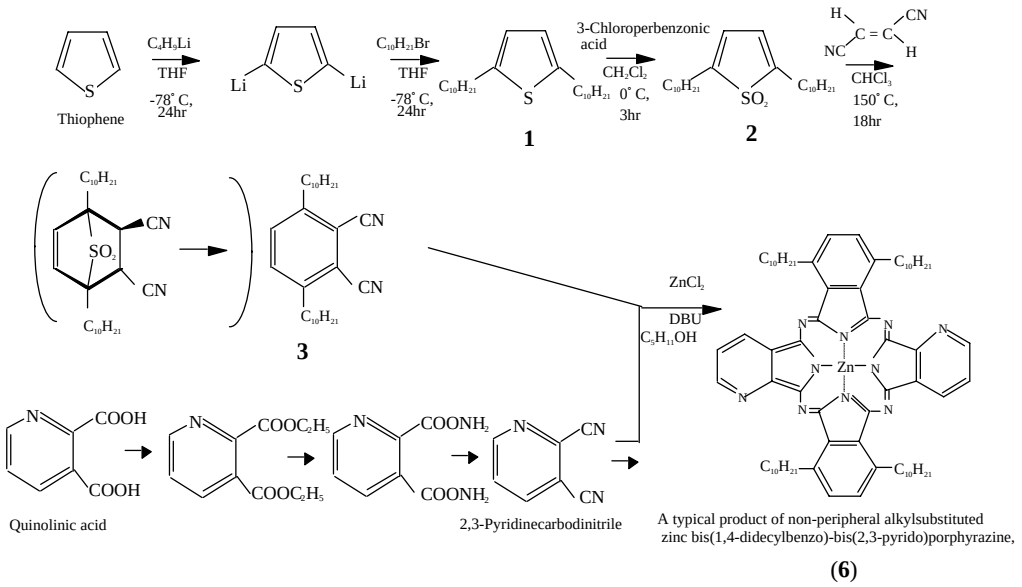

Scheme 2.

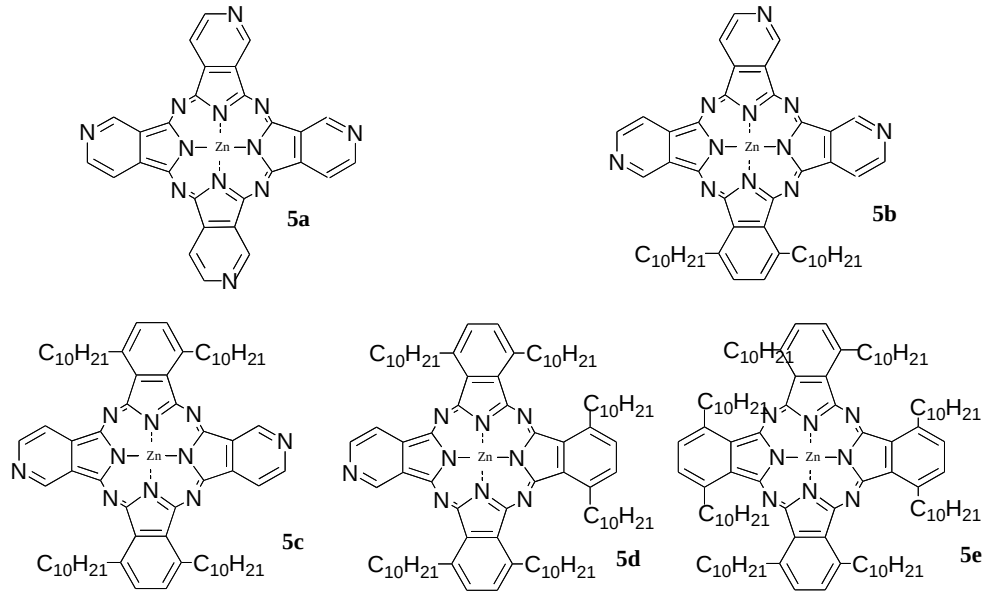

Figure 1. Molecular structures of zinc tetrapyridoporphyrazine *5a*, zinc 1,4-didecylenzo-tris(3,4-pyrido)porphyrazine *5b*, zinc bis(1,4-didecylbenzo)-bis(3,4-pyrido)porphyrazine *5c*, zinc tris(1,4-didecylbenzo)-3,4-pyridoporphyrazine *5d*, and zinc octadcylphthalocyanine *5e*.

In the case of related compounds, 2,3-pyridoporphyrazines are known to have not longer wavelength but stronger absorption intensity than corresponding phthalocyanines and 3,4-pyridoporphyrazines [27]. In accordance with the literature [27], it is expected that *6* and its quaternation compounds have stronger absorption intensities than that of before reported *5c* [28-35]. Therefore, novel compound, *6* and its quaternation compounds are expected

excellent photosensitizer for PDT. Electron transfer ability of *6* is estimated with cyclic voltammetry (CV) technique.

The *6* was evaluated the PDT efficacy by cancer cell culture.

SYNTHESIS

Phthalocyanines can be prepared from cyclization of the appropriate phthalic acid derivatives such as the anhydride, imide or dinitrile.

Zinc non-peripheral substituted phthalocyanine derivatives *5* and *6* were synthesized by cross cyclotetramerization. Synthesized zinc non-peripheral substituted phthalocyanine derivatives *5* have different numbers of pyridine rings in the molecule (Figure 1).

The intermediates 1 - 3 and 4 were analysed by infrared (IR), proton nuclear magnetic resonance (^{1}H-NMR), mass (MS) spectra and elemental analysis, and the results are shown in Table 1. The analytical data for all compounds were in good agreement with the proposed structures.

The compound *5a* was also obtained by condensation of *4* with zinc chloride in the presence of 1,8-diazabicyclo[5,4,0]undec-7-ene (DBU). As a non-pyridinoide phthalocyanine derivative, non-peripheral substituted *5e* of which the substituents were 1, 4, 8, 11, 15, 18, 22, 25 region was synthesized from *3* and zinc chloride in the presence of DBU in accordance with the literature [29, 30]. The preparation of the alkylbenzopyridoporphyrazines was carried out by statistical condensation of zinc chloride, a catalytic amount of DBU, and mixtures of *3* and *4*, 3:1, 1:1 and 1:3 mol ratio, respectively.

A typical synthetic procedure of *5c* is described as following; a mixture of *3* and *4* for 1 (0.12 g, 0.29 mmol):1 (0.04 g, 0.29 mmol) mol ratio was dissolved in pentanol (7 cm^3) and anhydrous zinc (II) chloride (0.05 g) was added. The mixture was heated at 137 °C for 4 h in the presence of DBU as a catalyst. After cooling, the reaction mixture was dissolved in toluene (50 cm^3) and the solution filtered. The solvent was removed by evaporation. The products were separated and purified by thin layer chromatography (TLC) (Merk Silica gel 60 F_{254} on aluminium sheet, eluent: toluene). Blue solid (0.18 g; yield 84%). ^{1}H-NMR (δ 400 MHz, benzene-d_6 (C_6H_6-d_6)/ppm) 0,9 (m, 12H, CH_3), 1.61-2.61 (m, 64H, CH_2), 4.18-4.36 (m, 8H, α-CH_2), 7.45 (m, 4H, arom), 8.26 (m, 6H, Py); IR(ν KBr/cm^{-1}) 2970 (ν_{C-H}), 1600 (ν_{C-C}), 1500 (ν_{C-C}), 1470 (ν_{C-C}), 1450 (ν_{C-C}), 1210 (δ_{C-H}), 1090 (δ_{C-H}), 720 (δ_{C-H}); UV-Vis [λ_{max} toluene/nm (log ε_{max})] 686 (4.814), 636, 617; Anal Calcd. for $C_{70}H_{94}N_{10}Zn$: C. 73.68: H. 8.30: N.12.28. Found: C.73.67: H. 8.30: N. 12.28.

The compounds *5b* - *5d* and octadecylphthalocyanine *5e* were characterized by IR, ultraviolet-visible (UV-Vis) spectroscopy and elemental analysis.

The compounds *5a* and *5e* are composed of only one constituent. Whereas it is expected that the alkylbenzopyridoporphyrazines synthesized from mixed raw materials are prepared as a mixture of products, which have different numbers of pyridine rings in the molecule [26, 36]. Therefore, the alkylbenzopyridoporphyrazines can be separated into more than three blue-colored constituents. Then, each alkylbenzopyridoporphyrazine synthesized from mixed raw materials has the desired molecular structure for its main constituents [26, 36].

Table 1. Synthetic data of intermediates 1-4 of 5

Compound	Yield (%)	ν max KBr/cm⁻¹	δ (¹H 90MHz)/ppm CHCl3-d	Formula	MS[M]+ m/z	Found (calculation)		
						C	H	N
1	71	2960 (ν C-H),1610(ν C-C), 1490(ν C-C), 1460(ν C-C), 1370 (ν C-C),1230(δC-H), 730(δC-H),680(ν C-S)	0.88(t,6H), 1.26(m,32H), 2.72(t,4H), 6.52(s,2H)	$C_{24}H_{44}S$	365	79.06 (79.04)	12.06 (12.06)	-
2	39	2970 (ν C-H),1650(ν C-C), 1480(ν C-C), 1440(ν C-C),1370(ν C-C), 1290 (ν S=O), 1220(δC-H),1140 (ν S=O),730(δC-H), 680(ν C-S)	0.88(t,6H), 1.26(m,32H), 2.47(t,4H), 6.25(s,2H)	$C_{24}H_{44}SO_2$	397	72.66 (72.67)	11.18 (11.18)	-
3	26	2960 (ν C-H),2240(ν C-N), 1560(ν C-C), 1460(ν C-C),1410(ν C-C), 1230 (δC-H), 730(δC-H),	0.88(t,6H), 1.26(m,32H), 2.85(t,4H), 7.46(s,2H)	$C_{28}H_{44}N_2$	409	82.26 (82.29)	10.84 (10.85)	6.84 (6.86)
4	17	3090 (ν C-H),2240(ν C-N), 1600(ν C-C), 1550(ν C-C),1470(ν C-C), 1220 (δC-H), 750(δC-H),	7.26(s,1H), 7.75(s,1H), 9.09(s,1H)	$C_7H_3N_3$	129	65.12 (65.11)	2.34(2.34)	32.56(32.55)

Table 2. Characterization of *5* after purification by TLC

Compound	Yield (%)	Formula	Found (calculation)			Q-band	ν max KBr/cm^{-1}
			C	H	N	λ_{max} toluene/nm	
5a	29	$C_{28}H_{12}N_{12}Zn$	57.81(57.79)	2.11(2.08)	28.90(28.89)	675*, 664*, 603*	2960 (ν C-H),1500(ν C-C), 1470(ν C-C), 1450 (ν C-C),1210(δC-H), 1090(δC-H), 790(δC-H)
5b	65	$C_{49}H_{53}N_{11}Zn$	68.31(68.32)	6.22(6.20)	17.90(17.89)	686, 635, 617	2960 (ν C-H),1600(ν C-C), 1460(ν C-C), 1440 (ν C-C),1210(δC-H), 1080(δC-H), 720(δC-H)
5c	84	$C_{70}H_{94}N_{10}Zn$	73.67(73.68)	8.30(8.30)	12.28(12.28)	686, 636, 617	2970 (ν C-H),1600(ν C-C), 1500(ν C-C), 1470 (ν C-C),1450 (ν C-C), 1210(δC-H), 1090(δC-H),720(δC-H)
5d	84	$C_{91}H_{135}N_{9}Zn$	76.94(76.94)	9.57(9.58)	8.86(8.88)	686, 635, 617	2970 (ν C-H),1600(ν C-C), 1500(ν C-C), 1470 (ν C-C),1210(δC-H), 1100(δC-H), 720(δC-H)
5e	96	$C_{112}H_{176}N_{8}Zn$	79.12(79.13)	10.41(10.43)	6.61(6.59)	703,	2960 (ν C-H),1600(ν C-C), 1500(ν C-C), 1460 (ν C-C),1210(δC-H), 1100(δC-H), 730(δC-H)

* In pyridine under line; main peak.

Table 3. The relative number of each types of hydrogen atoms determined on 90MHz ^{1}H-NMR spetra *5* after purification by TLC

Compound	Number of hydrogen atom (calculation)			
	0.9 ppm	1.3 ppm	2.8 ppm	7.4 ppm
5b	6.7 (6)	33.4 (32)	4.2 (4)	11.0 (11)
5c	12.3 (12)	63.8 (64)	8.4 (8)	10.0 (10)
5d	18.8 (18)	95.9 (96)	12.3 (12)	9.0 (9)
5e	24.1 (24)	128.0 (128)	16.0 (16)	8.0 (8)

The analytical data of *5* are summarized in Table 2. These elemental analyses data agree with the desired molecular structure. It is concluded that compounds *5* synthesized from mixed raw materials are compounds *5b* - *5d*, respectively.

The compounds *5b* - *5d* and octadecylphthalocyanine *5e* exhibited solubility in common organic solvents such as benzene (C_6H_6), toluene, dichloromethane (CH_2Cl_2), chloroform ($CHCl_3$), *N*,*N* -dimethylformamide (DMF) and dimethylsulfoxide (DMSO), etc.

Each synthesized product was purified by TLC (eluent: toluene). After purification, each product had only one blue-colored constituent together with colorless raw materials. The each constituent of the synthesized compounds was recovered from each TLC plate.

The compounds *5* displayed strong absorption peaks around 680 nm as the Q-band which could be attributed to the allowed π - π^* transition [25, 29, 30, 34-42]. The Q-band absorption of *5* was shifted by 50 - 80 nm to a longer wavelength in comparison with unsubstituted phthalocyanines.

Table 3 shows the ^{1}H-NMR spectral data (90 MHz in $CHCl_3$-d) of *5b* - *5d* synthesized from mixed raw materials, and *5e*. Each constituent of *5b* - *5d* obtained after purification by TLC gave satisfactory analytical data by proposed molecular structures.

It was confirmed that each product synthesized from the mixed raw materials of *3* and *4* was not included in the mixture of phthalocyanine analogous having a different pyridine ring number. Then, each product was obtained as the stoichometric compound in accordance with the mole ratio of mixed raw materials, and contained their regio isomers except for *5d*.

The target compound *5c* synthesized from a 1:1 mol ratio raw material of *3* and *4* has five regio isomers (Figure 2).

Compound *5c* has two non-peripheral substituted benzenoid and pyridinoid rings, which are different locations. In the molecule, the pyridinoid rings are adjacent and opposite to each other. In the case of adjacent to the pyridinoido rings, three types of isomer exist in accordance with the orientation of the ring. Meanwhile, two types of isomers exist in the case of opposite to the pyridinoid rings.

Compound *6* was synthesized as following; *3* (0.12 g, 0.29 mmol) and 2,3-dicyanopyridine (0.04 g, 0.29 mmol) were dissolved in pentanol (7 cm^3) and zinc chloride (0.05 g) was added; the ensuing mixture was heated for 4 h in the presence of DBU as

catalyst. After cooling, the reaction mixture was dissolved in toluene (50 cm^3) and filtered; the solvent was removed by evaporation. The product was purified by TLC (eluent : toluene) yielding a blue solid (0.13 g; yield 80%). ^{1}H-NMR (δ 400 MHz, C_6H_6-d_6/ ppm) 0.9 (m, 12H, CH_3), 1.61-2.61 (m, 64H, CH_2), 4.18-4.36 (m, 8H, α-CH_2), 7.45 (m, 4H, arom), 8.26 (m, 6H, Py); IR(ν KBr / cm^{-1}) 2960 (ν_{C-H}), 1600 (ν_{C-C}), 1500 (ν_{C-C}), 1420 (ν_{C-C}), 1200 (δ_{C-H}), 1100 (δ_{C-H}), 750 (δ_{C-H}); UV-Vis [λ_{max}toluene / nm (log ε_{max})] 665 (5.494); Anal Calcd. for $C_{70}H_{94}N_{10}Zn$: C. 73.68: H. 8.30: N.12.28. Found: C.73.67: H. 8.30: N. 12.28.

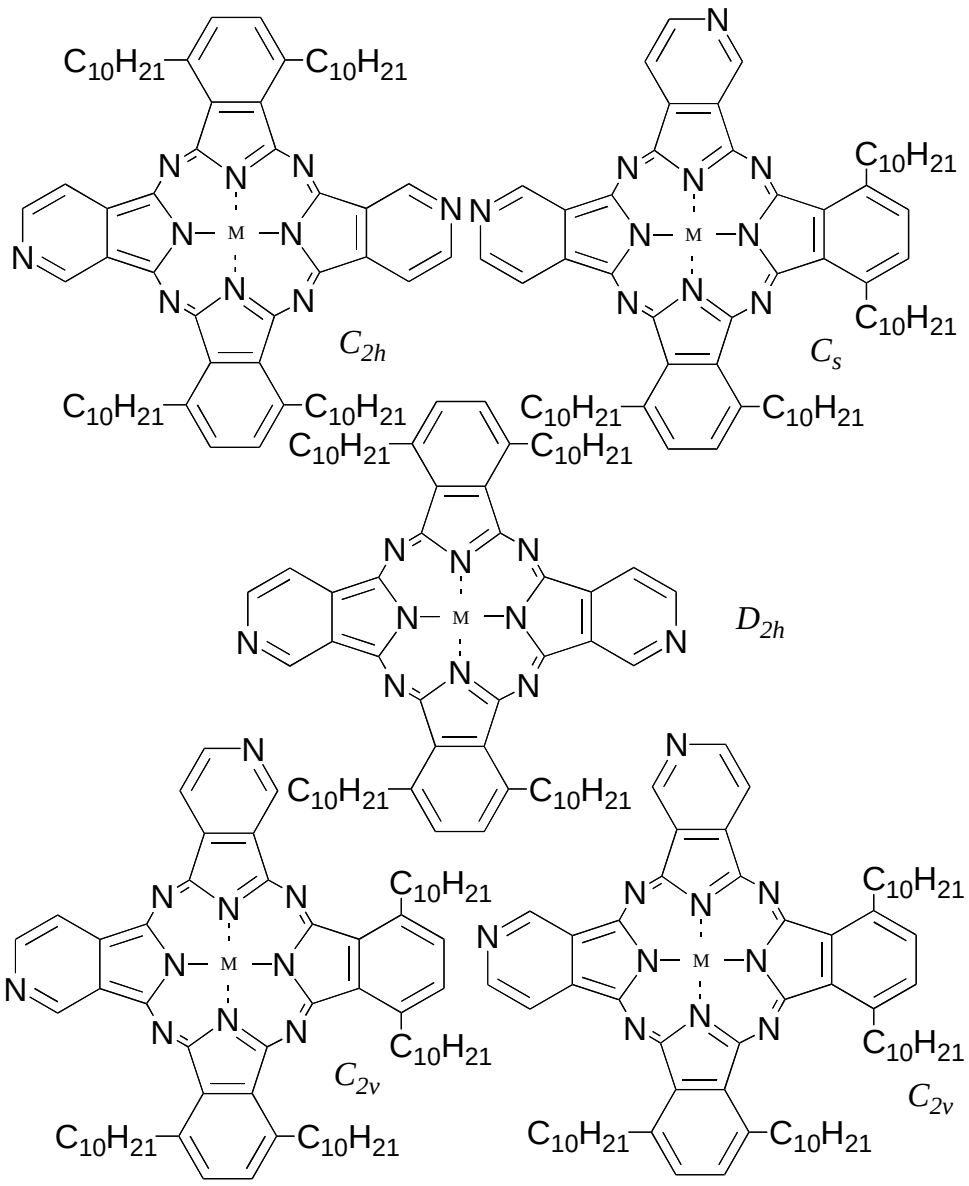

Figure 2. Molecular structures of resio isomers in *5c*.

CHARACTERIZATION OF REGIO ISOMERS

We attempted to separate the regio isomers of the compound, *5c* using TLC (eluent: toluene - pyridine, 7:3). The compound *5c* was separated into four green- to blue-colored fractions by TLC. These fractions were numbered from 1, 2, 3 and 4, according to the R_f values, and the R_f values were 0.95, 0.91, 0.75 and 0.65, respectively. Each fraction was recovered by scraping from the TLC plate, dissolved in pyridine, the solution filtered, and the solvent removed. The four fractions have different ^{1}H-NMR, UV-Vis and fluorescent spectra. The four fractions separated by TLC have been attributed to four of five possible regio isomers of the *5c*. The total amounts of fractions 1 - 4 are 26.1, 17.4, 17.4 and 39.1%, respectively.

The ^{1}H-NMR spectra (400 MHz, in C_6H_6-d_6) of the four fractions are shown in Table 4.

In this table, the assignment of hydrogens is the following; around 0.9 ppm is methyl protons; around 1.2 - 1.8 ppm is methylene protons γ or further removed from aromatic rings; 1.8 - 2.7 ppm is methylene protons β to aromatic rings; peaks around 4 and 4.3 ppm are metylene protons α to aromatic rings; peaks at 7.4 - 8.0 ppm are aromatic protons; more than 8.0 ppm are pyridyl protons.

The peaks of fractions in C_6H_6-d_6 around 8.3 ppm are separated after the addition of pyridine-d_5 [43-45]. The pyridyl protons of fractions appear as follows; the fraction 1: δ = 9.32 (d, 2H), 9.47 (d, 2H), 11.19 (s, 2H); the fraction 2: δ = 9.23 (d, 2H), 9.47 (d, 2H), 11.10 (s, 2H); the fraction 3: δ = 9.11 (d, 1H), 9.16 (d, 1H), 9.34 (d, 1H), 9.40 (d, 1H), 10.98 (s, 1H), 11.06 (s, 1H); fraction 4: δ = 9.04 (d, 1H), 9.11 (d, 1H), 9.38 (d, 1H), 9.44 (d, 1H), 10.97 (s, 1H), 11.05 (s, 1H).

The UV-Vis spectra of the four fractions are shown in Figure 3.

The UV-Vis spectra of four fractions show the typical pattern for phthalocyanine derivatives and analogous, mainly the π–π* transition with the heteroaromatic 18 π electron system. The Q bands around 700 nm are accompanied by characteristic weak satellite bands. In the UV-Vis spectra, the Q band is split into two bands (Q_1 and Q_2), except fraction 3.

Table 4. Spectral data (400 MHz ^{1}H-NMR in benzene-d_6) of fractions of 5c

Compound	Chemical shift δ / ppm
Fraction 1	0.93 (t,12H) 1.21-1.88 (m,48H) 1.88-2.23 (m, 8H) 2.24-2.69 (m, 8H) 4.13 (t, 4H) 4.32 (t, 4H) 7.35 (d, 2H) 7.49 (d, 2H) 8.30 (m, 6H)
Fraction 2	0.92(t,12H) 1.24-1.80 (m, 48H) 1.82-2.29 (m, 8H) 2.32-2.62 (m, 8H) 4.12 (t, 4H) 4.30 (t, 4H) 7.36 (d, 2H) 7.49 (d, 2H) 8.31 (m, 6H)
Fraction 3	0.92 (t, 12H) 1.16-1.95 (m, 48H) 1.95-2.20(m, 4H) 2.20-2.36 (m, 4H) 2.36-2.70 (m, 8H) 3.99 (t, 4H) 4.23 (t, 4H) 7.36 (d, 2H) 7.49 (d, 2H 8.30 (m, 6H)
Fraction 4	0.92 (t, 12H) 1.27-1.83 (m, 48H) 1.83-2.26(m, 8H) 2.30-2.68 (m, 8H) 4.07 (t, 4H) 4.29 (t, 4H) 7.35 (d, 2H) 7.48 (d, 2H) 8.31 (m, 6H)

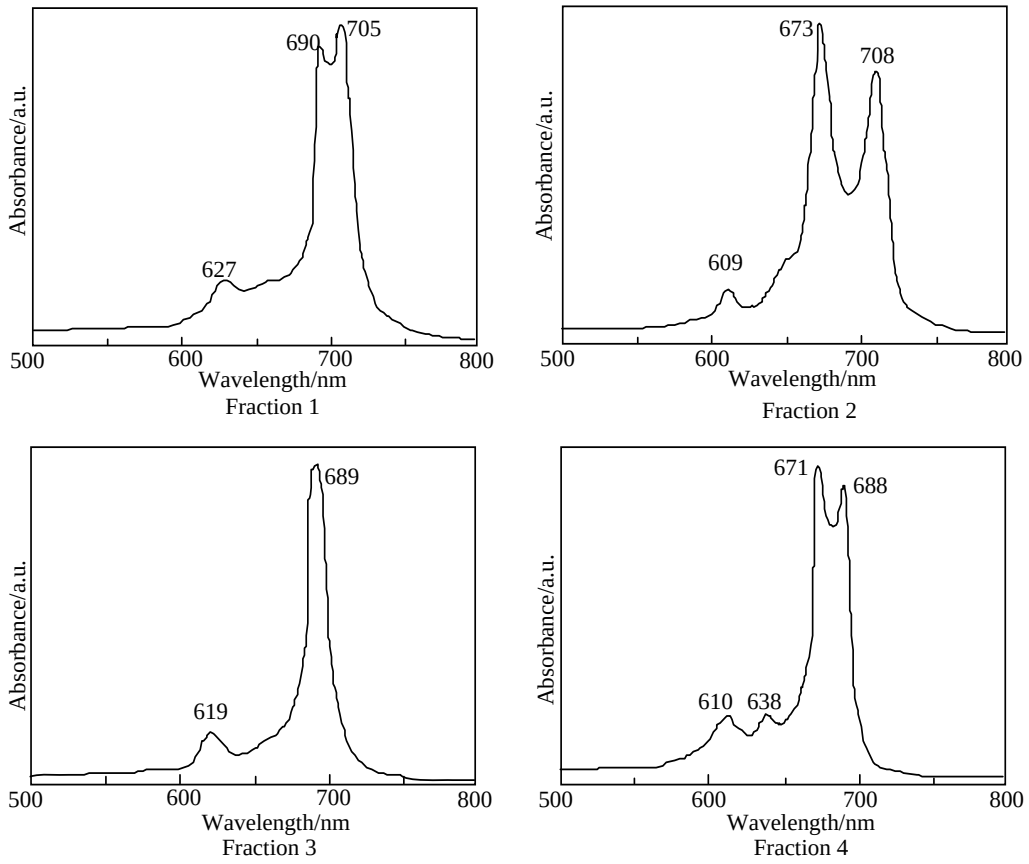

Figure 3.

The fluorescent spectra of the four fractions have different maxima at 703.6, 705.8, 694.8 and 701.0 nm for fraction 1, 2, 3 and 4, respectively (Figure 4). The fluorescence maxima were almost the same values for the four fractions. Similar phenomena were observed in the UV-Vis spectra of the four fractions.

It is known that fluorescence is expected in the molecules, which are aromatic and/or conjugation double bond with a high degree of resonance stability. The difference in the fluorescence maxima of the four fractions means dependence on the π electron environment of molecular structure.

The symmetry of the regio isomers of *5c* was decreased in the orders C_{2h}, D_{2h}, C_{2v}, C_s. The assignment of the spectra obtained from each fraction has been based on the theory of the relationship between symmetry and Q band [37-42], and consideration of the most probable formed isomer. Of the highest isomer symmetry, the Q band splits into two peaks, the splitting Q band is decreased with decreasing symmetry [23]. The Q band appearing at a higher wavelength corresponds to an electron transition from HOMO to LUMO, while the other is based on the one from HOMO to NLUMO.

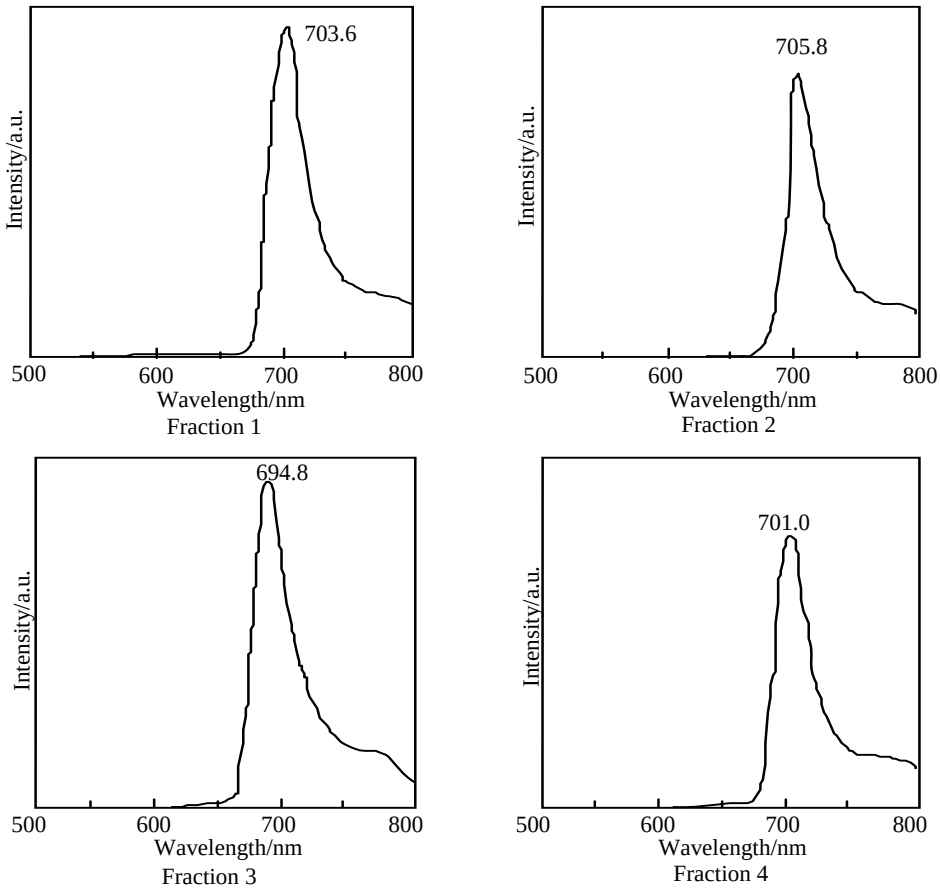

Figure 4.

The Q band absorption for fraction 2 is split into two peaks at λ_{max} 708 and 673 nm, the observation attributes to the highest symmetry isomer C_{2h}. The lowest symmetrical isomer C_s probably corresponds to the single absorption peak shown in fraction 3. The Q band absorption of fraction 1 is split into two peaks at λ_{max} 705 and 690 nm, and that of fraction 4 is at λ_{max} 688 and 671 nm. Fractions 1 and 4 are associated with C_{2v} or D_{2h} isomers. However, the confirmation between C_{2v} or D_{2h} is difficult since the difference of Q band has almost same, and two C_{2v} isomers cannot be isolated and identified.

The molecular orbital calculation of the isomers was achieved in order to obtain their theoretical Q band absorptions with the ZINDO/S semi-empirical CI configurations which were performed using HyperChem 5.1Pro software. The theoretical data of Q band regions and splits are as follows; C_{2h} : λ_{max}, 717.0 nm, 685.6 nm; $\delta_{Q1\text{-}Q2}$, 31.4 nm; D_{2h} : λ_{max}, 702.6 nm, 684.6 nm; $\delta_{Q1\text{-}Q2}$, 18.0 nm; C_{2v} : λ_{max}, 703.3 nm, 691.7 nm; $\delta_{Q1\text{-}Q2}$, 11.6 nm; C_{2v} : λ_{max}, 702.5 nm, 694.3 nm; $\delta_{Q1\text{-}Q2}$, 8.2 nm; C_s : λ_{max}, 700.4 nm, 697.3 nm; $\delta_{Q1\text{-}Q2}$, 3.1 nm. The theoretical Q band splits in the isomers are decreased in the orders C_{2h}, D_{2h}, C_{2v}, C_s, and are in good agreement with the experimental data.

CV can be used to make an estimation of the electrochemical difference for regio isomers. CV was carried out with a BAS CV-50W voltammetric analyzer at room temperature in acetonitrile containing a 0.01 mol dm^{-3} solution of *tert*-butylammonium perchlorate (TBAP). CVs were recorded by scanning the potential at the rate of 50 mV s^{-1}. The working and counter electrodes were platinum wires, and the reference electrode was a silver/silver chloride (Ag/AgCl) saturated sodium chloride electrode. The area of the working electrode was 2.0×10^{-2} cm^2.

The important parameters of a CV are the reduction and oxidation potentials for irreversible peaks, and the mid-point potential for a reversible couple, E_{mid} (Table 5).

Before separation of regio isomers, the reduction and oxidation potentials of *5c* are sorted into six irreversible peaks.

After separation, fractions 1 - 3 have one pair of reversible oxidation potential and four irreversible peaks. Fraction 4 has one pair of reversible oxidation and three irreversible reduction waves. The reduction and oxidation of metal phthalocyanine derivatives are due to the interaction between the phthalocyanine ring and the central metal [43-50].

The porphyrazine ring in the molecules of metal phthalocyanine derivatives or analogous is influenced by the π electrons about the closed system [49-53]. Although the π electron system of *5c* and fractions 1 - 4 consist of one porphyrazine, two pyridinoido and two didecyl substituted phenylene rings, the locations of these rings except for porphyrazine are different from each regio isomer.

Table 5. Reduction and oxidation potential of 5c and dits position isomers (fractions 1-4)

Materials	Potential (V vs. Ag/AgCl)	
	Reduction	Oxidation
5c, before separation of position isomers	-0.97* -0.71* -0.45* - 0.15*	0.37* 0.93*
Fraction 1	-1.00* -0.58* -0.24*	0.44 0.93*
ΔE^{**}		0.17
Fraction 2	-1.05* -0.60* -0.19*	0.37 0.90*
ΔE^{**}		0.10
Fraction 3	-0.96* -0.65* -0.22*	0.37 0.89*
ΔE^{**}		0.13
Fraction 4	-0.87* -0.63* -0.21*	0.34
ΔE^{**}		0.01

Potentials of reversible wave are midpoint potential of anodic and cathodic peaks for each couple, E_{mid}
* Irreversible peak.
** The anodic peak to cathodic peak separation for reversible couple.

The irreversible peaks are attributed to the oxidation of the central metal and the reversible couples represent the redox of the phthalocyanine ring [54].

Substituents and pyridinoid rings influenced the π electron environment in the *5c* and fractions 1 - 4. It is thought that the effect of pyridinoid rings gives rise to changes of the electron density of the metal phthalocyanine derivative. The difference of reduction and oxidation peaks between fractions 1 - 4 is attributed to the effect of the variation of the interaction between the central metal and the alkylbenzoporphyrazine. And then, the difference of cyclic voltammogram between the *5c* and fractions 1 - 4 is also the effect of the interaction, since *5c* is a mixture of its regio isomers.

The ΔE values are the anodic peak to cathodic peak separation located in the oxidation potential region. The ΔE values are around 100 mV and the redox processes are the same for regio isomers, except for fraction 4. This means that the electron process of regio isomers between fractions 1 - 3 involve approximately one electron transfer. The ΔE values of fraction 4 show different behaviour in comparison to the others. It is thought that the different behavior for fraction 4 is attributable to the mixture of two types of C_{2v} regio isomers. In other words, the reduction and oxidation potentials of fraction 4 are based on the interaction between two types of C_{2v} regio isomers. No observation on the reversible couple in *5c* resulted in the interaction between the regio isomers.

The potential difference between the reduction and oxidation is expressed in the HOMO - LUMO energy gap [55]. The values of λ_{max} in the Q band correlated with the potential difference between the reduction and oxidation.

The compound *6* fluoresced on exposure to ultraviolet light. Although fluorescence spectra generally were known to be mirror images of UV-Vis spectra at the longer wavelengths, the Q bands nearly overlapped with the wavelengths at which fluorescence occurs in the case of *6*, thus, the differences between λ_{max} of UV-Vis and the F_{max} of fluorescence spectra, called the Storks shift, were very small. These observations are similar to that seen with the *6*.

LASER-FLASH PHOTOLYSIS OF ALKYLBENZOPYRIDOPORPHYRAZINES

The absorption maxima of the compounds appeared around 660 – 710 nm in the solutions. The UV-Vis spectra of *5a*, *5c* and *5e* show the typical shape for phthalocyanine derivatives. The strongest peaks are assigned as the Q band, which could be attributed to the allowed $\pi - \pi^*$ transition of a phthalocyanine ring. The *5c* had the strongest absorption intensity of the products. The λ_{max} and log ε_{max} of products are summarized in the Table 6.

Laser flash photolysis in film was performed using a total reflection sapphire cell (10 x 30 mm, 1 mm thick, and both of the short side were cut at a 45° angle), which was spin-coated with a 1.2 μm thick photopolymer film. An excitation light pulse (20 ms, 355 nm and 10 mJ per pulse) from a YAG laser was expanded and exposed over the entire sample cell. A monitoring light from a xenon lamp passed through the multireflection cell which was connected to the head of an optical fiber attached to a monochrometer equipped with a photomultiplier or to a spectral multichannel analyzer system[57-65].

Table 6. UV-Vis spectral data of 5a-5c in toluene atat 5.0 X 10^{-5} M, and 5e in pyridine at 2.6 X 10^{-5} mol dm^{-3}

Compounds	λ_{max} / nm	log emax
5a*	675	4.243
5b	686	4.472
5c	687	4.814
5d	686	4.661
5e	707	4.720

* Pyridine solution.

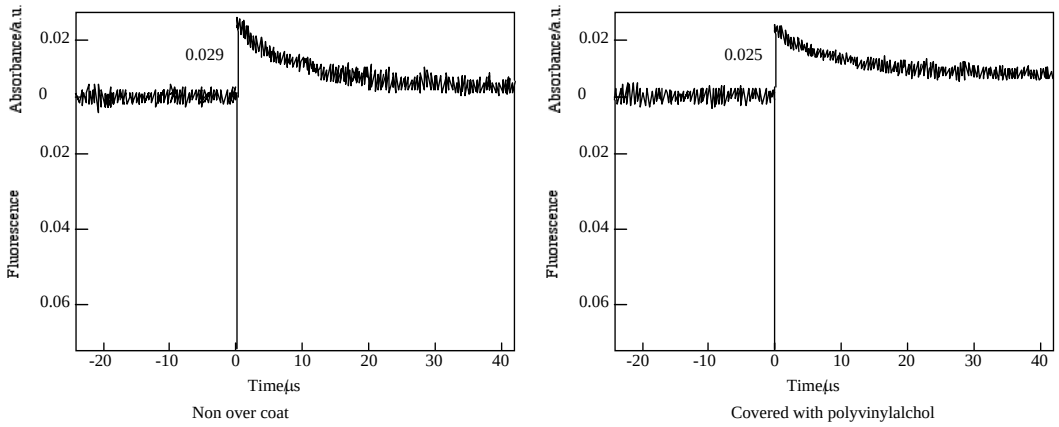

Figure 5. Decay trace of *5c* in PMMA film on 560 nm.
Wxcitation wavelength Is 355 nm in the presence and absence of PVA coatings.

The films were prepared as follows: A 10 wt% poly(methyl methacrylate) (PMMA) solution was made up in cyclohexanone, allylbenzopyridoporphyrazines were added to this solution by dissolving to a thickness of 1.2 μm thick by spin-coating a solution onto a sapphire cell. After that the films were covered with a poly(vinyl alcohol) (PVA) solution.

Figure 5 shows the time profiles of the triplet state for one of the alkylbenzopyridoporphyrazines, *5c* in PMMA was observed using laser-flash photolysis.

The triplet state lifetime of alkylbenzopyridoporphyarazines, *5b – 5d* and *5e* were also summarized in Table 7.

In each alkylbenzopyridoporphyrazine *5*, it is shown that *5b* and *5c* have longer triplet lifetimes than *5d* and *5e*. The length of the triplet lifetime for alkylbenzopyridoporphyrazine depends upon its molecular structure. The triplet lifetime of alkylbenzopyridoporphyrazines increased with increasing pyridine numbers in the molecule. It seems that if

tetrapyridoporphyrazine *5a* can be soluble in common solvents and measured for laser-flash photolysis, its triplet lifetime will be shown the longest value.

The photoexcited triplet state lifetimes of *5b* and *5c* in PMMA without a PVA coating were estimation to be 11.4 and 10.1 μs, respectively. While covered with a PVA coating, the photoexcited triplet state lifetimes of *5b* and *5c* were estimated as 51.8 and 46.9 μs, respectively. Compared with each compound, the triplet state lifetime in PMMA covered with PVA was longer than without the PVA coating.

The Q-band absorption of *5* in PMMA films was similar to that in solution, but the profile of Q-band in PMMA film became wider than that in solution and moved to a longer wavelength, except for *5e*.

Non-transition metal phthalocyanine derivatives were known to be excellent photosensitizers because of their chemical stability and high absorbance in the 650 – 700 nm region [56]. In the presence of a photosensitizer, photooxidation progresses via singlet state oxygen [57–66]. Phthalocyanine derivatives in the excited triplet state react with ground triplet state dioxygen. The triplet state dioxygen generated singlet excited state oxygen. The singlet excited oxygen reacts with a substrate to produce oxide, Equations. (1) – (3) [23, 35].

Both, covered with a coating and without PVA, the photooxidation proceeded as the same mechanism. However, in the case of being covered with PVA, the photoexited triplet state lifetimes of alkylbenzopyridoporphyrazines, *5b – 5d* and *5e*, were longer than in the case of non-overcoating with PVA. In the case of non-coated with PVA the shorter decay time was considered due to M-PC quenching by oxygen existing in an air atmosphere. While under the coated state with PVA, they suppressed the oxygen-permeation from the air atmosphere into the photopolymer layer. As a result, grand triplet state dioxigen was not furnished from the surrounding to the system.

Compounds *5* in the case of being covered with PVA behaved as a model for a practical photosensitizer in tumors or cancer cells.

Table 7. Triplet lifetime of 5b-5e

Compound	Q-band/nm in PMMA film	Lifetime/μ s	
		non over coat	over coat
5b	675.2	11.4	51.8
5c	717.6	10.1	46.9
5d	670.0	5.7	18.2
5e	703.9	2.6	17.9

$$\text{M-PC} \xrightarrow{h\nu} {}^1\text{M-PC} \xrightarrow{\text{intersystem crossing}} {}^3\text{M-PC} \quad (1)$$

$${}^3\text{M-PC} + {}^3\text{O}_2 \longrightarrow \text{M-PC} + {}^1\text{O}_2 \quad (2)$$

$${}^1\text{O}_2 + \text{substrate} \longrightarrow \text{substrate oxide} \quad (3)$$

In comparison with *5b* and *5c*, the photoexcited triplet lifetime of *5b* was slightly longer than *5c*, the absorption intensities for *5c* were stronger than *5b*. So that in these aspects, there is little to choose as a sensitizer for PDT between the two. As pyridine rings in the molecule of *5* increased, the water-solubility is expected to increase. In the case of the *N*,*N*',*N*",*N*''',*N*''''-tetramethylated quaternized forms of tetrapyridoporphyrazines, it was reported that the complexes do not form an aggregation in an aqueous solution [35, 67, 69]. Although the long alkyl-chain substituents in *5b* and *5c* will occur in aggregation, *5b* and *5c* are expected to undergo rapidly photodecomposition after the photooxidation process, similar to alkyl phthalocyanine derivatives [15].

Consequently, since *5b* and *5c* have the most intense absorption and a longer triplet state lifetime, we think *5b* and *5c* will become a useful sensitizer for PDT. The photosensitizer should be made in isomerically pure form [15]. Isomers of *5b* have not been reported yet, but *5c* has been separated and identified [23]. Thereupon, isomers of *5c* were examined by laser-flash photolysis, and *5b* will be reported next time.

LASER- FLASH PHOTOLYSIS OF REGIO ISOMERS

The regio isomers of the compound, *5c* were separated into four green- to blue-colored fractions by TLC [24]. The four fractions have a different ^{1}H NMR, UV-Vis and fluorescent spectra. The four fractions separated by TLC have been attributed to four of the five possible regio isomers of *5c*.

Figure 6 shows the fluorescence and excitation spectra of *5c*. The excitation spectra of *5c* and its fractions have almost the same profile. No significant change on the fluorescence spectra was observed for *5c* and its fractions.

Table 8 shows the Q-band and fluorescent maximum of fractions of *5c*. The assignment of the Q-band from each fraction was carried out on the theory of the relationship between symmetry and the Q-band [37, 38, 40, 41]. The Q-band splits into two peaks of the highest isomer symmetry, the splitting Q-band is decreased with a decreasing symmetry [41]. The symmetry of the position isomer of *5c* was decreased in orders of C_{2h}, D_{2h}, C_{2v}, C_s [21].

The position isomers of *5c* were the symmetry of molecular structures as D_{2h}, C_{2h}, C_s and C_{2v} for fractions 1, 2, 3 and 4, respectively [23]. Two types of C_{2v} isomers were not able to be isolated [23].

Table 9 shows the photoexcited triplet lifetime of fractions separated from *5c*. In spite of the presence or absence of PVA coatings, the triplet lifetime was increased with a decreasing symmetry of position isomers, which were ordered as C_{2h}, D_{2h}, C_{2v} and C_s for fractions 2, 1, 4 and 3, respectively. The photoexcited triplet state lifetimes of fraction 3 in PMMA absence and presence of a PVA coating were estimated to be 14.29 and 25.97 μs, respectively. Of each fraction except for fraction 3, the length of the lifetime was shorter than *5c*, and the sensitivities of triplet-triplet (T-T) absorptions were observed as very low.

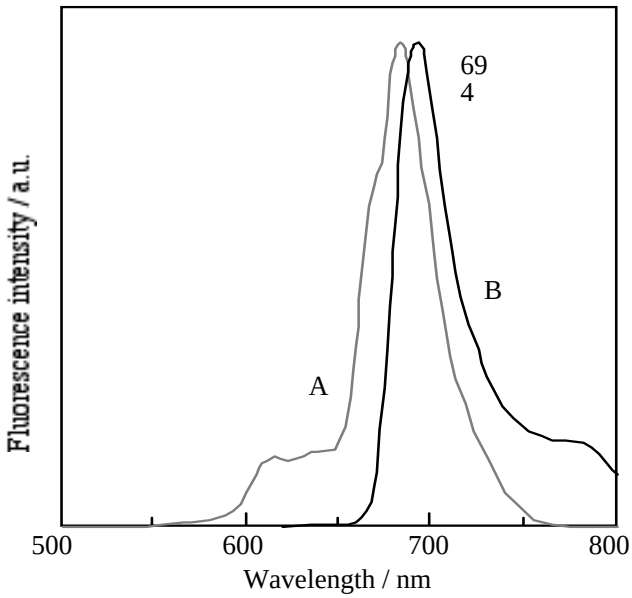

Figure 6. Fluorescence and excitation spectra of *5c* in DMF. A: Excitation spectrum, B: fluorescence spectrum.

Table 8. Absorption and fluorescence maxima for each fraction of *5c* in solution

Compound	Absorption Q band / nm	Fluorescence / nm	Symmetry
Fraction 1	627, 690, 705	704	D_{2h}
Fraction 2	609, 673, 708	706	C_{2h}
Fraction 3	619, 689	695	C_s
Fraction 4	610, 638, 671, 688	701	C_{2v}

═══ : Most intense peak

——— : Next intense peak

Although the length of the triplet lifetime of *5c* was observed by approximately 4 times that of the absence of a PVA over coating, the fractions of *5c* were only about 1.5 times as long as triplet lifetimes in comparison with the absence and presence of PVA coatings.

Unfortunately, a precise solution to the cause cannot be obtained. However, it seems to be the followings. Phthalocyanine derivatives were well known to aggregate in water and non-coordinating solvents. Zinc non-peripheral phthalocyanine derivatives having long side chains formed an aggregation at least 10^{-5} mol dm^{-3} in cyclohexane [18, 64]. It is enough thought that the samples in this study for laser-flash photolysis were formed in aggregation in the experimental condition. The aggregation degree for *5c* and its isomers is different from each other. And then, the ability of aggregation for *5c* and each of its isomers is a difference and complication. Since compounds *5b* and *5c* were consisted mixtures of their isomers, the aggregation and relationships of the energy levels between samples and the triplet state of dioxygen became a complication. For this reason, compounds *5b* and *5c* could measure relatively long lifetimes. The molecular structure of fraction 3 is suitable to occur in the T-T absorption in the system.

In order to estimate the photoexcitation mechanism, the triplet lifetime of each fraction was measured, containing *N,N'*-tetramethyl-4,4'-diaminobenzophenon (Michler's keton) as an additional quencher. As using Micher's keton, the lifetimes without PVA coatings were estimated as 21.19 and 14.03 μs for fractions 3 and 4, respectively (Table 10). These values of lifetime were longer than in the absence of Micher's keton. In the case of fractions 1 and 2, no T-T absorption occurred. The results were thought to be that each fraction has different energy levels of grand and excited states. The T-T absorption took place via the interactions between the energy levels of grand or excited states of fractions and the triplet of dioxygen or Michler's keton.

Table 9. Triplet lifetime of each fraction of *5c*

Compound	Q-band/nm in PMMA film	Lifetime/μ s	
		non over coat	over coat
Fraction 1	728.2, 681.6, 653.5	7.0	11.3
Fraction 2	670.0	0.9	1.6
Fraction 3	696.4	14.29	25.97
Fraction 4	665.5	6.4	9.2

Table 10. Triplet lifetime of each fraction of *5c* using Micher's keton as a quencher

Compound	Lifetime/μ s	
	non over coat	over coat
Fraction 1	-	-
Fraction 2	-	-
Fraction 3	21.19	72.72
Fraction 4	14.03	47.32

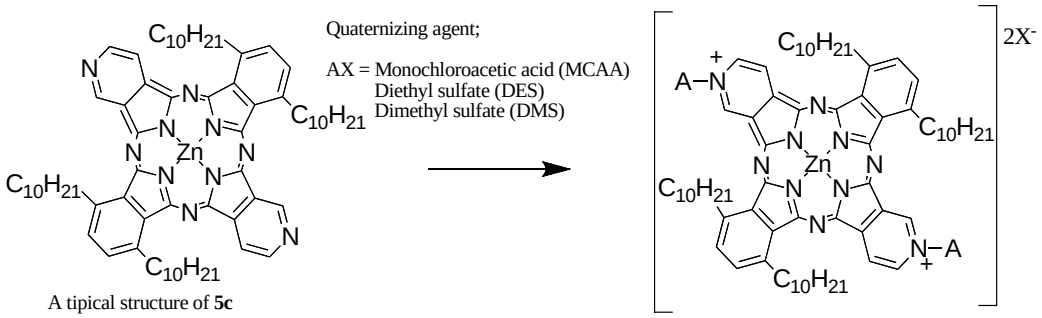

A tipical structure of **5c**

Scheme 3.

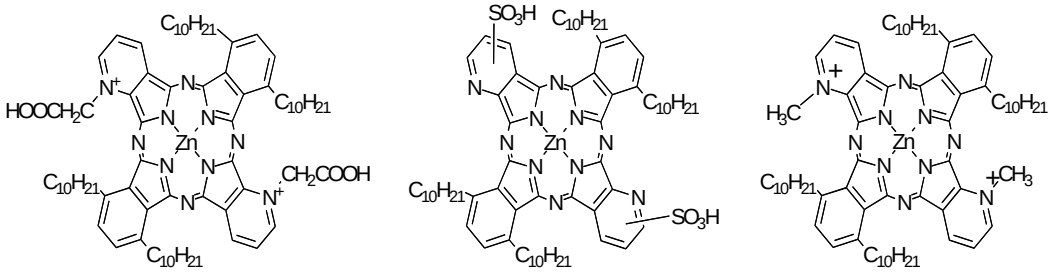

Afterreaction with MCAA of **6** Afterreaction with DES of **6** Afterreaction with DMS of **6**

Scheme 4.

QUATERNATION OF ALKYLBENZOPYRIDOPORPHYRAZINE

Compound *5c* and *6* were reacted with quaternizing agents such as monochloroacetic acid (MCAA), diethyl sulfate (DES) and dimethyl sulfate (DMS) (Scheme 3 & 4).

Quaternized *5c* is performed as followings: *5c* (0.17 g, 0.15 mmol) was reacted with quaternizing agents such as MCAA(0.57 g, 6 mmol), DES (0.1 g, 0.6 mmol) and DMS (0.2 g, 1.5 mmol), respectively, in DMF as solvent at 140 °C for 2h. The reaction mixture was dissolved in acetone (20 cm^3), cooled to room temperature and the solution filtered. The solvent was removed. The products were purified by TLC (eluent: THF-toluene, 8 : 2). Each product was recovered by scraping from the TLC plate, dissolved in pyridine, the solution filtered, and the solvent removed.

Yields of products were 23%, 17% and 28% for MCAA, DES and DMS as quaternizing agents, respectively. After reaction with quaternizing agents, *5c* were identified through spectroscopic techniques such as ^{1}H-NMR, IR and UV-Vis spectra.

(a) Product with MCAA: dark blue solid (32 mg; yield 23%). ^{1}H-NMR (δ 400 MHz, DMSO-d_6/ppm) 0.85 (m, 12H, CH_3), 1.19-1.71 (m, 48H, γ-CH_2), 1.79-2.12 (m, 8H, β-CH_2), 2.27-2.68 (m, 8H, β-CH_2), 4.15 (m, 4H, α-CH_2), 4.39 (m, 4H, α-CH_2), 6.19 (s, 2H, CH_2), 7.37 (m, 4H, arm), 8.32 (m, 6H, Py); IR (ν KBr/cm^{-1}) 3050 (ν_{C-H}), 2980 (ν_{C-H}), 1730 (ν_{C-O}), 1620 (ν_{C-C}), 1400 (ν_{C-C}), 1210 (δ_{C-H}), 1080 (δ_{C-H}), 790 (δ_{C-H}), 690 (δ_{C-H}); UV-Vis (λ_{max} toluene/nm) 686: (λ_{max} pyridine/nm) 690: (λ_{max} water/nm) 681; Anal Calcd. for $C_{74}H_{100}N_{10}O_4Zn$: C. 45.05: H. 2.52: N.17.50. Found: C.45.02: H. 2.49: N. 17.48;

(b) Product with DES: blue solid (37 mg, yield 17%). ^{1}H-NMR (δ 400 MHz, DMSO-d_6/ppm) 0.86 (m, 12H, CH_3), 1.02-1.70 (m, 48H, γ-CH_2), 1.88-2.11 (m, 8H, β-CH_2), 2.30-2.68 (m, 8H, β-CH_3), 4.11 (m, 4H, α-CH_2), 4.25 (m, 4H, α-CH_2), 7.38 (m, 4H, arom), 8.18 (m, 4H, Py); IR(ν KBr/cm^{-1}) 3050 (ν_{C-H}), 2960 (ν_{C-H}), 1500 (ν_{C-C}), 1450 (ν_{C-C}), 1400 (ν_{C-C}), 1340 (ν_{S-O}), 1180 (ν_{S-O}), 1250 (δ_{C-H}), 920 (δ_{C-H}), 760 (δ_{C-H}), 590 (δ_{C-S}); UV-Vis (λ_{max} toluene/nm) 687: (λ_{max} pyridine/nm) 731: (λ_{max} water/nm) 679; Anal Calcd. for $C_{70}H_{98}N_{10}S_2O_6Zn$: C. 37.11: H. 1.78: N.18.54. Found: C.37.10: H. 1.78: N. 18.49;

(c) Product with DMS: dark blue solid (53 mg, yield 28%). ^{1}H-NMR (δ 400 MHz, DMSO-d_6/ppm) 0.88 (m, 12H, CH_3), 1.14-1.72 (m, 48H, γ-CH_2), 1.82-2.17 (m, 8H, β-CH_2), 2.29-2.62 (m, 8H, β-CH_2), 4.06 (s, 6H, CH_3), 4.27 (m, 4H, α-CH_2), 4.51 (m, 4H, α-CH_2), 7.34 (m, 4H, arom), 8.23 (m, 6H, Py); IR (ν KBr/cm^{-1}) 3060 (ν_{C-H}), 2980 (ν_{C-H}), 1500 (ν_{C-C}), 1450 (ν_{C-C}), 1400 (ν_{C-C}), 1250 (δ_{C-H}), 1100 (δ_{C-H}), 950 (δ_{C-H}), 830 (δ_{C-H}), 660 (δ_{C-H}); UV-Vis (λ_{max} toluene/nm) 739: (λ_{max} pyridine/nm) 739: (λ_{max} water/nm) 684; Anal Calcd. for $C_{72}H_{100}N_{10}Zn$: C. 49.03: H. 3.09: N.21.43. Found: C.49.03: H. 3.08: N. 21.40.

Compound *6* (0.17 g, 0.15 mmol) was also reacted with MCAA (0.57 g, 6 mmol), DES (0.1 g, 0.6 mmol) and DMS (0.2 g, 1.5 mmol), respectively, in *N*, *N*-dimetylformamide (DMF) 140 °C for 2h. The reaction mixture was dissolved in acetone (20 cm^3), cooled to room temperature and the resulting solution was filtered. The solvent was removed and the product was purified by TLC (eluent: THF-

toluene, 8:2); the product was recovered from the TLC plate, via dissolution in pyridine followed by filtration and solvent removal.

(d) Product with MCAA: dark blue solid (yield 25%). ^{1}H-NMR (400 MHz, C_6H_6-d_6/ ppm) 0.87(m, 12H, CH_3), 1.13-1.70(m, 56H, γ-CH_2), 1.82-2.61(m, 8H, β-CH_2),4.11-4.38(m, 4H, α-CH_2), 6.20(s, 2H, CH2), 7.14-7.27(m, 4H, Arom), 8.73-.16(m, 6H, Py): IR(KBr / cm^{-1}) 3480(ν_{O-H}), 3050, 2970(ν_{C-H}), 1740($\nu_{C=O}$), 1600, 1500, 1400($\nu_{C=C}$), 1210, 1100, 940, 790, 690(δ_{C-H});

(e) Product with DES: blue solid (yield 21%). ^{1}H-NMR (400 MHz, C_6H_6-d_6/ ppm) 0.86(m, 12H, CH_3), 1.02-1.63(m, 56H, γ-CH_2), 1.88-2.61(m, 8H, β-CH_2), 4.26-4.50(m, 4H, α-CH_2), 7.37(m, 4H, Arom), 8.22(m, 4H, Py): IR(ν KBr / cm^{-1}) 3480(ν_{O-H}), 3050, 2960(ν_{C-H}), 1600, 1460, 1400($\nu_{C=C}$), 1350, 1150($\nu_{S=O}$)1250, 920, 770(δ_{C-H}), 580(δ_{C-S});

(f) Product with DMS: dark blue solid (yield 25%). ^{1}H-NMR (400 MHz, C_6H_6-d_6/ ppm) 0.90(m, 12H, CH_3), 0.95-1.45(m, 56H, γ-CH_2), 1.60-2.41(m, 8H, β-CH_2),4.05(s, 6H, CH_3), 4.25-4.42(m, 4H, α-CH_2),7.45(m, 4H, Arom), 8.02(m, 6H, Py): IR(ν KBr / cm^{-1}) 3070, 2980(ν_{C-H}), 1500, 1400($\nu_{C=C}$), 1250, 1100, 950, 810, 660(δ_{C-H}).

When MCAA or DMS was employed as the quaternizing agent, it is confirmed that *N*-CH_2COOH or *N*-CH_3 bond was obtained on the pyridinoide rings in *5c* and *6*, while as DES was used, we verified quaternation was not achieved but sulfonation occurred [18]. The shapes of UV-Vis spectra of pyridine solution changed after quaternation. It is thought that interactions between molecules are complicated, when DES and DMS were used as quaternizing agents. Then the quaternized products give rise to easy aggregation in aqueous media.

After reaction with quaternizing agents, all compounds gave the water solubility, and got amphiphilic property (Table 11).

Table 11. Solubilities of 5c, 6 and quaternized compounds with MCAA, DES and DMS in solvents

Compound	Toluene	Chloroform	Pyridine	Water
5c or **6**	○	○	○	×
Quaternized with MCAA	○	○	○	○
Quaternized with DES	○	○	○	○
Quaternized with DMS	○	○	○	○

○ : Soluble, × : insoluble

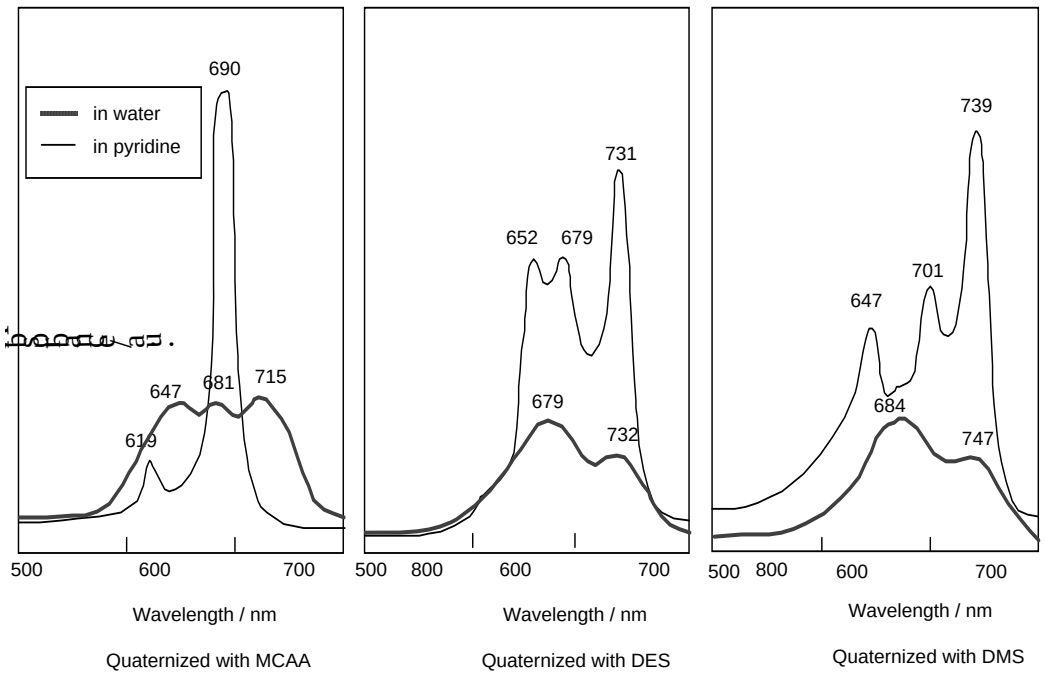

Compounds *5c* and *6* are readily soluble in pyridine with strongest absorption at 687 nm (log ε_{max} 4.81). The Q band absorption of the compound quaternized with DMS showed 739 nm and shifted by 56 nm to longer wavelength in comparison with compounds reacted with MCAA and DES. After react with MCAA, DES and DMS, all compounds are very soluble in water, they show strongest absorptions in the Q band at 715, 731 and 747 nm for *5c*, and 676, 687 and 687 nm for *6* , respectively (Figure 7 & Table).

Table 12. Uv-vis and fluorescence spectral data of quaternized *6*.

Quaternizing agent	Q-band		Fluorescence	
	λ_{max} pyridine/nm	λ_{max} water/nm	F_{max} pridine/nm	F_{max} water/nm
DMS	746, 673, 649, 606 [a]738, 668, 641, 600	723, 676, 646	683	681
DES	693, 658, 628, 597 [a]673, [a]645, 605	708, 687, 652	698	691
MCAA	679, 650 [a]677, [a]620	687, 647	692	688

underline; main peak.
[a] in toluene.

Table 13. Redox potentials of 5c and its quaternized compound with MCAA, DES and DMS in DMF solution containing with TBAP

Compound	Potential (V vs. Ag/AgCl)	
	Reduction	Oxdation
5c	-0.97* -0.71* -0.45* -0.15*	0.37* 0.93*
Quaternized with MCAA	-0.95* -0.45* -0.14*	0.45* 0.97*
Quaternized with DES Δ *E* **	-0.95* -0.89 -0.65* -0.19* 0.13	0.50* 1.01*
Quaternized withDMS Δ *E* **	-0.78 -0.58* -0.14* 0.10	0.31* 0.50* 1.13*

Potentials of reversible wave are midpoint potential of anodic and cathodic peaks for each couple, E_{mid}
* Irreversible peak.
** The anodic peak to cathodic peak separation for reversible couple.

Table 14. Potentials of quaternized *6* in DMF with TBAP

Compound	Potential (V vsAg/AgCl)	
	Reduction	Oxydation
6	-0.94* -0.62* -0.29* -0.03*	0.32* 0.48* 0.97*
Quaternized with DMS Δ E**	-1.15* -0.77 -0.14* -0.05* 0.11	0.50*
Quaternized with DES Δ E**	-0.83 -0.51* -0.05* 0.14	0.25* 1.05*
Quaternized with MCAA Δ E**	-0.75* -0.52* -0.12*	0.96* 1.28*

Potentials of reversible wave are midpoint potential of anodic and cathodic peaks for each couple.
* Irreversible peak.
** The anodic peak to cathodic peak separation for reversible couple.

The important parameters of a CV are the reduction and oxidation potentials for irreversible peaks, and the mid-point potential for a reversible couple, E_{mid} (Tables 13 & 14). The reduction and oxidation potentials of *5c* are sorted into six irreversible peaks. The irreversible peaks are attributed to the oxidation of the central metal and the reversible couples represent the redox of the phthalocyanine ring.

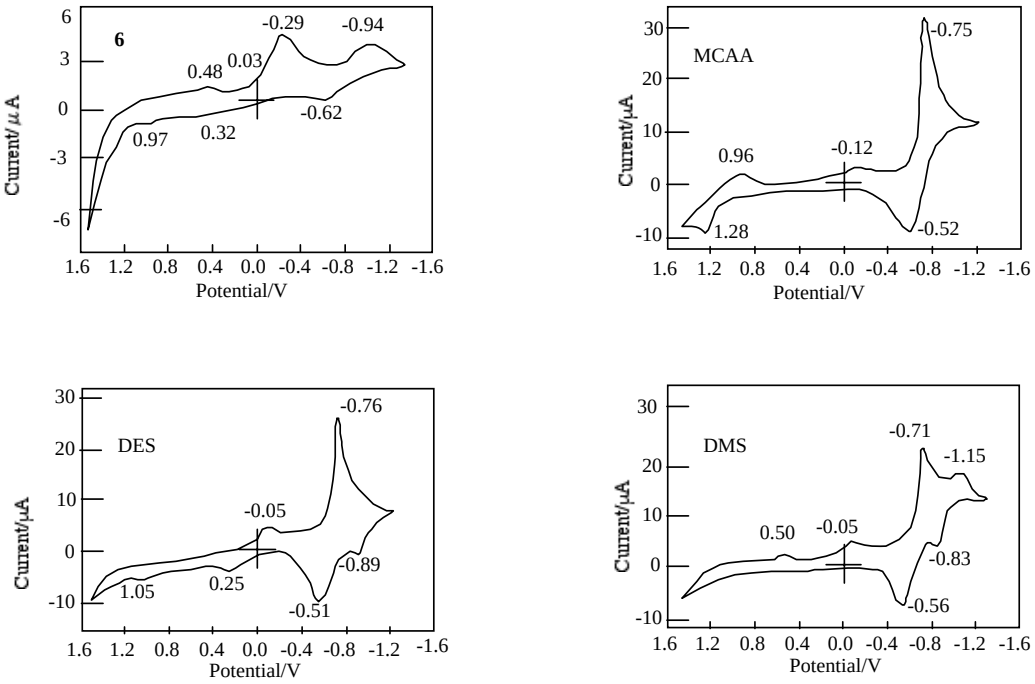

Figure 8. CVs of 6 and its quaternized compounds with MCAA, DES and DMS.

Shapes of CVs were changed between before and after reaction. The redox potential of *5c* have six irreversible peaks. The redox potentials of quaternized compound were different from each other. The CVs of compounds quaternized with MCAA, DMS showed three anodic peaks and two cathodic peaks, while DES had four anodic peaks and two cathodic peaks. It is thought that no effect on quaternation takes place for redox properties of phthalocyanione analogous, because redox potentials were not changed.

The reduction and oxidation potentials of *6* comprise seven irreversible peaks which consist of three anodic and four cathodic peaks (Figure 8). The irreversible peaks can be attributed to oxidation of the central metal and the reversible couples represent the reduction and oxidation of the phthalocyanine ring [1-3, 51, 52].

The potential difference in CVs between the reduction and oxidation correspond to the HOMO-LUMO energy gaps of the compound [58]. Just as chemical reactions occur during the electron transfer between HOMO and LUMO energy levels, photochemical reactions are also based on similar phenomena of energy transfer. Before and after the quaternization, the HOMO-LUMO energy gap of *6* was unchanged.

QUATERNATION OF REGIO ISOMERS

The separated regioisomers of *5c* were quaternized with DMS.

Quaternized regio isomers *5c*: Regio isomers of *5c* (0.4 mg, 0.35 μmol) was reacted with quaternizing agent as DMS (0.5 mg, 3.5 μmol) in DMF as solvent at 140 °C for 2h. The products were purified with TLC (eluent: THF-toluene, 8: 2). Each product was recovered by

scraping from the TLC plate, dissolved in pyridine, the solution filtered, and the solvent removed.

Yields of products were 11%, 9%, 15% and 11% for fractions 1, 2, 3 and 4, respectively. Quaternized regio isomers were also identified through spectroscopic techniques such as ^{1}H-NMR, IR, UV-Vis and fluorescence spectra.

(a) Fraction 1 with DMS: dark blue solid (0.053 mg, yield 13 %). ^{1}H-NMR (δ 400 MHz, DMSO-d_6/ppm) 0.86 (t, 12H, CH_3), 1.15-1.70 (m, 48H, γ-CH_2), 1.82-2.12 (m, 8H, β-CH_2), 2.19-2.49 (m, 8H, β-CH_2), 3.67 (s, 6H, CH_3), 3.92 (t, 4H, α-CH_2), 4.19 (t, 4H, α-CH_2), 7.37 (m, 4H, arom), 8.20 (m, 6H, Py); IR (ν KBr/cm^{-1}) 3070 (ν_{C-H}), 2980 (ν_{C-H}), 1500 (ν_{C-C}), 1400 (ν_{C-C}), 1250 (δ_{C-H}), 1100 (δ_{C-H}), 950 (δ_{C-H}), 820 (δ_{C-H}), 660 (δ_{C-H}); UV-Vis (λ_{max} toluene/nm) 680: (λ_{max} pyridine/nm) 703: (λ_{max} water/nm) 690; Fluorescence (F_{max} pyridine/nm) 687: (F_{max} water/nm) 695; Anal Calcd. for $C_{72}H_{100}N_{10}Zn$: C. 49.03: H. 3.09: N.21.43. Found: C.49.00: H. 3.01: N. 21.33;

(b) Fraction 2 with DMS: dark blue solid (0.065 mg, yield 15 %). ^{1}H-NMR (δ 400 MHz, DMSO-d_6/ppm) 0.87 (t, 12H, CH_3), 1.16-1.73 (m, 48H, γ-CH_2), 1.73-2.10 (m, 8H, β-CH_2), 2.10-2.55 (m, 8H, β-CH_2), 3.90 (s, 6H, CH_3), 3.99 (t, 4H, α-CH_2), 4.17 (t, 4H, α-CH_2), 7.23 (m, 4H, arom), 8.25 (m, 6H, Py); IR (ν KBr/cm^{-1}) 3070 (ν_{C-H}), 2980 (ν_{C-H}), 1500 (ν_{C-C}), 1400 (ν_{C-C}), 1250 (δ_{C-H}), 1100 (δ_{C-H}), 980 (δ_{C-H}), 830 (δ_{C-H}), 660 (δ_{C-H}); UV-Vis (λ_{max} toluene/nm) 689: (λ_{max} pyridine/nm) 675: (λ_{max} water/nm) 686; Fluorescence (F_{max} pyridine/nm) 684: (F_{max} water/nm) 690; Anal Calcd. for $C_{72}H_{100}N_{10}Zn$: C. 49.03: H. 3.09: N.21.43. Found: C.48.99: H. 2.98: N. 21.22;

(c) Fraction 3 with DMS: dark blue solid (0.055 mg, yield 11 %). ^{1}H-NMR (δ 400 MHz, DMSO-d_6/ppm) 0.85 (m, 12H, CH_3), 1.09-1.63 (m, 48H, γ-CH_2), 1.70-2.11 (m, 8H, β-CH_2), 2.11-2.42 (m, 8H, β-CH_2), 3.86 (s, 6H, CH_3), 3.97 (t, 4H, α-CH_2), 4.21 (t, 4H, α-CH_2), 7.23-7.33 (m, 4H, arom), 8.21 (m, 6H, Py); IR (ν KBr/cm^{-1}) 3080 (ν_{C-H}), 2970 (ν_{C-H}), 1500 (ν_{C-C}), 1400 (ν_{C-C}), 1250 (δ_{C-H}), 1100 (δ_{C-H}), 950 (δ_{C-H}), 830 (δ_{C-H}), 660 (δ_{C-H}); UV-Vis (λ_{max} toluene/nm) 681: (λ_{max} pyridine/nm) 689: (λ_{max} water/nm) 689; Fluorescence (F_{max} pyridine/nm) 690: (F_{max} water/nm) 698; Anal Calcd. for $C_{72}H_{100}N_{10}Zn$: C. 49.03: H. 3.09: N.21.43. Found: C.49.03: H. 3.03: N. 21.40;

(d) Fraction 4 with DMS: dark blue solid (0.078 mg, yield 19 %). ^{1}H-NMR (δ 400 MHz, DMSO-d_6/ppm) 0.87 (t, 12H, CH_3), 1.20-1.63 (m, 48H, γ-CH_2), 1.71-2.17 (m, 8H, β-CH_2), 2.17-2.47 (m, 8H, β-CH_2), 3.85 (s, 6H, CH_3), 4.09 (t, 4H, α-CH_2), 4.27 (t, 4H, α-CH_2), 7.21-7.36 (m, 4H, arom), 8.22 (m, 6H, Py); IR (ν KBr/cm^{-1}) 3070 (ν_{C-H}), 2980 (ν_{C-H}), 1500 (ν_{C-C}), 1400 (ν_{C-C}), 1250 (δ_{C-H}), 1100 (δ_{C-H}), 950 (δ_{C-H}), 830 (δ_{C-H}), 660 (δ_{C-H}); UV-Vis (λ_{max} toluene/nm) 677: (λ_{max} pyridine/nm) 730: (λ_{max} water/nm) 673; Fluorescence (F_{max} pyridine/nm) 686: (F_{max} water/nm) 687; Anal Calcd. for $C_{72}H_{100}N_{10}Zn$: C. 49.03: H. 3.09: N.21.43. Found: C.49.02: H. 3.08: N. 21.43.

In comparison with UV-Vis spectra of before and after the quaternation of regio isomers with DMS, the Q band absorption of quaternized regio isomer were split into two or more. Then after quaternation, the Q band absorptions were moved to longer wavelength (Figure 9).

In general, fluorescence spectra are measured as mirror image of excitation spectra. Excitation spectra show the same profile of absorption bands. Fluorescence spectra show longer wavelength than absorption and excitation spectra.

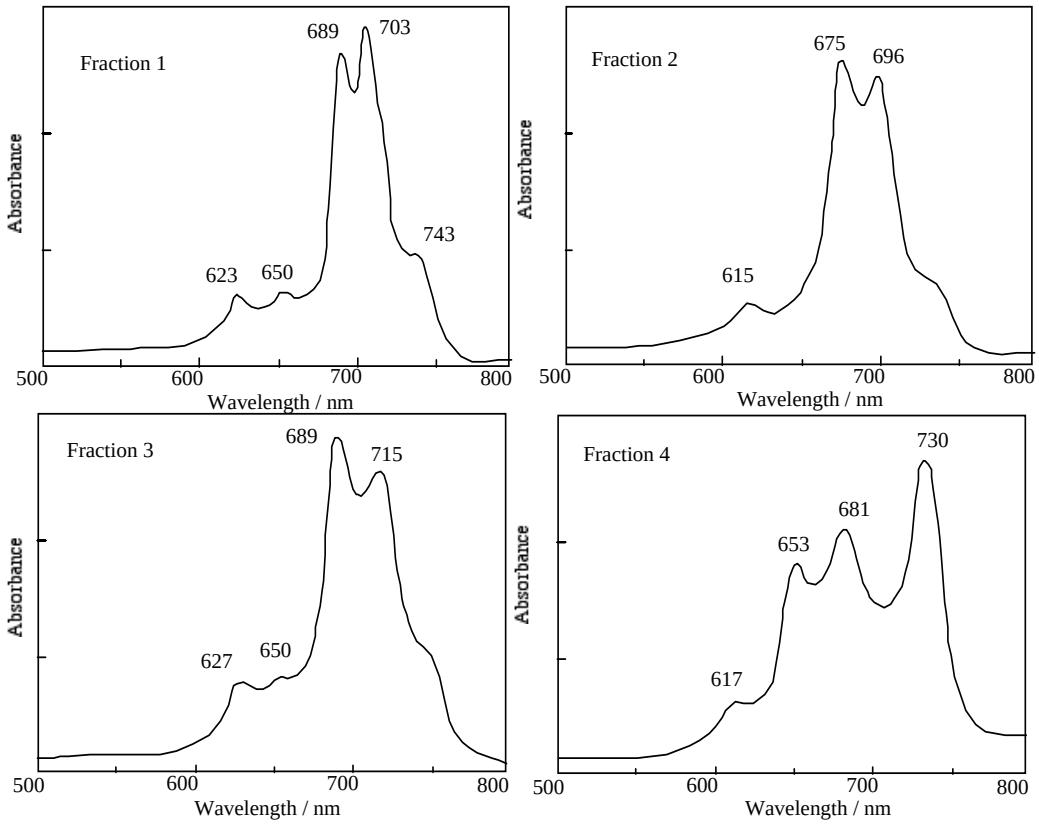

Figure 9. UV-Vis spectra of each regioisomer in 5c quaternized with DMS. The UV-Vis spectra of each quaternized isomer was measured in pyridiene.

For quaternized products except for fractions 1and 4, fluorescence spectra showed longer wavelength than their own absorption spectra.

In fraction 1 and 4, the degree of overlaps between absorption and fluorescence spectra was determined. These phenomena result from re-absorption or re-emission of fluorescence.

Accordingly, fluorescence spectra of fractions 1 and 4 showed shorter wavelength than the longest wavelength of absorption bands.

The CVs of fractions 1-3 have one pair of reversible oxidation potential and four irreversible peaks. Fraction 4 has one pair of reversible oxidation and three irreversible reduction waves. The reduction and oxidation of metal phthalocyanine derivatives are due to the interaction between the phthalocyanine ring and the central metal.

The porphyrazine ring in the molecules of metal phthalocyanine derivatives or analogous is influenced by the π electrons about the closed system. Although the π electron system of *5c* and fractions 1-4 consist of one porphyrazine, two pyridinoido and two didecyl substituted phenylene rings, the locations of these rings except for porphyrazine are different from each regio isomer.

The irreversible peaks are attributed to the oxidation of the central metal and the reversible couples represent the redox of the phthalocyanine ring.

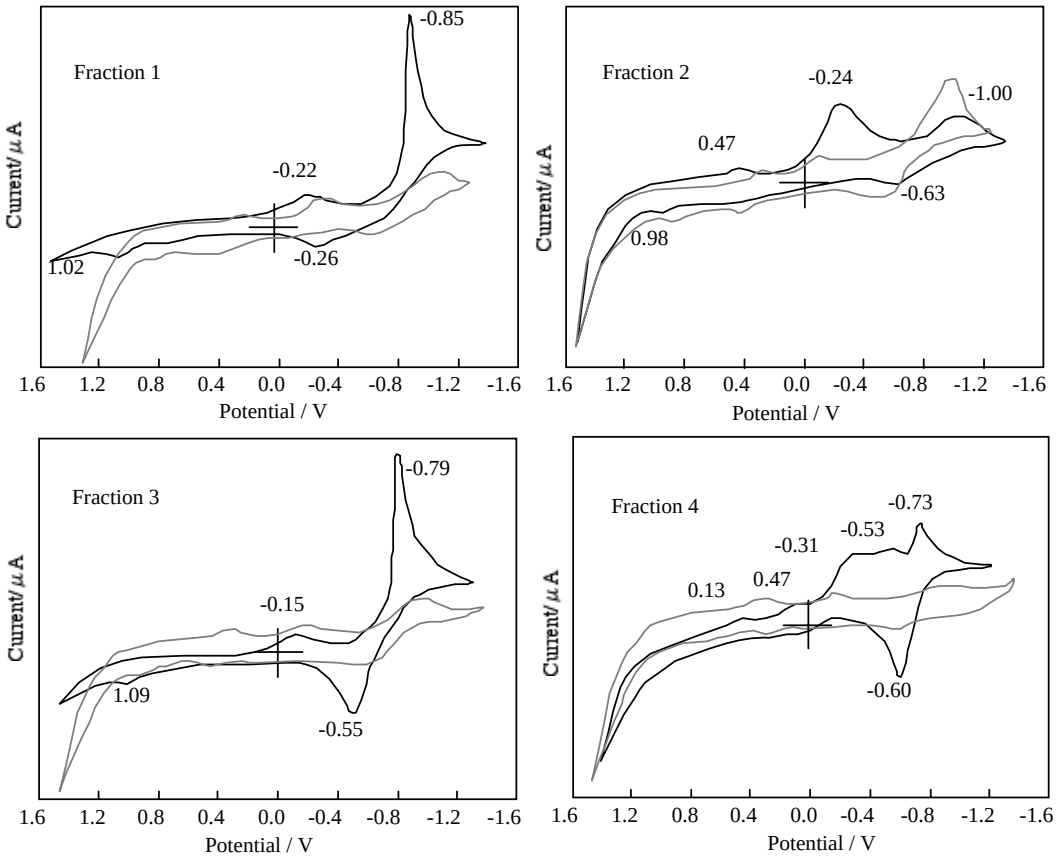

Figure 10. Cyclic voltammograms of each regioisomer in *5c* quaternized with DMS. Black line; After quaternation with DMS, Gray line; before quaternation.

Substituents and pyridinoid rings influenced the π electron environment in the fractions 1–4 of *5c*. It is thought that the effect of pyridinoid rings gives rise to changes of the electron density of the metal phthalocyanine derivative. The difference of reduction and oxidation peaks between fractions 1-4 is attributed to the effect of the variation of the interaction between the central metal and the alkylbenzoporphyrazine. And then, the difference of CV between *5c* and fractions 1-4 is also the effect of the interaction, since *5c* is a mixture of its resio isomers (Figure 10).

The ΔE values are the anodic peak to cathodic peak separation located in the oxidation potential region. The ΔE values are around 100 mV and the redox processes are the same for regio isomers, except for fraction 4. This means that the electron process of regio isomers between fractions 1-3 involve approximately one electron transfer. The ΔE values of fraction 4 show different behaviour in comparison to the others. It is thought that the different behaviour for fraction 4 is attributable to the mixture of two types of C_{2v} isomers. The redox potentials of fraction 4 are based on the interaction between two types of C_{2v} regio isomers. No observation on the reversible couple in *5c* resulted in the interaction between the regio isomers.

The redox potential of quaternized regio isomer were varied. After quaternation of regio isomers, the shapes of CVs appeared clearly. It is thought that electron transfer ability of regio isomers have been increased remarkably by the acquisition of cation groups. The CVs showed two anodic and two cathodic peaks, two anodic and three cathodic peaks, two anodic and two cathodic peaks, and one anodic and five cathodic peaks for fractions 1, 2, 3 and 4, respectively. Fractions 1 and 4 have a reversible couple in a reduction potential region at –0.24 and –0.57 V vs. Ag/AgCl, respectively. For quaternized regio isomers, some of redox potentials are recognized before the reaction.

Consequently, it suggested that the photoelectron transfer ability is kept unchanged regardless of the quaternation.

CELL CULTURE

IU-002 cells were maintained in MEM medium supplemented 5% fetal calf serum.

Cells seeded into 96-well tissue culture plates and incubated to allow attachment to the plates. The sensitizer was. Cells were incubated for 3h. The medium was removed, the cells were washed with phosphate-buffered saline (PBS), and fresh medium was added. Cells were exposed halogen light for 10 minutes. Appearance of cells was observed used a fluorescence microscope.

The uptake of DMS quaternized *6* was done in IU-002 cells. IU-002 cells were incubated at 37°C. After incubation for 3h, Cellular quaternized *6* was observed with a fluorescence microscope.

A fluorescent substance was noted when the uptake of DMS quaternized *6* in IU-002 cells was carried out.

Cell rupture can be detected. Intact cells selectively concentrated fluorescence. After exposed halogen light for 10 minutes showed damage and loss of fluorescence, although fluorescence in cells occurred in perinuclear area (Figure 11).

Consequently, the light exposed DMS quaternized *6* in cells produces cell disruption that can be detected as a decrease as fluorescence.

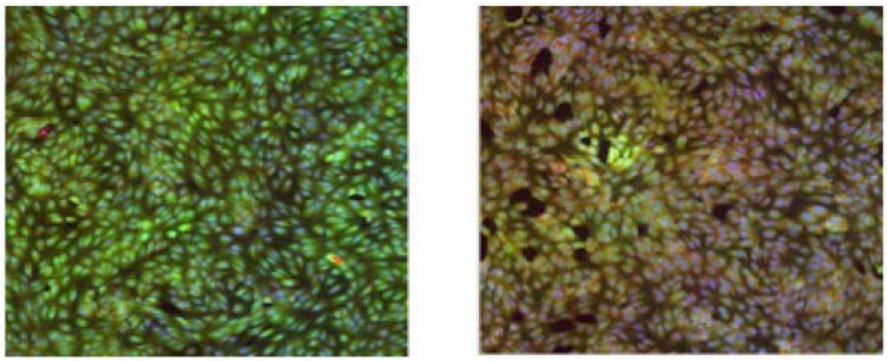

(a)

Figure 11. Fluorescence image of IU-002 cells. (a) Control, (b) Incubated with DMS quaternized *6* and irradiated with halogen light for 10 minutes.

CONCLUSION

The compound *5c* and *6* were synthesized from an equimolar mixture of *3* and *4* or 2,3-pyridine carbonitrile in the presence of basic catlist as DBU.

The triplet state of *5* was measured using laser-flash photolysis in PMMA film.

The triplet life times of *5* increased with an increasing pyridine number in the molecule. One of the zinc non-peripheral substituted alkylbenzopyridoporphyrazines, *5c* in the PMMA layer showed the most intense absorption and a longer triplet state lifetime. The photoexcited triplet state lifetimes of *5b* and *5c* in PMMA without a PVA coating were estimated to be 11.4 and 10.1 μs, respectively. While covered with a PVA coating, the photoexcited triplet state lifetimes of *5b* and *5c* were estimated as 51.8 and 46.9 μs, respectively. The compound *5c* was suitable for use of the sensitizer for PDT, since *5c* has the most intense absorption and a longer triplet state lifetime.

The triplet lifetime for position isomers in *5c* was increased with the decreasing symmetry of position isomers, which were ordered as C_{2h}, D_{2h}, C_{2v} and C_s for fractions 2, 1, 4 and 3, respectively. The photoexcited triplet state lifetime of fraction 3 in PMMA in the absence and presence of PVA coatings were estimation to be 14.29 and 25.97 μs, respectively.

The compound *5c* and *6* having two pyridine and two alkyl-substituted benzene rings were reacted with DMS, DES and MCAA as quaternizing agents.

When MCAA or DMS was employed as quatenization agents, *5c* and *6* were change to quatrenized compounds, while as DES was used, we verified quaternation was not achieved but sulfonation occurred. All compounds showed amphiphilic property.

After quaternation, the shapes of CVs appeared clearly. It is thought that electron transfer ability have been increased remarkably by the acquisition of cation groups. It suggested that the photoelectron transfer ability is kept unchanged regardless of the quaternation.

The uptake of DMS quaternized *6* was done in IU-002 cells.

The light exposed DMS quaternized *6* in cells produces cell disruption that can be detected as a decrease as fluorescence.

ACKNOWLEDGEMENT

The authors are favored to have the assistance of Mr. Taku KATO and Mr. Masaki WATAMABE who contributed his experimental skill, sustained effort, and grasp of objectives to the accomplishment of experimental program.

The assistance of Miss T. KOMORIYA, Research Associate of Nihon University, in the taking of data for part of cell culture is greatly appreciated. We also thank Professor Dr. KOHONO for his helpful advice given to us regarding our paper.

This research work was supported financially by Advanced Research Center for Life Science and Human Environment, Graduate School of Industrial Technology, Nihon University, which was adopted by a project for the promotion of high technology within The Ministry of Education and Science, Japan's Academic Frontier Project.

REFERENCES

[1] Lezonoff, CC. & Lever, AB. Phthalocyanines -Properties and Applications- Vol. 1. NewYork: VCH Publishers; 1989.

[2] McKeown, NB. Phthalocyanine Materials. Cambridge: Cambridge Univ. Press: 1998.

[3] Hirohasi, R; Sakamoto, K. & Ohno-Okumura, E. Phthalocyanines as Functional Dyes. Tokyo: IPC; 2004.

[4] Ao, R; Kummert, L. & Haarer, D., 1995, *Adv. Mater., 5*, 495.

[5] Maruta, M.1999, *J. Jpn. Soc. Colour Mater., 72*, 397.

[6] Wohrle, D. & Meissener, D. 1991, *Adv. Mater., 3*, 129.

[7] Frampton, CS; O'Connor; Peterson, JMJ. & Silver, J. 1988, *Display, 1998*, 74.

[8] Fernandez, DA; Awruch, J. & Dicello, LE. 1996, *Photochem. Photobiol. 63*, 784.

[9] Jori, G. 1990, *Photochem. Photobiol. 52*, 439.

[10] Kessel,D., 1990, Spectrum 3, 13.

[11] Tabata, K; Fukushima, K; Oda, K; & Okura, I., 2000, *J. Porphyrins Phtalocyanines 4*, 278.

[12] Moan, J. 1990, *J. Photochem. Photobiol. B: Biol. 5*, 521.

[13] Cook, MJ; Chambrier, I; Cracknell, SJ; Mayes, DA. & Russell, D.A. 1995, *Photochem. Photobiol. 62*, 542.

[14] De Filippis, MP., Dei, D., Fantetti, L., and Roncucci, G., 2000, *Tetrahedron Lett. 41*, 9143.

[15] Jori, G. 1996, *J. Photochem. Photobiol. B: Biol., 36*, 87.

[16] Yang, YC; Ward, JR; & Seiders, RP. 1985, *Inorganic Chem., 24*, 1765.

[17] Ogawa, K; Kinoshita, S; Yonehara, H; Nakahara, H & Fukuda, K. 1989, *J. Chem. Soc. Chem. Commun.,1989*, 477.

[18] Klech, H; Weitemeyer, A; Muller, S; & Wohrle, D. 1995, *Liebigs Ann., 1269*, 1273.

[19] Boyle, R. & van Lier JE.1993, *Synlett., 351*, 352.

[20] Shrman, WN., Kudrevich, SV. & van Lier, JE. 1996, *Tetrahydron Lett., 37*, 5831.

[21] Chan, WS; Brasseur, N; La Madeleine, C; Oullet, R & van Lier, JE. 1997, *Eur. J. Cancer, 33*, 1855.

[22] Urizzi, P; Allen, CM; Langlois, AR; Oullet, R; La Madeleine, C. & van Lier, JE. 2001, *J, Porphyrins Phthalocyanines, 5*, 154.

[23] Sakamoto, K; Kato, T. & Cook, M. J. 2001, *J.Porphyrins Phthalocyanines, 4*, 742.

[24] Yokote, M; Shibamiya, F. & Shoji, S.1964, *Kogyo Kagaku Zasshi , 67*, 166.

[25] Sakamoto, K; Kato, T; Kawaguchi, T; Ohno-Okumura, E; Urano, T; Yamaoka, T; Suzuki, S. & Cook MJ. 2002. *J Photochem Photobiol A: Chem.153*, 245.

[26] Sakamoto, K; Ohno-Okumura, E; Kato, T; Kawaguchi, T..2003. *J Prphyrins Phthalocyanine, 7*, 83.

[27] Sakamoto, K; Kato, T; Ohno-Okumura, E; Watanabe, M. & Cook MJ. 2005, *Dye Pigments, 64*, 63.

[28] Seotsanya-mokhosi, I; Kuznetsova, N. & Nyokong T. 2001, *J. Photochem Photobiol A: Chem., 140*, 215.

[29] Yokote, M; Shibamiya, F & Shoji, S. 1964, *Kogyo Kagaku Zasshi*, 67, 166.

[30] McKeown, NB., Chambrier, I. & Cook, M.J. 1990, *J. Chem. Soc. Perkin Trans. 1, 1990*, 1167.

[31] Chambrier, I; Cook, MJ; Cracknell, SJ. & McMurdo, J. 1993, *J. Mater. Chem., 3,* 841.
[32] Sakamoto, K. & Shibamiya, F. 1986, *J. Jpn. Soc. Colour Mater., 59,* 517.
[33] Hanack, M; Meng, D; Beck, A; Sommerauer, M. & Subramanian, L. R. 1993, *J. Chem. Soc. Chem. Commum., 1993*, 58.
[34] Markovitsi, D; Lecuyer, I. & Simon, J. 1991, *J. Phys. Chem., 95,* 3620.
[35] Khatib, NEL; Boudjema, B; Maitrot, M; Chermette, H. & Pote, L. 1988, *Can. J. Chem., 66*, 2313.
[36] Rollmann, LD. & Iwamoto, RT. 1968, *J. Am. Chem. Soc., 90*, 1455.
[37] Fierro, C; Anderson, AB. & Scherson, DA.1988, *J. Phys. Chem., 92*, 6902.
[38] Cook, MJ. & Jafari-Fini, A. 1997, *J. Mater Chem., 7,* 2327.
[39] Sommerauer, M; Rager, C. & Hanack, M. 1996, *J. Am. Chem. Soc., 118,* 10085.
[40] Gaspared, S. & Maillard, PH. 1987, *Tetrahydron, 43*, 1083.
[41] Negrimovskii, VM; Bouvet,M; Luk'yanets, EV. & Simon, J. 2000, *J. Porphyrins Phthalocyanines, 4*, 248.
[42] Kobayashi, N. & Konami, H. 1996, Phthalocyanines -Properties and Applications- Vol. 4", (Ed.) Lezonoff, C. C., and Lever, A. B. P. VCH Publishers, New York, 343.
[43] Kasuga, K. & Tsutsui, M. 1980, *Coordination Chem. Rev., 32,* 67.
[44] Lever, ABP; Licoccis, S; Magrell, M. & Ramanamy, B. S. 1982, *Adv. Chem. Ser., 210,* 237.
[45] Sakamoto, K. & Ohno, E. 1996, *J. Soc. Dyers and Colorists, 112,* 368.
[46] Sakamoto, K. & Ohno, E., 1997, *Dyes Pigments, 35*, 375.
[47] Sakamoto, K. & Ohno, E., 1998, *Dyes Pigments, 37*, 291.
[48] Sakamoto, K. & Ohno, E., 1997, *Prog. Org. Coat., 31*, 139.
[49] Sakamoto, K. & Ohno-Okumura, E., 1999, *J. Porphyrins Phthalocyanines, 3*, 634.
[50] Sakamoto, K. & Ohno-Okumura, E., 1999, *J. Jpn. Soc. Color Mater., 72*, 2.
[51] Kadish, KM; Moninot, G; Hu, Y; Dubois, D; Ibnlfassi, A; Barbe, J-M. & Guilard, R., 1993, *J. Am. Chem. Soc., 115*, 8153.
[52] Darwent, JR; Douglas, P; Harriman, A; Porter, G. & Richoux, MC. 1982, *Coord. Chem. Rev., 44*, 83.
[53] Ozomen, K., Kuznetsova, N. & Nyokong, T. 2001, *J. Photochem. Photobiol. A: Chem., 139*, 217.
[54] Murphy, ST; Konda, K. & Foote, CS. 1999, *J. Am. Chem. Soc., 121*, 3751.
[55] Gerdes, R; Wohrle, D; Spiller, W; Schmeider, G. & Schulz-Ekloff, G. 1997, *J. Photochem. Photobiol. A: Chem., 111*, 65.
[56] Lang, K; Wagnerova, DM. & Brodilova, J. 1993, *J. Photochem. Photobiol. A: Chem., 72*, 9.
[57] Iliev, V; Alexiev, V. & Bilyarska, L. 1999, *J. Mol. Catal. A: Chem., 137*, 15.
[58] Lukyanets, EA. 1999, *J. Porphyrins Phthalocyanines, 3*, 592.
[59] Kaliya, OL; Lukyanets, EA. & Vorozhtsov, GV. 1999, *J. Porphyrins Phthalocyanines, 3*, 592.
[60] Edrei, R; Gottfried, V; Van Lier, JE., & Kimel, S. 1998, *J. Porphyrins Phthalocyanines, 2*, 191.
[61] Dhami, D. & Phillips, D. 1996, *J. Photochem. Photobiol. A: Chem, 100*, 77.
[62] Spiller, W; Kliesch, H; Wohrle, D; Hackbarth, S; Roder, B. & Schmurpfeil, G. 1998, *J. Porphyrins Phthalocyanines, 2*, 145.
[63] Tokumaru, K. 2001, *J. Porphyrins Phthalocyanines, 5*, 77.

[64] Wohrle, D; Gitzel, J; Okura, I. & Aono,S. 1985, *J. Chem. Soc., Perkin Trans. II, 1985*, 1171.
[65] Yhamae, M. & Nyokong, T. 1999, *J. Electroanal. Chem., 470*, 126.